UNIVERSITÄTSKLINIKUM HAMBURG-EPPENDORF

Institut für Experimentelle Immunologie und Hepatologie

Prof. Dr. rer. nat. Gisa Tiegs

Influence of *in utero* Acetaminophen exposition on the T cell development of the offspring

Dissertation

zur Erlangung des Grades eines Doktors der Medizin

an der Medizinischen Fakultät der Universität Hamburg.

vorgelegt von:

Laura Enrica Mayer

aus Hamburg

Hamburg 2022

(wird von der Medizinischen Fakultät ausgefüllt)

Angenommen von der

Medizinischen Fakultät der Universität Hamburg am:
24.04.2023

Veröffentlicht mit Genehmigung der

Medizinischen Fakultät der Universität Hamburg.

Prüfungsausschuss, der/die Vorsitzende:
Prof. Dr. Eva Tolosa

Prüfungsausschuss, zweite/r Gutachter/in:
Prof. Dr. Gisa Tiegs

Above all, don´t fear difficult moments. The best comes from them.

Rita Levi-Montalcini

Meinen Eltern

Contents

Figure Legend

Table Legend

Abbreviations

AGM	aorta-gonad-mesonephros region
ALT	alanine aminotransferase
AM404	N-arachidonoylaminophenol
ANOVA	analysis of variance
APC	antigen-presenting cell
AST	aspartate aminotransferase
Bcl11b	B cell lymphoma/leukemia 11b
BM	bone marrow
BSA	bovine serum albumin
CoA	co-activator
CD	cluster of differentiation
CD4 SP	CD4 single positive cell
CD8 SP	CD8 single positive cell
COX	cyclooxygenase
d	day
DILI	drung-induced liver injury
DLL	Delta-like ligand
DMSO	dimethyl sulfoxide
DN	double negative cell
DNMTs	DNA-methyltransferases
DP	double positive cell
DPBS	Dulbecco´s phosphate buffered saline
E	embryonic day
EDTA	ethylenediaminetetraacetic acid
EML	erythroid, myeloid, lymphoid
ES	experimental setup
ETH	endothelial-to-haematopoietic-transition
ETP	early thymic progenitors
FACS	fluorescence-activated cell sorting
FCS	fetal calf serum
FITC	fluorescein isothiocyanate
Foxn1	forkhead box n1
Foxp3	forkhead box p3

GATA3	GATA binding protein 3
H&E	haematoxylin & eosin
HBSS	Hanks balanced salt solution
HSC	haematopoietic stem cell
ICN	intracellular region of Notch
Ig	immunoglobulin
IL	interleukin
i.p.	intraperitoneal
ISP8	immature single positive CD8 T cell
IVC	individually ventilated cages
Jag	Jagged
lin	lineage
MACS	magnetic cell sorting
MCSF	macrophage stimulating factor
MHC	major histocompatibility complex
NAC	N-acetylcysteine
NAPQI	N-acetyl-p-benzoquinone imine
NF-ATc1	nuclear factor of acitvated T cells c1
NK	natural killer cell
NSAIDs	non-steroidal anti-inflammatory drug
PBS	phosphate buffered saline
PE	phycoerythrin
PFA	paraformaldehyde solution
RPMI	Roswell Park Memorial Institute
Sca-1	stem cell atnigen-1
TCF-1	T cell factor-1
TCR	T cell receptor
TEC	thymic endothelial cell
TGF-β	transforming-growth factor β
Th	T helper cell
T_{reg}	regulaltory T cell
UGT	UDP-glucuronyltransferase

Aim of the study

APAP (N-Acetyl-para-aminophenol, Paracetamol, Acetaminophen) overdose, intentional or unintentional, represents the main cause for drug-induced liver injury (DILI) (Brune, Renner, and Tiegs 2015, W. M. Lee 2017). It is commonly prescribed by physicians to treat fever and pain, but it is also available over the counter and often taken as self-medication. Also, in pregnancy it is the analgetic and antipyretic substance of choice, as it is considered to be safe for the mother and the child (Bremer et al. 2017).

However, epidemiological studies revealed that maternal application of APAP also bears risks: For example, it was found that children prenatally exposed to APAP had less haematopoietic stem cells (HSC) in cord blood (Bremer et al. 2017). These reduced HSC frequencies were also found in murine fetal livers after APAP exposition *in utero* (Karimi et al. 2015). Furthermore, an association between a higher susceptibility for the children to develop T cell-mediated childhood asthma and maternal APAP treatment during pregnancy was observed (Persky et al. 2008, Rebordosa et al. 2008, Eyers et al. 2011).

All these findings raised doubts on the safety of APAP in pregnancy, as it seems to have a potential effect on the offspring´s immune system, or more precisely: on the HSC compartment and the differentiation of T cells from HSC.

Hence, the major aim of this study was to investigate potential alterations in T cell development from murine fetal liver HSC due to prenatal exposition to APAP. For this purpose, T cell differentiation was studied *in vitro* by co-culturing fetal liver HSC isolated from *in vivo* pretreated pregnant mice with OP9 cells, a stromal cell line that express the Notch-ligand, Delta-like ligand 1 (DLL1), essential for T cell development (Brandstadter and Maillard 2019).

To provide suitable experimental conditions for investigation of T cell development from fetal liver HSC in the OP9 co-culture system, a most reliable experimental set up needed to be established. It was important that it meets the criteria of good practicability but also best cell survival, proliferation and differentiation.

The second part of these studies investigated the effect of APAP application in pregnancy on maternal health and pregnancy outcome as well as the impact on offspring´s immune development. To study this, initially fetal liver HSC were co-cultured with OP9-DLL1 cells to induce T cell differentiation. Developing cells were analyzed at different time points of co-culture regarding potential alterations of T cell development induced by *in vivo* APAP exposition.

Finally, it was assessed whether additional treatment with N-acetylcysteine (NAC), the APAP-specific antidote, might have protective effects on maternal health, pregnancy outcome and fetal T cell development.

1 Introduction

1.1 Acetaminophen

APAP (N-Acetyl-para-aminophenol, Paracetamol, Acetaminophen) is commonly used to treat fever and pain. It is frequently prescribed by physicians but is also available over the counter.

Although APAP is one of the most applied medications, it also bears risks. It is responsible for most of the deaths due to acute liver failure in industrialized countries (Lee 2004, Larson et al. 2005, Brune, Renner and Tiegs 2015). In the United States alone it causes 500 deaths and 10.000 hospitalizations per year (W. M. Lee 2017). Furthermore, APAP overdose is the main reason for drug-induced liver injury (DILI) culminating in liver transplantations (Brune, Renner, and Tiegs 2015, W. M. Lee 2017). Inconsistent package labeling of APAP-containing drugs in different countries may lead to unintentional overdose causing acute liver failure. Additionally, the fact that APAP is easily available in big package sizes contributes to, intentional or unintentional, APAP-intake greater than the daily recommended dose of 4 g eventually resulting in liver damage.

The mechanism of pharmacological action of APAP is not yet fully understood, however, it is considered as an inhibitor of prostaglandin synthesis. Prostaglandins are lipid mediators that play a role in inflammation, fever, and pain (Smyth et al. 2009). Their synthesis is catalyzed by cyclooxygenases (COX) (Mazaleuskaya et al. 2015). APAP impairs the function of different isotypes of COX which leads to its analgesic and antipyretic effect. However, studies revealed that APAP does not have the same effect on all COX enzymes. In fact, it is more selective to inhibit COX-2 compared to COX-1 (Hinz, Cheremina, and Brune 2008).

Nevertheless, studies also consider central mechanisms responsible for the analgesic effects of APAP. For example, it influences the serotonergic descending pain pathways (Graham and Scott 2005). Moreover, Anderson *et al.* propose that p-aminophenol, an active metabolite of APAP, is conjugated with arachidonic acid to form the metabolite N-arachidonoylaminophenol (AM404) which affects cannabinoid receptors that mediate analgesia (Anderson 2008).

In general, APAP is metabolized in the liver. When used in therapeutic doses, it is mainly converted into inactive non-toxic conjugates *via* glucuronidation (85 %) mediated by UDP-glucuronyltransferase (UGT) and sulfation which is catalyzed by sulfotransferases (Prescott 1983, Gelotte et al. 2007). The final products are excreted *via* the kidneys. Nevertheless, a smaller amount of APAP is oxidized to an active and toxic metabolite, N-acetyl-p-benzoquinone imine (NAPQI), by cytochrome P450 isoenzymes (Dong et al. 2000).

When APAP is taken in therapeutic doses, NAPQI is conjugated with hepatic glutathione forming APAP-GSH that can be finally excreted *via* urine as cysteine and mercapturic acid conjugates (Bessems and Vermeulen 2001, Hodgman and Garrard 2012, Mazaleuskaya et al. 2015). However, APAP overdoses lead to an excessive formation of NAPQI which causes a depletion of glutathione

stores in the liver. NAPQI can no longer be detoxified and accumulates. Unconjugated NAPQI reacts preferably with sulfhydryl groups generating protein adducts. This causes a loss of liver enzyme activity and alteration of mitochondrial proteins which results in an inhibition of energy production and can finally lead to hepatocellular necrosis (Bessems and Vermeulen 2001, Hodgman and Garrard 2012, Mazaleuskaya et al. 2015). APAP also indirectly leads to liver damage through activation of the innate immune system by damage-associated molecular patterns released from dying hepatocytes and the resulting increased production of inflammatory cytokines (Han et al. 2013, Imaeda et al. 2009).

1.2   N-acetyl-cysteine

N-acetyl-cysteine (NAC) is a derivative of the thiol-containing amino acid, cysteine, with a wide range of medical applications. NAC has a direct antioxidative effect by binding electrophilic groups of free radicals through its thiol side-chain (Pei et al. 2018). NAC has also been shown to have antimicrobial properties through eradication of biofilms (Pérez-Giraldo et al. 1997). Furthermore, NAC exerts anticarcinogenic effects by inducing DNA repair, inhibiting genotoxicity and cell transformation, as well as regulating cell survival and apoptosis (Pei et al. 2018, De Flora et al. 2001). In the clinic, NAC is often used as an expectorant and an antidote for APAP poisoning. Through excessive APAP intake, glutathione stores in the liver are depleted leading to an accumulation of the toxic and active intermediate NAPQI and finally to hepatocellular necrosis. In this case, NAC can serve as a cysteine-donor, which is the rate-limiting amino acid in glutathione biosynthesis. NAC can therefore help to replenish hepatic glutathione stores, hence, ensuring NAPQI detoxification (Bessems and Vermeulen 2001, Hodgman and Garrard 2012, Mazaleuskaya et al. 2015). Patients are usually treated with an initial dose of 150 mg/kg over one hour, a maintenance dose of 50 mg/kg over 4 hours followed by 100 mg/kg of NAC over another 16 hours intravenously (Prescott et al. 1977).

1.3   Paracetamol in pregnancy

Almost every second pregnant woman (47 %) takes analgesic drugs at least once during pregnancy, whereby the majority uses APAP (86 %) (Bremer et al. 2017). It is frequently prescribed by physicians to treat fever and pain in pregnancy as it is considered to be safe for the mother as well as for the unborn child.

However, APAP freely crosses the placental barrier and may therefore have direct effects on the unborn child (Thiele et al. 2015). Although more and more studies describe potential negative effects of APAP on the offspring (Brune, Renner, and Tiegs 2015), so far, there is no reliable data that explain the mechanisms behind the effects of maternal APAP intake on the baby.

An association between maternal APAP application and the reduction of the number of haematopoietic stem cells (HSC) in cord blood has been observed in humans, especially when applied in the third trimester of pregnancy (Bremer et al. 2017). Thiele *et al*. showed that maternal APAP application during pregnancy might correlate with higher rates of abortions, lower birth weights, and preterm birth (Thiele et al. 2013, 2015). Surprisingly, Karimi *et al.* found that pregnant mice were more prone to APAP-induced hepatic injury compared to non-pregnant mice that received the same dose of APAP. This was represented by elevated plasma levels of ALT, AST, and bilirubin as well as increased centrilobular necrosis in pregnant mice treated with APAP (Karimi et al. 2015). Also, a connection between infertility of male offspring and maternal APAP intake in pregnancy has been suggested (David Møbjerg Kristensen et al. 2011, David M. Kristensen et al. 2016, Jensen et al. 2010).

Studies also revealed that maternal APAP intake during pregnancy increases the risk for impaired neuronal development and the onset of attention-deficit and hyperactivity (Hay-Schmidt et al. 2017, Petersen et al. 2018, Liew et al. 2014, Tovo-Rodrigues et al. 2018).

Moreover, several epidemiological studies implicated a correlation between maternal APAP intake during pregnancy and a higher susceptibility for the development of childhood asthma in the offspring (Persky et al. 2008, Rebordosa et al. 2008, Eyers et al. 2011). Furthermore, newborns *in utero* exposed to APAP were more likely to develop wheezing after birth (Rebordosa et al. 2008). A meta-analysis indicated, that especially the treatment with APAP during the first trimester seems to increase the risk of childhood asthma (Cheelo et al. 2015).

In mice, Karimi *et al*. also showed that the offspring prenatally exposed to APAP was more susceptible to the development of allergic airway inflammation after antigen sensitization and challenge. They additionally demonstrated that prenatal exposure to APAP is negatively associated with the frequency of HSC in fetal livers which may be a sign of immune-deviation and therefore potentially causal for overshooting airway inflammation in the offspring (Karimi et al. 2015).

Despite all these findings, the causality of how *in utero* APAP exposition and childhood asthma are associated is still missing. Therefore, the connection between APAP exposition during embryogenesis and the higher susceptibility for the development of asthma later in life still needs to be elucidated. As asthma and allergies are T cell-mediated, the effect of maternal APAP intake during pregnancy especially on HSC development and T lymphopoiesis still needs to be investigated.

1.4 Asthma bronchiale

Asthma bronchiale is a chronic inflammatory disease of the airways which is accompanied by a transient bronchial obstruction as well as hyperreactivity of the bronchial system. The range of symptoms goes from mild physical constraints, such as light cough and sore throat to life-threatening dyspnoea. Over time, mucosal and submucosal tissue remodelling results in airway narrowing (Mims 2015).

The aetiology of asthma bronchiale is not yet fully understood. However, it is known that a variety of cells and cellular components play a crucial role (Tumes et al. 2017). It can be categorized into allergic (extrinsic) and non-allergic (intrinsic) asthma, dependent on the trigger that causes an asthmatic attack.

The majority of allergic asthmatic patients exhibit a type 2 inflammation which is also associated with atopic diseases (Fahy 2015).

Type 2 immune responses are characterized by the occurrence of T helper cells (Th) type 2 which secrete type 2 cytokines, such as interleukin (IL)-4, IL-5, and IL-13. These cytokines induce hyperplasia of mast cells and eosinophil granulocytes as well as the production of immunoglobulin E (IgE) by plasma cells (Holgate 2012).

Furthermore, regulatory T cells (T_{reg}), are the main actors in regulating the immune response mediated by Th2 cells. Reduced T_{reg} activity might be one of the main reasons for an overshooting immune response by type 2 T cells and the pathogenesis of asthma (Zhao and Wang 2018). In mice, it was shown that removal of T_{reg} resulted in more severe airway inflammation and airway hyperreactivity after allergen exposition (Fahy 2015, Zhao and Wang 2018, Lewkowich et al. 2005).

The pathogenesis of asthma bronchiale is very complex because several immunological mechanisms play a role.

As T cells seem to be crucial in airway inflammation, the potential causality between altered T cell development due to prenatal APAP exposition and the development of asthma bronchiale remains to be elucidated.

1.5   Haematopoiesis

Haematopoiesis is a process that ensures the continuous supply of blood cells. All mature blood cells originate from a common multipotent HSC. In mice, HSC are characterized by specific surface markers: they are defined as Lineage- (lin$^-$), CD117$^+$ (c-Kit$^+$), Stem cell antigen$^+$ (Sca-1$^+$), and ST-2$^-$ (Seita and Weissman 2010).

HSC can either develop into the myeloid progenitor cell that can give rise to erythrocytes, thrombocytes, granulocytes, and monocytes, or they adopt the lymphoid fate which further develop into T cells as well as B cells.

In mammals, haematopoiesis already starts during embryogenesis and takes place at different sites.
In mice, primitive haematopoiesis starts on embryonic day (E) 7.5 in the yolk sac (Choi et al. 1998). Primitive haematopoiesis primarily provides haematopoietic cells that are required for oxygenation, such as erythroid progenitors, and cells needed for tissue remodelling and defence from pathogens, such as embryonic macrophages (Gao et al. 2018). A second wave of haematopoiesis starts on E 8.5 in the yolk sac and produces multipotent erythroid, myeloid, and lymphoid progenitors. Nevertheless, a third wave, starting on E 10.5, is necessary that generates HSC *via* a process called endothelial-to-haematopoietic-transition (ETH), which takes place in the aorta-gonad-mesonephros region (AGM) (Gao et al. 2018, Azzoni et al. 2018).

However, the main site of haematopoiesis during embryogenesis is the fetal liver, where HSC proliferate extensively from E 11.5 until E 16.5 (Gao et al. 2018).

While haematopoiesis still takes place in the fetal liver, HSC already seed into the thymus. This process happens in waves: The first wave of HSC migrating into the thymus starts on E 10.5 and the second wave occurs between E 12.5 and E 16.5. In the thymus pro-T cells already undergo positive- as well as negative-selection before they begin to mature into definite T cells (Nowell, Farley, and Blackburn 2007, Solano et al. 2011).

Positive-selection ensures that T cells with a sufficient affinity to major histocompatibility complex (MHC)-molecules, required for antigen recognition, get the signal for further proliferation. On the other hand, T cells binding to self-antigens are negatively selected and die *via* induction of apoptosis. These processes ensure that only self-tolerant T cells with the ability to recognize antigens with sufficient avidity are capable to further differentiate (Kondo, Ohigashi, and Takahama 2019).

From E 15.5 onwards, cells start to seed into the fetal spleen. Meanwhile, HSC activity in the fetal liver decreases. On E 17.5 the spleen has ultimately superseded the fetal liver as site of embryonic haematopoiesis. Simultaneously, the HSC start to migrate into the bone marrow where they are also found postnatally (Gao et al. 2018, Solano et al. 2011) *(Figure 1).*

1.6   T cells

T cells belong to the lymphatic cell lineage and develop from HSC which postnatally derive from the bone marrow. T cells are part of the adaptive immune response and recognize antigens, presented by MHC-molecules of antigen-presenting cells (APC), with their antigen-specific T cell receptor (TCR) (Kumar, Connors, and Farber 2018).

TCR have a high variability in order to be able to recognize a wide range of antigens. This is ensured by the high number of TCR encoding regions in the gene and by somatic rearrangement (Mahe, Pugh, and Kamel-Reid 2018). The TCR is a protein complex consisting of two protein chains bound together *via* disulphide bridges. Four different types of TCR chains exist, α, β, γ and δ proteins, that combine to form a functional TCR. Depending on whether the α and β chains cluster or the γ and δ proteins combine to form the TCR, two subtypes of T cells can be discriminated, the αβ type and the γδ type (Mahe, Pugh, and Kamel-Reid 2018). However, αβ T cells represent the vast majority of T cells (95 %), therefore, the knowledge about T cell recognition mechanisms mainly refers to αβ T cells (Vantourout and Hayday 2013).

TCR chains consist of a variable and a non-variable (constant) region. The N-terminal region of the TCR chain is the variable part (Vα and Vβ) that contributes to the antigen recognition, while the other C-terminal part of the chain is near the membrane and constant (Cα and Cβ). The signal transmission in T cells is not conducted *via* the TCR itself but through invariable membrane proteins, called cluster of differentiation (CD) 3 (CD3ε, CD3γ, and CD3δ). As these chains are identical in all TCR, CD3 serves as a specific surface antigen to define T cells (Mahe, Pugh, and Kamel-Reid 2018, Vantourout and Hayday 2013, Rojo, Bello, and Portolés 2008).

Furthermore, T cells can be discriminated by their surface expression of CD4 and CD8 molecules: CD8-expressing T cells differentiate into cytotoxic cells. They recognize antigens presented by MHC-class-I-molecules. MHC-class-I is expressed on every nucleated cell in the body and presents peptides formed through proteolytic degradation of proteins synthesized by the cell. Therefore, every cell in the body may be a potential target for cytotoxic CD8$^+$ T cells. Antigens recognized are e.g., viral or altered proteins that are produced in tumour cells. Recognition of pathological proteins *via* the TCR induces cell destruction (Mittrücker, Visekruna, and Huber 2014).

CD4-expressing T cells also play a crucial role in adaptive immunity. These cells recognize antigens that are presented *via* MHC-II by APC, such as dendritic cells, B cells, and macrophages. Their primary function is to coordinate the antibody production of B cell-derived plasma cells and to stimulate cytokine production. CD4$^+$ T cells may differentiate into different effector subpopulations, e.g. Th1, Th2, Th17 cells, and T$_{reg}$ (P. Li et al. 2014). The subtypes have different functions, as they stimulate the production of a variety of cytokines, hence activating various other immune cells. Their

differentiation is dependent on the cytokines produced in the inflamed tissue (Romagnani 1994, Cosmi et al. 2014, G. R. Lee 2018).

An additional type of T cell exists: T_{reg} are activated by the immunosuppressive cytokine IL-10 which is secreted by Th2 cells as well as by T_{reg} itself. They produce IL-10 and transforming growth factor (TGF)-β and suppress the activation of the immune system by inactivating a variety of immune cells, including B and T lymphocytes, macrophages, and dendritic cells (Okeke and Uzonna 2019). This facilitates self-tolerance by impeding exaggerated immune reactions provoked by non-pathogenic and self-antigens. This prevents the development of autoimmune diseases and allergies. However, they also play a crucial role in controlling non-autoimmune diseases. T_{reg} require forkhead box p3 (Foxp3) for their differentiation which is induced through antigen-stimulation and co-stimulation (G. R. Lee 2018, Okeke and Uzonna 2019, Kanamori et al. 2016).

1.6.1 T cell development

T cells are named according to the site where they initially differentiate, the thymus.
The thymus consists of thymic epithelial cells (TEC) and is divided into medulla and cortex. The organization into those two compartments is important as the different T cell maturation processes are spatially separated and take place in either of them (van Ewijk, Shores, and Singer 1994).
TEC development relies on the expression of transcription factors, such as forkhead box n1 (Foxn1), GATA binding protein 3 (GATA3), and nuclear factor of activated T cells c1 (NF-AT c1) (Su et al. 2003, Hosoya et al. 2009, Patra et al. 2013). They create a microenvironment that promotes T cell development through receptor activation and cytokine production. For example, IL-7, produced by TEC, is essential for differentiation, survival, and proliferation of immature T cell precursors (Shah and Zúñiga-Pflücker 2014, Puel et al. 1998).
Early thymic progenitors (ETP) originate from the adult bone marrow and seed the thymus. Required for successful T cell development is thymic crosstalk which describes the interaction between ETP and TEC (van Ewijk, Shores, and Singer 1994).

During intrathymic T cell differentiation, T cell precursors progress through different intermediate stages before a mature T cell is generated: ETP, recently migrated from the adult bone marrow, belong to the double negative (DN) thymocytes. These cells are characterized by the absence of CD4 and CD8 expression on their cell surface. DN cells are further divided into four subgroups (DN1-4) distinguished *via* the surface expression of CD44 and CD25 (Shah and Zúñiga-Pflücker 2014). Firstly, T cell precursors progress through the DN1 stage (CD44$^+$, CD25$^-$). DN1 thymocytes are still able to adopt several different cell fates, such as T cells, natural killer (NK) cells, dendritic cells, macrophages, and B cells (Shah and Zúñiga-Pflücker 2014, Porritt et al. 2004). After DN1 cells have

committed to the T cell lineage, CD25 expression is upregulated and DN2 cells are generated (CD44$^+$, CD25$^+$). They mature in the cortex where TCR-β, TCR-γ , and TCR-δ gene segment rearrangement is initiated. Although DN2 cells are likely to become a T cell they still have limited potential to give rise to dendritic cells or NK cells. Only after the transition from DN2 to DN3 (CD44$^-$ CD25$^+$) irreversible commitment to the T cell lineage occurs. At that stage, the pre-TCR-complex has already evolved, and CD3 is already expressed on the cell surface. This facilitates an essential process for further T cell maturation, called β-selection. This crucial step selects T cells that successfully rearranged their TCR-β chain locus and enables only them for further maturation processes (Shah and Zúñiga-Pflücker 2014, Ciofani and Zúñiga-Pflücker 2007, Hosokawa and Rothenberg 2018). In the subscapular region of the thymus, β-selection occurs which finally leads to downregulation of CD25 and subsequently to the formation of DN4 (CD44$^-$, CD25$^-$) thymocytes (Ciofani and Zúñiga-Pflücker 2007, Shah and Zúñiga-Pflücker 2014) *(Figure 1)*.

After T cells passed through the DN stages, CD8 is upregulated and the intermediate state of the immature single positive CD8$^+$ T cell (ISP8) has formed. These cells do not express TCR-β on their surface yet (Gegonne et al. 2018).

CD4 and CD8 upregulation finally results in the development of double positive (DP) T cells. In this state, TCR-α-gene rearrangement is initiated. This is important for the diversity of antigen recognition by TCR. Finally, T cells that have successfully generated an $\alpha\beta$-TCR are positively as well as negatively selected in the cortex and medulla. Only cells that are self-tolerant – on the one hand – and still extreme variable in antigen recognition – on the other, are released for circulation in the periphery (Shah and Zúñiga-Pflücker 2014, Singer, Adoro, and Park 2008).
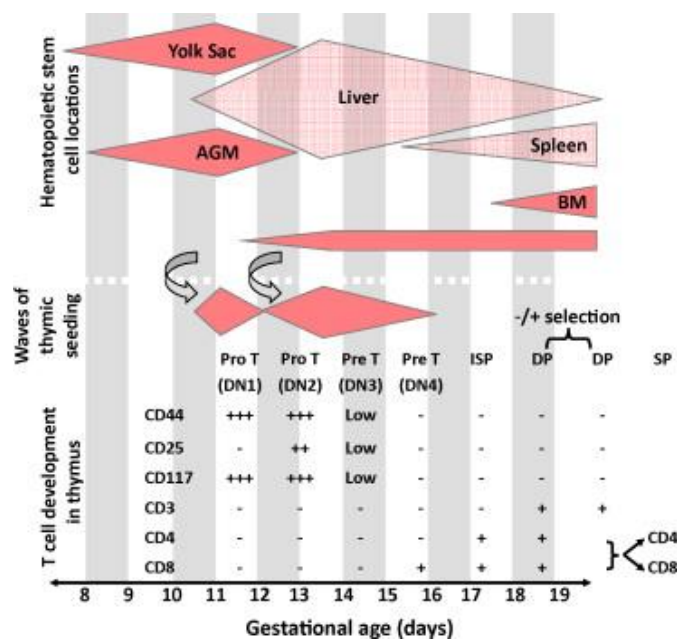
Figure 1: Embryonic development of T cells (Solano et al. 2011).
This figure shows fetal immune cell development in mice. Locations of HSC development are displayed. At the beginning of gestation HSC develop in the yolk sac and the AGM region. From gestational day 10.5 HSC colonize the fetal liver, which becomes the main site of heamatopoiesis during embryogenesis. At the end of gestation, the bone marrow (BM) takes over as site of HSC development. In the BM, HSC are still found postnatally.
While HSC still develop in the fetal liver, they already begin to seed the thymus in waves. This process starts on gestational day 10.5 and ends on gestational day 16.5.
The lower part of the diagram shows that T cells already mature in the fetal thymus where they progress through the distinct double negative (DN) stages 1-4, that neither express CD4 nor CD8. The cells of the different DN stages are differentiated by their expression of CD25 and CD44 (Solano et al. 2011).

1.7 Notch-Signaling

The Notch-signaling pathway is essential for T cell development. The Notch-receptor is expressed by thymocytes and interacts with thymic stromal cells that express Notch-ligands. In mammals, four Notch-receptors are known (Notch 1-4). All four subtypes are heterodimeric receptors that bind to two groups of Notch-ligands, the Delta-like (DLL-1, -3, and -4) family and the Serrate family, in mammals called Jagged (Jag)-1 and Jag-2 (Shah and Zúñiga-Pflücker 2014, Bray 2006). After ligand binding, the intracellular domain of Notch is transported to the nucleus where it binds to downstream factors, such as T cell factor-1 (TCF-1). TCF-1 itself activates T cell-specific transcription factors, including GATA3 and B-cell lymphoma/leukemia 11b (Bcl11b). The absence of TCF-1 and subsequently GATA3 and BCl11b resulted in the inhibition of ETP differentiation, which shows the importance of Notch-dependent activation of TCF-1 for T cell differentiation (Hosoya et al. 2009, Weber et al. 2011). Notch-ligand-interaction leads to suppression of B cell development and myeloid cell differentiation and facilitates T cell development instead (Brandstadter and Maillard 2019). Studies have demonstrated that Notch-1-deficient mice were not able to develop mature

T cells, instead B cells evolved in these thymi (Radtke et al. 1999). Notch-signals regulate the rearrangement of the TCR-β-gene and facilitate CD4$^+$- versus CD8$^+$-T cell fate decision (Zúñiga-Pflücker 2004, Fowlkes and Robey 2002). However, the intensity of Notch-signaling decreases physiologically after the pre-TCR-complex has been formed. For further T cell development, Notch-signaling - to that extent - is not required anymore. DP thymocytes need only weak Notch-signaling, whereas positive- and negative-selection is not dependent on Notch at all (Hosokawa and Rothenberg 2018, Brandstadter and Maillard 2019) *(Figure 2)*.
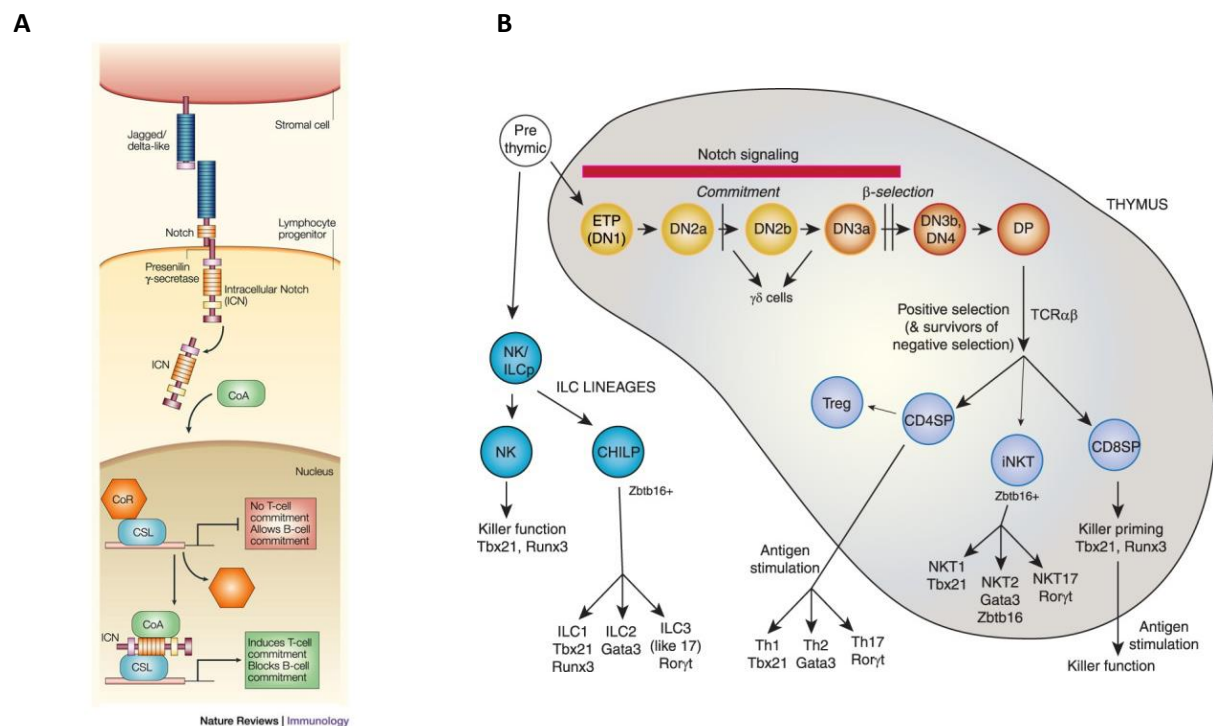
Figure 2: Notch Signaling cascade and Notch-dependent T cell development (Rothenberg 2019).
(A) The Notch signaling pathway is induced by interaction between Jagged or Delta-like-ligand on a stromal cell, e.g., the thymic stromal cell, and the Notch-receptor expressed on HSC or T cells. After binding, presenilin-dependent y-secretase-mediated cleavage of the intracellular domain of Notch (ICN) is activated and ICN is translocated to the nucleus. There it interacts with a Co-activator (CoA, mastermind-family member), which leads to the inhibition of a repressor (CoR) which usually allows B cell commitment instead of T cell commitment. CoA interacts with the DNA-binding protein CSL (CBF1/RBP-Jk) which induces transcription of T cell-specific genes (Artavanis-Tsakonas, Rand, and Lake 1999, Wu et al. 2000, Zúñiga-Pflücker 2004).
(B) shows T cell development schematically. Pre-thymic cells invade the thymus and give rise to early T cell precursors (ETP, DN1). The cells further differentiate Notch-dependently into DN3a cells. At that stage TCR-β gene rearrangement takes place. The transition from DN3a to DN3b and DN4 stages occurs due to β-selection. This developmental step is already Notch-independent. Cells mature into DP cells, where TCR-α gene rearrangement occurs. After positive selection mature T cells have evolved (CD4SP, T$_{reg}$, CD8 SP, or iNKT). γδ T cells already diverge from the αβ T cell development pathway between stage DN2a and DN2b (Rothenberg 2019).

1.8 OP9 cells

OP9 cells are stromal cells that originally derive from bone marrow of OP/OP mice. These mice are deficient of macrophage-stimulating factor (MCSF), therefore inhibit clonal expansion of myeloid cells (Kodama et al. 1994, Ueno et al. 2003, Nakano 1995). Originally, OP9 cells were only used for the investigation of B cell differentiation. T cells were initially not able to develop in cultures with simple OP9 cells, not expressing DLL1 (Zúñiga-Pflücker 2004).

However, the generation of OP9-DLL1 cells by transfecting the cells with the Notch-ligand, DLL-1, led to the loss of the ability to promote B cell development and facilitated T cell development instead. This brought light into the field of *in vitro* T cell studies (Zúñiga-Pflücker 2004, Tsukamoto 2019).

OP9-DLL1 cells support differentiation of CD4$^+$, CD8$^+$, DP, and mature single positive CD8$^+$ (CD8 SP) cells. HSC co-cultured with OP9-DLL1 cells are able to develop into αβ-, as well as, γδ-T cells. As simple OP9 cells express both homologues of the Jagged-ligand but not the Delta-like family and are able to induce B cell development but not T cell development, demonstrates that Delta-like ligands are essential for T cell lymphopoiesis (Zúñiga-Pflücker 2004, Schmitt and Zúñiga-Pflücker 2002). Although OP9-DLL1 cells are commonly used (also in these studies), OP9 cells transfected with DLL4 are also able to induce T cell development, as it has the same sequence identity and properties as DLL1 (Zúñiga-Pflücker 2004, Dorsch et al. 2002).

2 Materials and Methods

2.1 Materials

2.1.1 Technical equipment

Table 1: equipment

Equipment	Supplier
ATILON ATL-423-I	Acculab Sartorius group, Göttingen
Centrifuge 5417R	Eppendorf, Hamburg
Centrifuge 5810 R	Eppendorf, Hamburg
BD FACSAria™Fusion Flow Cytometer	Becton Dickinson, Heidelberg
BD FACSAria™Illu Flow Cytometer	Becton Dickinson, Heidelberg
BD LSRFortessa™ Cell Analyzer	Becton Dickinson, Heidelberg
Cobas Integra® 400 plus	Roche, Basel CH
Eppendorf Research® Plus Pipettes	Eppendorf, Hamburg
Eppendorf ThermoMixer® 5436	Eppendorf, Hamburg
G3013 Comfort	Liebherr, Biberach an der Riss
Handy Step® electronic	BRAND GmbH, Wertheim
Hera cell 240	Thermo Fisher Scientific, Waltham, USA
Hera Safe	Heraeus, Hanau
Integra Pipetboy2	Integra, Biebertal
MDF U53V Ultra low freezer	Sanyo, München
Mr. Frosty® cryo-container	Fisher Scientific, Waltham, USA
MSC Advantag, Clean Bench	Thermo Fisher Scientific, Hamburg
Microscope CK40	Olympus, Hamburg
Neubauer Improved	Chamber Roth, Karlsruhe
quadroMACS separation unit	Miltenyi Biotec, Bergisch Gladbach
Constant displacement pump	Medorex e.K., Nörten-Hardenberg
Vortex Mixer	Heidolph, Schwabach

2.1.2 Consumables

Table 2: consumables

Consumable	Supplier
Abgene PCR tubes	Abgene, Thermo Fisher Scientific, Hamburg
Cell culture flask	Sarstedt, Nümbrecht
Cell culture plates, flat (24-well, 48-well)	Sarstedt, Nümbrecht
Dispenser-tips PD-Tips II	BRAND GmbH, Wertheim
FALCON tubes	
Hollow needles / canulaes	B. Braun, Melsungen AG, Melsungen
MACS pre-separation filters	Myltenyi Biotec, Bergisch Gladbach
MACS separation colums (LD, LS, MS)	Myltenyi Biotec, Bergisch Gladbach
Nylon meshes (40 µm)	BD Falcon, Heidelberg
Parafilm M	American National Can. USA
Pipette tips (10 µl, 200 µl, 1000 µl)	Sarstedt, Nümbrecht
Reaction tubes (1,5 ml, 2 ml)	Sarstedt, Nümbrecht
Reaction tubes (15 ml, 50 ml)	Sarstedt, Nümbrecht
Syringe	B. Braun, Melsungen AG, Melsungen
Tubes for flow cytometer	Sarstedt, Nümbrecht

2.1.3 Reagents and Kits

Table 3: reagents and kits

Reagents and Kits	Supplier
Acetaminophen	Sigma Aldrich, Taufkirchen
ALT reagents	Roche, Basel CH
AST reagents	Roche, Basel CH
Anti-APC MicroBeads (lyophilized)	Miltenyi Biotec, Bergisch Gladbach
Bovine serum albumin (BSA)	Serva, Heidelberg
Brefeldin A (BFA)	Sigma-Aldrich, Taufkirchen
Calcium chloride ($CaCl_2$)	Merck, Whitehouse Station, USA
D-glucose	Roth, Karlsruhe
Dimethylsulfoxid (DMSO)	Roth, Karlsruhe
di-sodiumhydrogenphosphatlydrate (Na_2HPO_4)	Roth, Karslruhe
EDTA	Roth, Karlsruhe
Ethanol	Roth, Karlsruhe
Fetal calf serum (FCS)	Lonza, Cologne
GBSS	Sigma-Aldrich, Taufkirchen
L-Glutamine	Gibco® Invitrogen, Darmstadt
Magnesium chloride hexahydrate (MgCl)	Roth, Karlsruhe
Magnesium sulfate hexahydrate ($MgSO_4$)	Roth, Karlsruhe
Methanol	Roth, Karlsruhe
MEM alpha Medium	Gibco® Invitrogen, Darmstadt
Mouse Flt3-Ligand	Miltenyi Biotec, Bergisch Gladbach
Mouse IL-7	Miltenyi Biotec, Bergisch Gladbach
Mouse SCF	Miltenyi Biotec, Bergisch Gladbach
N-acetylcysteine	Hexal, Holzkirchen
Paraformaldehyd	Roth, Karlsruhe
Penicillin/ streptomycin (100 U/ ml)	Gibco® Invitrogen, Darmstadt
Potassium chloride (KCl)	Roth, Karlsruhe
Potassium dihydrogen phosphate (KH_2PO_4)	Roth, Karlsruhe
RPMI	Gibco® Invitrogen, Darmstadt
Sodium azide (NaN_3)	Roth, Karlsruhe
Sodium chloride (NaCl)	AppliChem, Darmstadt
Sodium hydrogencarbonate ($NaHCO_3$)	Roth, Karlsruhe
Sodium hydroxide (NaOH)	Roth, Karlsruhe
Trypan Blue	Sigma-Aldrich, Taufkirchen

2.1.4 Buffers and Solutions

Table 4: buffers and solutions

Buffer or solution	Recipe
HBSS	5.4 mM KCl
	0.3 mM Na_2HPO_4 x 7 H_2O
	4.2 mM $NaHCO_3$
	1.3 mM $CaCl_2$
	0.5 mM $MgCl_2$ x 6 H_2O
	0.6 mM $MgSO_4$ x 7 H_2O
	137 mM NaCl
	5.6 mM D-glucose
	pH 7.4

PBS	137.9 mM NaCl 6.5 mM Na_2HPO_4 x 2 H_2O 1.5 mM KH_2PO_4 2.7 mM KCl pH 7.4
MACS buffer	PBS 0.5% BSA 2 mM EDTA
FACS buffer	PBS 1% BSA 15.4 mM NaN_3 (0.1 %)
4% Paraformaldehyd (pH 7,4)	8 g Paraformaldehyd 20 ml PBS$^-$ (10x) 10 mM NaOH ad 200 ml ddH_2O
OP9 medium (500 ml)	375 ml H_2O 5 g MEMalpha powder 14.65 ml $NaHCO_3$ 5 ml pen/ strep 5 ml L-Glutamine 1000 ml FCS
Freezing medium 1	90% FBS 10% DMSO
Freezing medium 2	50% RPMI 40% FBS 10% DMSO

2.1.5 Software

Table 5: software

Software	Company
BD FACS Diva	BD Biosciences, Heidelberg
FlowJo™10	BD Biosciences, Heidelberg
GraphPad Prism 6	GraphPad Software, San Diego, USA
MacBook Air	Apple, Cupertino, USA
MS Office 2019	Microsoft, Redmond
Windows XP	Microsoft, Redmond

2.2 Methods

2.2.1 Animals

All experiments which involved mice were registered and implemented in compliance with the German Animal Protection Law. For this study, female C57Bl/6J and male BALB/c mice, purchased from Charles River Laboratories (Sulzfeld, Germany), were used.

Mice were delivered to the UKE animal facility two weeks before the start of experiments to allow for adaptation to the new environment. Mice were maintained in individually ventilated cages (IVC) at 20 °C ± 2 °C, humidity of 55 %, 12-hour day /night rhythm with autoclaved chow and water *ad libitum*. The animals received human care according to the criteria outlined in the "Guide for the Care and Use of Laboratory Animals" prepared by the US Academy of Sciences and published by the National Institutes of Health and legal requirements in Germany.

2.2.2 Mating

Female wild-type C57Bl/6J mice at the age of 6 to 10 weeks and male wild-type BALB/c mice were allogeneically mated. Two female mice were put into a cage with one male mouse overnight. An existing vaginal plug the next morning was the criteria for successful mating. This day was considered as E 0.5. To confirm pregnancy, weight control of dams was performed on E 7.5 and E 10.5.

2.2.3 Treatment

On E 11.5 mice were transferred to a new cage and food was withdrawn overnight in order to equalize glutathione levels. On E 12.5 mice were treated. APAP solution was prepared by dissolving 20 mg/ml APAP powder in sterile Dulbecco's phosphate buffered saline (DPBS, Gibco, Life Technologies GmbH, Darmstadt, Germany). Mice were injected intraperitoneally (i.p.) with 250 mg/ kg body weight APAP or 250 mg/ kg body weight APAP and additional 1200 mg/ kg body weight NAC. The control group was treated with 12.5 ml/ g body weight phosphate buffered saline (PBS), which resulted in an injection volume of 250 ml, approximately.

2.2.4 Analysis of plasma transaminase levels

On E 13.5 APAP-induced liver damage was assessed by measuring plasma levels of the liver specific ALT using the COBAS Integra 400 plus system (Roche Diagnostic, Mannheim, Germany). For that purpose, mice were anaesthetized with CO_2/O_2 and retrobulbar blood was taken. Blood samples were centrifuged for 1 minute at 4 °C at 1000 x g in order to obtain the plasma for the measurement.

2.2.5 Tissue sampling

On E 14.5 pregnant mice were anaesthetized by CO_2/O_2 and sacrificed by cervical dislocation. After opening the abdomen and peritoneum, cardiac blood was taken by punctuation of the heart. The livers of the dams were removed. The quadrate lobe was stored in 4 % paraformaldehyde-solution (PFA) for histology. The uterus was removed from the abdomen and numbers of implantations and abortions were documented. Fetuses were separated from the embryonic membrane and weighed. For purification of fetal liver HSC, fetal livers were collected and stored at 6 °C in Hanks balanced salt solution (HBSS) until further processing.

2.2.5.1 Isolation of HSC from fetal livers

Freshly harvested fetal livers per dam were pooled. The fetal liver tissues were passed through a 40 µl cell strainer in 10 ml of OP9 medium and centrifuged for 5 minutes at 4 °C at 500 x g. Cells were then resuspended in 4 ml of OP9 medium and counted *(Cell counting and viability)*. After washing the cells with MACS buffer and centrifugation for 5 minutes at 4 °C at 500 x g, they were prepared for lineage negative magnetic cell separation (MACS) according to the manufacture´s protocol (Miltenyi Biotec, Bergisch Gladbach, Germany).

The purpose of MACS-sorting was to deplete lineage positive cells, including, T cells, B cells, monocytes, macrophages, granulocytes, erythrocytes, as well as their precursors. Lineage positive cells were labelled with an APC conjugated antibody mix (Miltenyi Biotec, Bergisch Gladbach, Germany) *(Table 6)*. After 10 minutes of incubation at 4 °C and a washing step with MACS buffer, anti-APC microbeads that bind to APC linked cells, were added to the cells. Magnetic columns were prepared according to the manufacture´s protocol. Prepared cells were put on the magnetic columns and the microbead-labelled cells (lineage positive) were retained by the magnetic column, so lineage negative cells were enriched in the solution. Lineage negative cells were then washed with MACS buffer and centrifuged for 5 minutes at 4 °C at 500 x g, resuspended in PBS and counted.

Table 6: list of antibodies used for MACS

name	host	clone	conjugate	dilution	supplier
APC Mouse Lineage Antibody Cocktail (T cells, B cells, monocytes/ macrophages, granulocytes, NK cells, erythrocytes)	mouse	n.a.	APC	1:10	BioLegend (San Diego, USA)

In order to test for ideal experimental conditions, three independent experiments were performed using slightly different protocols *(Figure 3)*. However, the steps until the MACS separation were the same. In the following the differences between the three experiments after MACS are displayed:

- Experimental set up one (ES1): Prior to the final HSC purification step by fluorescence-activated cell sorting (FACS), lineage depleted fetal liver cells were frozen and stored in liquid nitrogen for one week *(Freezing and thawing of cells)*. Cells were then thawed and prepared for FACS sorting *(Figure 3)*.
- Experimental set up two - three (ES2 - ES3): Lineage depleted cells by MACS were not frozen and directly prepared for further HSC enrichment *via* FACS *(Figure 3)*.

To further purify the HSC, they were prepared for FACS *(Flow cytometric sort)*. Cells were stained using the antibodies with their corresponding dilutions, listed below *(Table 7)*. Finally, cells were washed with PBS, centrifuged for 5 minutes at 4 °C at 500 x g and resuspended in 500 µl of OP9 medium. Sca-1$^+$, c-Kit$^+$ HSC were sorted and collected in cold OP9 medium. Cells were counted and prepared for co-culture.

Figure 3: Experimental set up ES1-ES3.
This figure shows the differences between the three experimental set ups. Mice were mated and treated with APAP, APAP+NAC or PBS on E 12.5. On E 14.5 dams were sacrificed and fetal liver cells were isolated. In ES1 fetal liver HSC were frozen prior to final HSC purification *via* fluorescence-activated cell sorting. In ES2 and ES3 cells were directly sorted. Then, purified fetal liver HSC were co-cultured with OP9-DLL1 cells on either 24- (ES1, ES2) or on 48-well plates (ES3) and reanalysed.

2.2.6 Freezing and thawing of cells

For ES1 lineage depleted fetal liver cells were prepared for freezing. Two freezing mediums were used *(Table 4)*. Isolated fetal liver cells of one dam were diluted in a total volume of 1 ml. First, cells were resuspended in 500 µl of freezing medium one (90 % RPMI + 10 % FBS) and then mixed with 500 µl of freezing medium two (50 % RPMI + 40 % FBS + 10 % DMSO) *(Table 4)* in a 1:1 ratio. Vials with fetal liver cells in freezing medium were slowly cooled down using a pre-cooled (6°C) cryo container (Thermo Scientific® Mr. Frosty, Fisher Scientific, Waltham, USA) which was stored in -80 °C for one day before cells were put into liquid nitrogen for one week.

After one week of cryo-preservation cells were put into a water bath (37 °C) until cells were thawed. They were then washed with warm OP9 medium and prepared for final HSC sort *via* FACS *(Flow cytometric sort)*.

2.2.7 Flow Cytometry

Flow cytometry is a common method to analyze different cell types through identification of cell specific expression of extra-, as well as intracellular molecules. Cells flow in a fluidic stream where they pass several lasers. These lasers activate fluorochromes linked to antibodies that bind to intra- and extracellular molecules of the cells. The intensity of fluorescence correlates with the marker expression (Givan 2011).

2.2.7.1 Flow cytometric sort

To isolate fetal liver HSC (lineage$^-$, ST-2$^-$, c-kit$^+$, Sca-1$^+$) from fetal liver tissues, cells were flow cytometrically sorted (cells were gated for lymphocytes, single, cells, living cells, lineage$^-$, ST-2$^-$, c-Kit$^+$, Sca-1$^+$). Staining was performed at 4 °C for 30 minutes in PBS. Fetal livers cells were stained applying a standard protocol, including blocking of Fc receptors using an anti-CD16/32 antibody in a 1:100 dilution and a total volume of 100 µl FACS buffer. The monoclonal antibodies and the corresponding dilutions used for fetal liver HSC isolation are listed in *(Table 7)*. After a final washing step with PBS and centrifugation for 5 minutes at 4 °C at 500 x g, cells were diluted in 500 µl of OP9 medium. Cell sorting was performed using the FACS Aria Fusion and the FACS Aria Illu (BD Biosciences, Heidelberg, Germany) provided by the core unit of the University Medical Center Hamburg-Eppendorf, Germany. Data were recorded and evaluated using BDFACSDiva™ software and FlowJo™10 (both BD Biosciences, Heidelberg, Germany).

Table 7: list of antibodies for flow cytometric sort of fetal liver HSC

name	host	clone	conjugate	dilution	supplier
anti-mouse c-Kit	rat	2B8	APC	1:100	BioLegend (San Diego, USA)
FITC anti-mouse Lineage cocktail (T cells, B cells, monocytes/ macrophages, granulocytes, NK cells, erythrocytes)	hamster	n.a.	FITC	1:500	BioLegend (San Diego, USA)
anti-mouse Sca-1	rat	D7	PE	1:100	BioLegend (San Diego, USA)
anti-mouse ST-2	rat	RMST2-2	PE-Cy7	1:100	Invitrogen (San Diego, USA)
viability dye: eflour 506	n.a.	n.a.	Amcyan	1:1000	eBiosciences (San Diego, USA)

n.a.= not applicable

2.2.7.2 Preparation for flow cytometric analysis in co-culture with OP9 cells

To investigate T cell development in the co-culture system with OP9-DLL1 cells, cells were reanalyzed *via* FACS on different days of co-culture (***Co-culture system of OP9 cells and fetal liver HSC***).

In general, staining was performed at 4 °C for 30 minutes with FACS buffer. 1×10^6 HSC of fetal livers were stained applying a standard protocol, including blocking of Fc receptors using an anti-CD16/32 antibody in a 1:100 dilution and a total volume of 100 µl FACS buffer. The monoclonal antibodies and the corresponding dilutions used are listed in *(Table 8)*. After a final washing step with FACS buffer and centrifugation for 5 minutes at 4 °C at 500 x g, cells were resuspended in 250 µl of FACS buffer and then analyzed.

On d0 of co-culture 10×10^3 of the FACS sorted fetal liver HSC were prepared for FACS and stained with the T cell panel (antibodies and their corresponding dilutions listed in ***Table 8***).

On the other reanalysis days (d4, d7, d11, 14, d18) cells were removed from the plates, washed and finally stained as described above. The antibodies and the corresponding dilutions are displayed in *(Table 8)*. The cells were then analyzed *via* flow cytometry using a LSRFortessa (BD Biosciences, Heidelberg, Germany) kindly provided by the core facility of the University Medical Center Hamburg-Eppendorf, Germany. Data were recorded and evaluated using BDFACSDiva™ software (BD Biosciences, Heidelberg, Germany) and FlowJo™10 (both BD Biosciences, Heidelberg, Germany).

Table 8: list of antibodies used for flow cytometric analysis of T cells

name	host	clone	conjugate	dilution	supplier
anti-mouse c-Kit	rat	2B8	APC	1:50	BioLegend (San Diego, USA)
anti-mouse Sca-1	rat	D7	PE	1:50	BioLegend (San Diego, USA)
anti-mouse TCRβ	hamster	H57-597	FITC	1:50	BioLegend (San Diego, USA)
anti-mouse TCRγδ	hamster	GL3	PerCP/Cy5.5	1:50	BioLegend (San Diego, USA)
anti-mouse CD4	rat	RM4-5	BV650	1:50	BioLegend (San Diego, USA)
anti-mouse CD5	rat	53-7.3	BV605	1:250	BD Horizon (New Jersey, USA)
anti-mouse CD8a	rat	53-6.7	BV785	1:50	BioLegend (San Diego, USA)
anti-mouse CD25	rat	PC61	BV421	1:50	BioLegend (San Diego, USA)
anti-mouse CD28	mouse	E18	PE-Cy7	1:100	BioLegend (San Diego, USA)
anti-mouse CD44	rat	IM7	V500	1:50	BD Pharmingen (San Jose, USA)

| anti-mouse CD69 | hamster | H1.2F3 | AF-700 | 1:50 | BioLegend (San Diego, USA) |
| viability dye: Zombi NIR | n.a. | n.a. | APC-Cy7 | 1:1000 | BioLegend (San Diego, USA) |

n.a.= not applicable

2.2.8 Cell culture

2.2.8.1 Cultivation of OP9 cells

To investigate T cell development *in vitro*, isolated fetal liver HSCs were co-cultured with DLL1-expressing OP9 cells, that create a thymus-like environment.

The OP9 cells, either transfected with a vector including DLL1 (OP9-DLL1) or an empty vector (OP9-LIE), were kindly provided by Prof. Eva Tolosa (UKE, Hamburg, Germany). OP9 cells were cultured in OP9 medium *(Table 4)* under sterile conditions in a CO_2 / O_2 incubator with 5 % CO_2 and 40 % O_2 at 37 °C. OP9-cells were passaged before they reached a confluency of 80 %. For passaging, the supernatant was removed from the cell flask and the adherent cells were dissociated using Trypsin / EDTA solution. Cells from passage 9 to 23 were used.

2.2.8.2 Co-culture system of OP9 cells and fetal liver HSC

To identify ideal conditions for the cells to proliferate and survive in the co-culture system, 24- or 48-well plates were coated with $6x10^3$ to $10x10^3$ OP9-DLL1 or OP9-LIE cells in 250 µl (48-well plate) or 500 µl (24-well plate) of OP9 medium per well *(Table 4)*. The cells were given 1 to 3 days to adhere to the plates.

After fetal liver HSC were sorted, cells were added to 24- (ES1, ES2) or 48- (ES3) well-plates coated with OP9-DLL1 cells or OP9-LIE cells: The supernatant from the OP9-coated 24- or 48-well plates was removed. Then, $5x10^3$ sorted fetal liver HSC in 250 µl (48-well plate) or 500 µl (24-well plate) of OP9 medium, containing IL-7 (10 ng/ml), SCF (10 ng/ml), Flt3-L (5 ng/ml), were plated per well and incubated for 11 (ES1), 7 (ES2) or 18 (ES3) days (see below) under sterile conditions in a CO_2 / O_2 incubator with 5 % CO_2 and 40 % O_2 at 37 °C.

In order to flow cytometrically analyze *(Preparation for flow cytometric analysis in co-culture with OP9 cells)* the developing HSC at different time points, cells were removed from the co-culture, pooled and approximately $5-10x10^3$ developing fetal liver HSC were sampled at d4, d7, d11, d14, d18, depending on the experiment (see below). The remaining fetal liver HSC, that were not used for flow cytometric analysis, were resuspended in OP9 medium *(Table 4)*, supplemented with IL-7 (10 ng/ ml), SCF (10 ng/ ml), Flt3-L (5 ng/ ml), and distributed to a freshly coated 24- (ES1, ES2) or 48- (ES3) well plate. In ES1 and ES3, the expanding HSC were split (1:2) when seeded on a new plate, from d7 onwards.

- <u>ES1:</u> Purified fetal liver HSCs were co-cultured with OP9 cells in 24-well plates over 11 days *(Figure 3)*.
- <u>ES2:</u> Purified fetal liver HSCs were co-cultured with OP9 cells in 24-well plates over 7 days *(Figure 3)*.
- <u>ES3:</u> Purified fetal liver HSCs were co-cultured with OP9 cells in 48-well plates over 18 days *(Figure 3)*.

2.2.9 Cell counting and viability

Cell counting was performed using a Neubauer counting cell chamber. All 4 major squares with its altogether 64 squares were counted. The following formula was used to calculate the cell number per milliliter.

$$\frac{\text{Cell counts x dilution factor x 104 (chamber constant)}}{\text{Number of major squares}} = \frac{\text{cells}}{\text{ml}}$$

2.2.10 Haematoxylin/ eosin staining of liver sections

To analyze the architecture of liver tissue histologically, livers were fixed in 4 % PFA. Subsequently, fixed livers were embedded in paraffin and hepatic sections of 3 µm thickness were stained with Haematoxylin / eosin using a standard protocol. The stained liver sections were then analyzed by light microscopy (Olympus, Hamburg, Germany).

2.2.11 Statistical analysis

The results of this study were analyzed using GraphPad Prism6. If two groups were compared Student´s t test was applied. The comparison of more than two groups was performed using ANOVA. All data in this study are expressed as a mean of $\pm$ SEM. A p value of 0.05 was considered to be significant with the following ranges *p $\leq$ 0.05, **p $\leq$ 0.01, ***p $\leq$ 0,001, ****p $\leq$ 0.0001.

3 Results

3.1 Effects of APAP administration on liver functions of pregnant mice

Acute liver damage leads to the release of liver enzymes such as ALT and AST into the blood. The extent of liver damage can be identified by determining plasma ALT activity. In healthy mice, ALT levels range from 15 U/L to 85 U/L (Otto et al. 2016). For the purpose of these experiments, liver damage was defined as ALT > 150 U/L. On E 12.5 pregnant mice were treated with 250 mg/kg body weight APAP (n = 15), a combination of 1200 mg/kg body weight NAC and 250 mg/kg body weight APAP (n = 4), or PBS as the control treatment (n = 15). Blood samples were taken 24 h after treatment and plasma ALT levels were measured *(Figure 4A)*. Pregnant mice exposed to APAP had significantly increased plasma ALT levels compared to the group injected with APAP+NAC and the control group, treated with PBS. APAP-treated dams had average ALT levels of 596 U/L, whereas animals belonging to the PBS group had mean ALT levels of 15 U/L. APAP+NAC exposed mice had normal ALT levels of average 50 U/L. On E 14.5, 48 h after treatment, pregnant mice were sacrificed, liver tissue was collected, imbedded in paraffin, and sections were stained with H&E *(Figure 4B-D)*. Extensive necrotic areas were observed in liver sections of APAP-treated mice but not in livers of mice in the two other treatment groups. Histological observations are in line with the liver damage that was represented by elevated plasma ALT levels after APAP treatment.
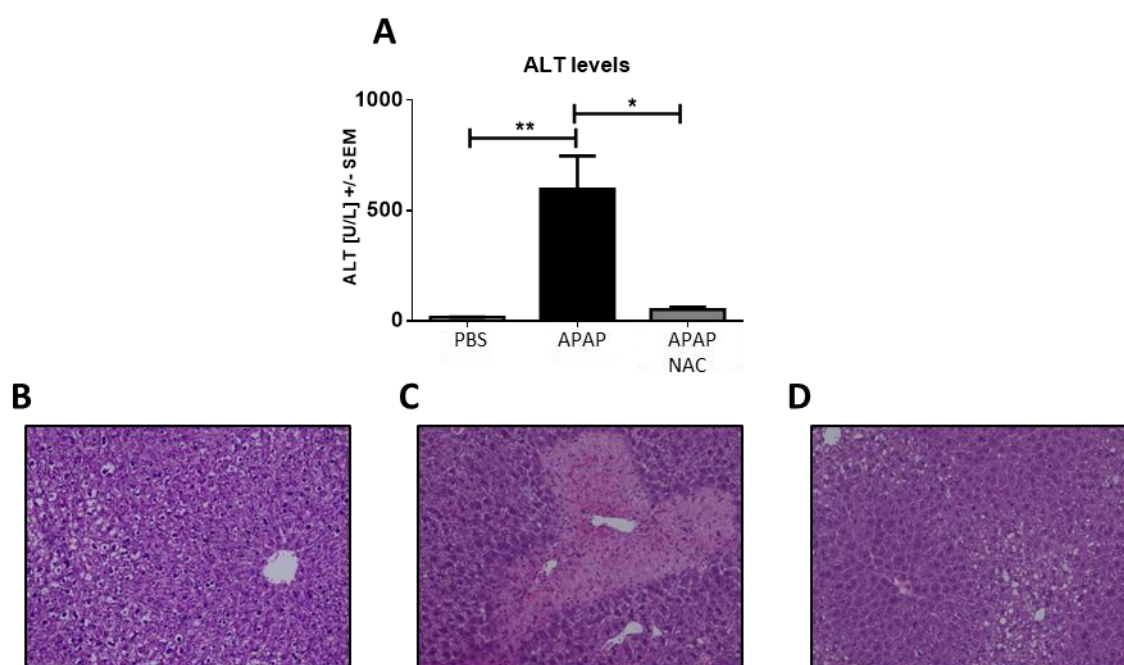
Figure 4: ALT levels and liver damage in APAP-, PBS- and APAP+NAC treated-dams.
Pregnant mice were treated on E 12.5 with 250 mg/kg APAP (n = 15), PBS (n = 15), or APAP+1200 mg/kg NAC (n = 4) i.p. One day after treatment plasma ALT levels were measured to detect liver damage (A). Paraffin-embedded liver sections of dams sacrificed on E 14.5 were stained with H&E for histological analysis. Representative liver sections of a PBS-treated mouse (B) and an APAP-treated mouse with liver damage (C) and liver tissue of APAP+NAC-treated mouse (D) are shown. *P ≤ 0.05, **P ≤ 0.01**.**

3.2   Pregnancy outcome after prenatal exposure to 250 mg/kg APAP

To analyze the effect of APAP treatment and the potential protective effect of additional NAC treatment on pregnancy outcome, litter sizes, number of miscarriages, average fetal weight, and maternal weight development throughout pregnancy were recorded *(Figure 5A-D)*.

When pregnant mice were sacrificed on E 14.5 litter sizes in all three treatment groups were similar. APAP treated mice (n = 15) had on average 7.8 fetuses, APAP+NAC treated animals (n = 4) 8 fetuses, and the control group, treated with PBS (n = 15), 8.4 fetuses *(Figure 5A)*. Additionally, the number of miscarriages per pregnant mouse was not influenced by APAP challenge *(Figure 5B)*. Dams in all three groups had less than one miscarriage per mother on average (APAP: 0.6 miscarriages, PBS: 0.3 miscarriages, APAP+NAC: 0 miscarriages).

Analysis of pregnancy outcome upon APAP treatment showed that there was no significant difference in fetal weight between the three treatment groups *(Figure 5C)*. On E 14.5 fetuses of mothers exposed to APAP (n = 15) had an average weight of 246 mg. Fetuses in the group that was additionally treated with NAC (n = 4) weighed on average 224 mg and offspring of the control group (n = 15) exhibited a mean weight of 263 mg.

Maternal weights were assessed on E 0.5 and E 14.5 and weight gains were calculated *(Figure 5D)*. In general, APAP exposed mice (n = 15) gained slightly less weight over the course of pregnancy, within the two days of APAP exposure than animals that were injected with either APAP+NAC (n = 4) or PBS (n = 15). APAP-treated mice had an average weight gain of 7.7 g. This was significantly lower than the average weight that was gained in the PBS group, which was 9.3 g. Dams treated with APAP and additional NAC had a 9.8 g higher weight on E 14.5 than on E 0.5 *(Figure 5D)* which was not significantly different to dams treated either with PBS or APAP alone. Overall, besides a slight reduction in weight gain during pregnancy, it seemed that prenatal APAP exposition did not influence pregnancy outcome (litter sizes, number of miscarriages, fetal weights) compared to the other treatment groups.
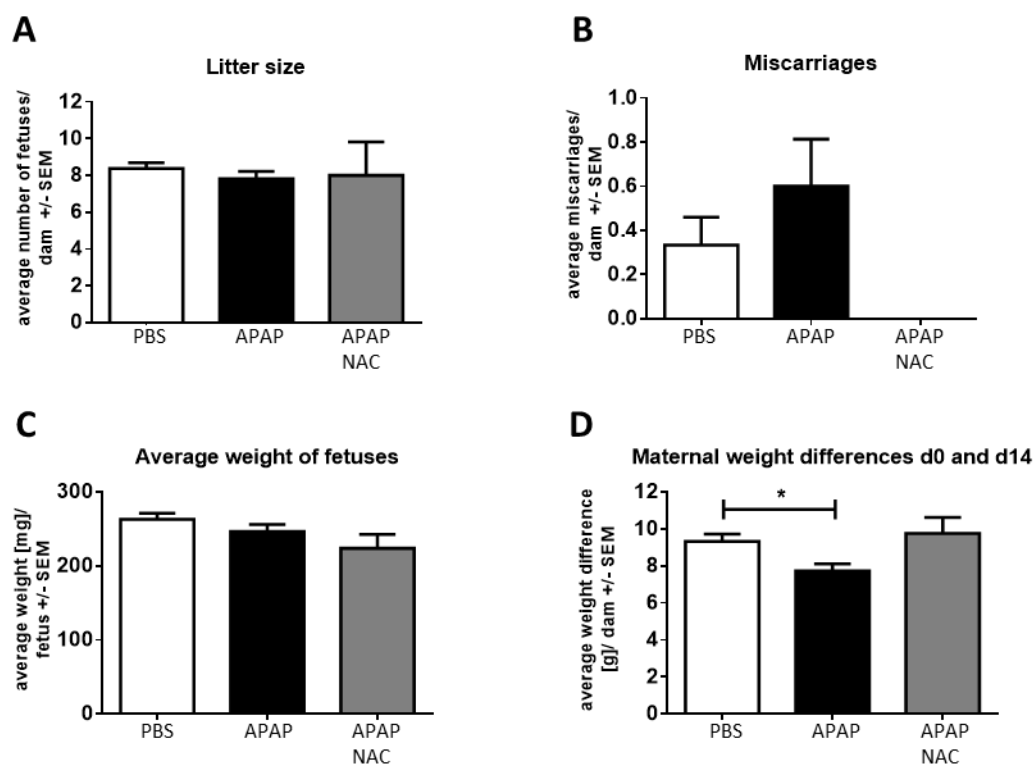
Figure 5: Effect of APAP and APAP+NAC treatment on pregnancy outcome.
Pregnant mice were treated on E 12.5 with 250 mg/kg APAP (n = 15), PBS (n = 15), or 250 mg/kg APAP+1200 mg/kg NAC (n = 4) i.p. On E 14.5, the day of tissue sampling and preparation of fetuses, litter sizes (A), and numbers of miscarriages per dam (B) were investigated. Fetuses were weighed (C) and maternal weight differences between the beginning of pregnancy, E 0.5, and the day of tissue sampling, E 14.5, were determined (D). *P ≤ 0.05.

3.3   Numbers of fetal liver HSC in response to APAP challenge

All hematopoietic and immune cells derive from HSC. During embryogenesis, the main source of HSC is the fetal liver, where hematopoiesis takes place before the bone marrow takes over (Seita and Weissman 2010, Gao et al. 2018).

Before fetal liver HSC were co-cultured with OP9-DLL1 or OP9-LIE cells, fetal liver HSC had to be purified. Fetal liver HSC (c-Kit$^+$, Sca-1$^+$) were isolated *via* MACS and subsequent FACS. In order to identify the optimal conditions for *ex vivo* T cell differentiation in the OP9 co-culture system, three slightly different experimental setups (ES) were used (for details see: ***Materials and Methods***). In short, in ES1 MACS sorted fetal liver cells were frozen and stored at -80 °C for one week prior to the final FACS sort and subsequent co-culture with OP9-DLL1 cells. In ES2 and ES3 MACS and FACS sort were performed on the same day prior to co-culture. For ES1 and ES2 co-culture was performed in 24-well plates, while in ES3 48-well plates were used.

To assess the initial effect of APAP on fetal liver HSC the number of cells that could be isolated from APAP-treated and control-treated fetal livers were compared (***Figure 6A-C***).
In all three independent experiments (ES1-ES3) the number of HSC extracted from the fetal livers were slightly lower when dams were treated with APAP. In ES1 the average cell number of HSC in

the PBS group (n = 7) was 6162 and in the APAP group (n = 7) 5896 HSC per fetal liver which was not significantly different *(Figure 6A)*. In ES2 cells were processed on the same day the dams were sacrificed and then incubated with OP9 cells in 24-well plates *(Figure 6B)*. Here, three treatment groups were compared, APAP (n = 4), APAP+NAC (n = 4), and PBS (n = 4). We observed that the average number of sorted fetal liver HSC of fetuses prenatally exposed to APAP was slightly lower than in offspring whose mothers were injected with PBS or APAP+NAC (APAP: 4210 HSC/fetal liver;   PBS: 6336 HSC/fetal liver   APAP+NAC: 6417 HSC/fetal liver). However, this difference was not significant. ES3 showed a similar HSC-reducing effect of APAP, which was also not significant. In ES3 on average 7604 fetal liver HSC could be isolated from APAP-exposed fetal livers (n = 4), which was less than in the PBS group (n = 4; 10266 HSC) *(Figure 6C)*.
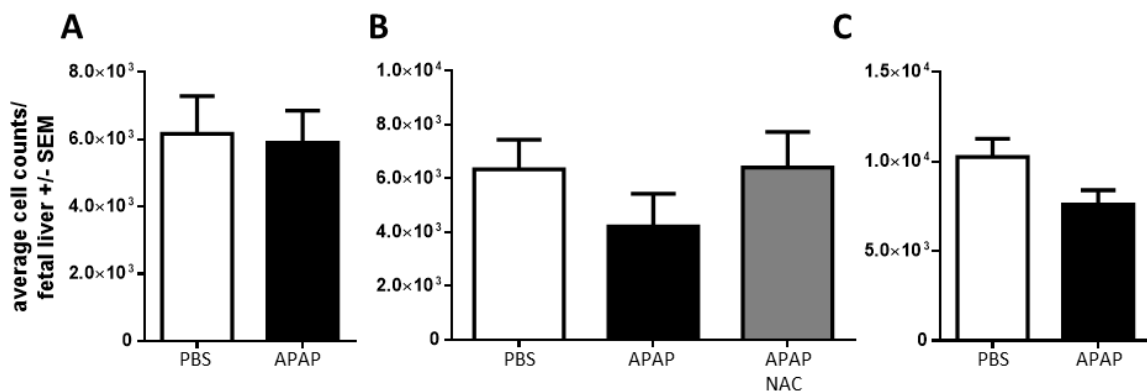
Figure 6: Frequencies of HSC in fetal livers upon maternal APAP administration with and without additional NAC.
After isolation of fetal liver HSC (c-Kit$^+$, Sca-1$^+$) on E 14.5, average HSC numbers per fetal liver were calculated. (A), (B) and (C) show HSC numbers of three different experiments. In (A) fetal liver cells were frozen prior to fluorescence-activated cell sorting. Pregnant mice in (A) and (C) were treated with either 250 mg/kg APAP (A: n = 7; C: n = 4), or PBS (A: n = 7; C: n = 4) i.p. In (B), a third group of pregnant mice was treated with a combination of 250 mg/kg APAP+1200 mg/kg NAC i.p. (n = 4 in all treatment groups). *P $\leq$ 0.05.

3.4   Impact of prenatal APAP exposure on stem cell characteristics of fetal liver cells during co-cultivation with OP9-DLL1 cells

On d0, before the isolated fetal liver HSC were co-cultured with OP9-DLL1 cells, the status quo was determined *via* flow cytometry. To evaluate the purity of HSC after FACS sort, the surface expression of c-Kit and Sca-1 was analyzed. To investigate how c-Kit and Sca-1 expression changes over time in co-culture with OP9-DLL1 cells, developing cells were reanalyzed throughout co-culture *(Figure 7, 8, 9)*.

In ES1 (frozen cells, 24-well plates) it was shown that on d0 of co-culture with OP9-DLL1 cells, almost all of the detected cells were c-Kit$^+$, Sca-1$^+$ and were therefore defined as HSC (PBS: 91.78 %; APAP: 93.07 %) *(Figure 7)*. Over time the frequency of c-Kit$^+$ and Sca-1$^+$ cells decreased significantly when compared to d0. After 4 days of co-culture, only a quarter of the cells expressed both c-Kit and Sca-1 on their surfaces (PBS: 23.24 %; APAP: 24.32 %). After 7 and 11

days in co-culture, almost no c-Kit$^+$, Sca-1$^+$ HSC could be detected (d7: PBS: 1.94 %; APAP: 1.47 %; d11: PBS: 0.79 %; APAP: 1.47 %). The decrease in the expression of stem cell markers is in line with the onset of differentiation. However, no difference in HSC frequency was seen between the two treatment groups, APAP and PBS.

Figure 7: Frequencies of HSC isolated from cryo-preserved fetal liver cells and co-cultured with OP9-DLL1 cells in 24-well plate.
On E 12.5 pregnant mice were treated with 250 mg/kg APAP (n = 7) or PBS (n = 7) i.p. On E 14.5 dams were sacrificed, fetuses collected, and fetal liver cells cryo-preserved prior to HSC (lin$^-$, c-Kit$^+$, Sca-1$^+$) isolation *via* fluorescence-activated cell sorting. HSC were co-cultured with OP9-DLL1 cells over 11 days in 24-well plates. Cells were analyzed by flow cytometry on d0, d4, d7, and d11 for the expression of c-Kit and Sca-1. The plotted significant stars refer to differences compared d0 of the respective treatment group. ****P ≤ 0.0001.

In ES2 fetal liver cells were not frozen before HSC purification *via* flow cytometric sort *(Figure 8)*. It was shown, that on d0 almost all cells expressed both c-Kit and Sca-1 (PBS 95.58 %; APAP: 92.98 %; APAP+NAC: 96.34 %). On d4 the frequency of c-Kit and Sca-1-expressing cells started to decrease (PBS: 36.5 %; APAP: 46.1 %; APAP+NAC: 42.08 %) until almost none of the co-cultured cells expressed both c-Kit and Sca-1 on d7 (PBS: 7.96 %; APAP: 9.71 %; APAP+NAC: 7.56 %). These differences in c-Kit$^+$ and Sca-1$^+$ cell frequencies were significant on d4 as well as on d7 when compared to d0. Therefore, it appeared that the isolated fetal liver HSC lost their c-Kit and Sca-1 surface expression during co-culture with OP9-DLL1 cells.

Figure 8: Frequencies of HSC isolated from fetal liver cells and co-cultured with OP9-DLL1 cells in 24-well plate.
On E 12.5 pregnant mice were treated with 250 mg/kg APAP (n = 4), PBS (n = 4), or 250 mg/kg APAP+1200 mg/kg NAC (n = 4) i.p. On E 14.5 dams were sacrificed, fetuses were collected and fetal liver HSC (lin$^-$, c-Kit$^+$, Sca-1$^+$) were isolated *via* fluorescence-activated cell sorting. HSC were co-cultured with OP9-DLL1 cells over 7 days in 24-well plates. Cells were analyzed by flow cytometry on d0, d4, and d7 for the expression of c-Kit and Sca-1. The plotted significant stars refer to differences compared to d0 of the respective treatment group. ****P ≤ 0.0001.

ES3 was performed in 48-well plates. Due to profound cell proliferation, cell numbers were higher, and more time points for reanalysis were considered. Similarly, to ES1 and ES2 described above, here HSC also appeared to differentiate as c-Kit and Sca-1 expression was downregulated over time *(Figure 9)*. Before co-culture (d0), nearly all of the purified HSC were c-Kit[+] and Sca-1^{+} (PBS: 93.75 %; APAP: 93.2 %). As HSC were incubated and co-cultured with DLL1-expressing OP9 cells, frequencies of cells that expressed both c-Kit and Sca-1 decreased. On d4 less than half of the HSC were still c-Kit[+] and Sca-1^{+} (PBS: 36.1 %; APAP: 40.3 %). On d7 of co-culture c-Kit[+] and Sca-1^{+} cell frequencies decreased further (PBS: 11.02 %; APAP: 8.76 %). When the co-cultured cells were reanalyzed on d11, frequencies of c-Kit- and Sca-1-expressing cells increased slightly compared to d7 (PBS: 18.18 %; APAP: 19.33 %). However, this effect was temporary. From d14 of co-culture onwards, around a tenth of all living cells could be defined as HSC on average (d14: PBS: 7.85 %; APAP: 10.77; d18: PBS: 12.08 %; APAP: 9.98 %). The decrease of HSC frequencies on each day of reanalysis was significant compared to the day before the start of the co-culture with OP9-DLL1 cells (d0). However, no significant difference was observed between APAP- and PBS-exposed cells.

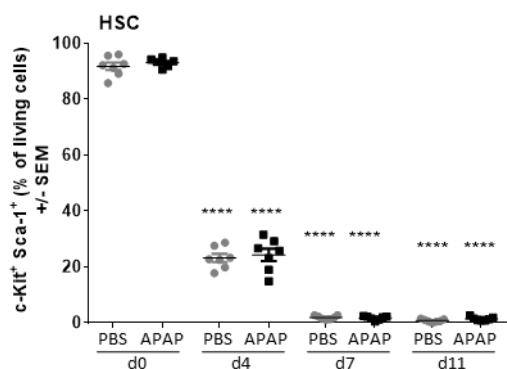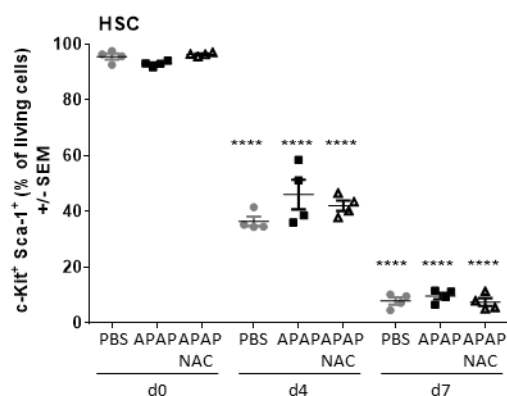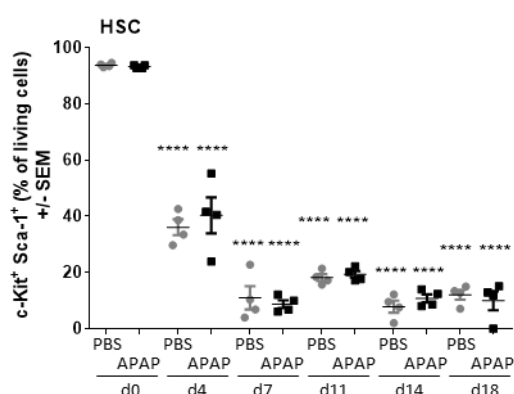**Figure 9: Frequencies of HSC isolated from fetal liver cells and co-cultured with OP9-DLL1 cells in 48-well plate.**
On E 12.5pregnant mice were treated with 250 mg/kg APAP (n = 4) or PBS (n = 4) i.p. On E 14.5 dams were sacrificed, fetuses were collected and fetal liver HSC (lin[-], c-Kit[+], Sca-1^{+}) were isolated *via* fluorescence-activated cell sorting. HSC were co-cultured with OP9-DLL1 cells over 18 days in 48-well plates. Cells were analyzed by flow cytometry on d0, d4, d7, d11, d14, and d18 of co-culture for the expression of c-Kit and Sca-1. The plotted significant stars refer to d0 of the respective treatment group. ****$P \leq 0.0001$.

3.5 Effects of prenatal APAP exposure on frequencies of CD4 and CD8 double negative cell kinetics during co-culture with OP9-DLL1 cells

When HSC give rise to T cells, they progress through different maturation stages. Developing T cells neither express CD4 nor CD8 at the beginning of differentiation and are referred to as double negative (DN) cells (Shah and Zúñiga-Pflücker 2014). During co-culture in ES1 (frozen cells, 24-well plates), the frequency of cells neither expressing CD4 nor CD8 initially increased from d0 to d4 (d0: PBS: 62.07 %; APAP: 61.51 %; d4: PBS: 74.51 %; APAP: 75.17 %) but then decreased slightly from d7 to d11 (d7: PBS: 73.79 %; APAP: 75.31 %; d11: PBS: 54.27 %; APAP: 50.07 %) *(Figure 10)*. However, these changes were not significant compared to d0 for any of the time points analyzed. Moreover, no differences between APAP-exposed and PBS-exposed cells were observed.

Figure 10: Frequencies of CD4 and CD8 double negative cells in co-culture of HSC isolated from cryo-preserved fetal liver cells with OP9-DLL1 cells in 24-well plate.
On E 12.5 pregnant mice were treated with 250 mg/kg APAP (n = 7) or PBS (n = 7) i.p. On E 14.5 dams were sacrificed and fetuses collected. Fetal liver cells were cryopreserved prior to HSC (lin⁻, c-Kit⁺, Sca-1⁺) isolation *via* fluorescence-activated cell sorting. HSC were co-cultured with OP9-DLL1 cells over 11 days in 24-well plates. Cells were analyzed by flow cytometry on d0, d4, d7, and d11 for the expression of CD4 and CD8.

In ES2 (fresh cells, 24-well plates), the frequencies of DN cells decreased throughout co-culture. At the beginning (d0), most of the cells neither expressed CD4 nor CD8 (PBS: 96.95 %; APAP: 94 %; APAP+NAC: 97.48 %) *(Figure 11)*. On d4 a significant decline in DN cells in the APAP-treated group (82.2 %) was detected compared to cells that were prenatally exposed to PBS (90.33 %) or APAP+NAC (91.4 %). Additionally, cell frequencies were significantly lower in comparison to d0 in the PBS-and APAP-treated group. Moreover, on d7 frequencies of DN cells decreased further (PBS: 84.45 %; APAP: 84.43 %; APAP+NAC: 88.38 %), so that frequencies of APAP- and PBS-exposed cells were again significantly lower than on d0. Nonetheless, at that time point, no significant differences between the treatment groups were observed.

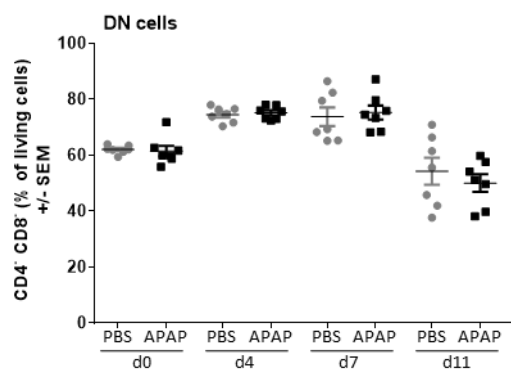**Figure 11: Frequencies of CD4 and CD8 double negative cells in co-culture of fetal liver HSC with OP9-DLL1 cells in 24-well plate.**
On E 12.5 pregnant mice were treated with 250 mg/kg APAP (n = 4), PBS (n = 4), or 250 mg/kg APAP+1200 mg/kg NAC (n = 4) i.p. On E 14.5 fetuses were collected and fetal liver HSC (lin⁻, c-Kit⁺, Sca-1⁺) were isolated *via* fluorescence-activated cell sorting. HSC were co-cultured with OP9-DLL1 cells over 7 days in 24-well plates. Cells were analyzed by flow cytometry on d0, d4, and d7 regarding the expression of CD4 and CD8. The plotted significant stars refer to d0 of the respective treatment group. *P ≤ 0.05, **P ≤ 0.01, ***P ≤ 0,001, ****P ≤ 0.0001.

In ES3 (fresh cells, 48-well plates) frequencies of DN cells declined throughout the co-culture *(Figure 12)*. However, this happened at later time points compared to the other two experiments (ES1, ES2) described above *(Figure 10, 11)*. From d0 to d7, there were high frequencies of DN cells. In both treatment groups, almost all of the cells belonged to the DN state (d0: PBS: 94.88 %; APAP: 93.2 %; d4: PBS: 90.88 %; APAP: 92.25 %; d7: PBS: 85.08 %; APAP: 88.1 %). Only from d11, frequencies of DN cells started to decline continuously (d11: PBS: 57 %; APAP: 58.88 %; d14: PBS: 61.1 %; APAP: 48.88 %; d18: PBS: 50 %; APAP: 26.33 %). Frequencies of PBS-exposed cells were already significantly lower on d11 compared to d0. On d14, significantly fewer APAP-exposed cells belonged to the DN stage compared to d0 and on d18 both treatment groups

had significantly lower DN cell frequencies compared to d0. The decline in DN frequencies over time was similar in both treatment groups, therefore, no significant differences were observed.
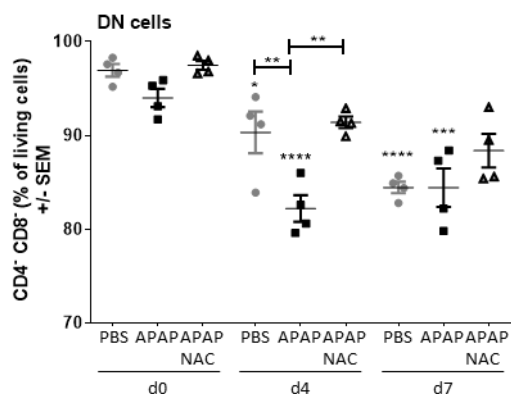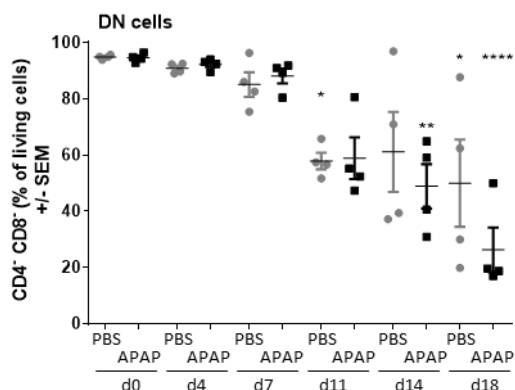

Figure 12: Frequencies of CD4 and CD8 double negative cells in co-culture of fetal liver HSC with OP9-DLL1 cells in 48-well plate.
On E 12.5 pregnant mice were treated with 250 mg/kg APAP (n = 4) or PBS (n = 4) i.p. Fetuses were collected on E 14.5 and fetal liver HSC (lin⁻, c-Kit⁺, Sca-1⁺) were isolated *via* fluorescence-activated cell sorting. HSC were co-cultured with OP9-DLL-1 cells over 18 days in 48-well plates. Cells were analyzed by flow cytometry on d0, d4, d7, d11, d14, d18 regarding the expression of CD4 and CD8. The plotted significant stars refer to d0 of the respective treatment group. *P ≤ 0.05, **P ≤ 0.01, ****P ≤ 0.0001.

3.6 Effects of prenatal APAP exposure on DN stages (DN1-DN4) of T cell maturation in the OP9-DLL1 co-culture system

During T cell maturation, cells undergo four different DN cell stages that can be distinguished *via* the expression of CD25 and CD44. The DN1stage is characterized by the expression of CD44 and the absence of CD25 expression (CD44⁺, CD25⁻) (Shah and Zúñiga-Pflücker 2014, Porritt et al. 2004).

In ES1 (frozen cells, 24-well plates) almost all of the DN cells belonged to the DN1 stage prior to co-culture (d0; PBS: 93.21 %; APAP: 94.98 %) *(Figure 13A-B)*. Over time, the frequency decreased slowly (d4: PBS: 90.14 %; APAP: 89.77 %; d7: PBS: 88.56 %; APAP: 89.59 %) until this decline in frequency of DN1 cells was significant on d11 (PBS: 35.4 %; APAP: 45.03 %) compared to d0 of co-culture. At that time point, there were significantly lower DN1 cell frequencies in the PBS-treated group than in the APAP-treated group.

DN2 cells are characterized as CD25⁺ and CD44⁺ DN cells (Shah and Zúñiga-Pflücker 2014, Ciofani and Zúñiga-Pflücker 2007, Hosokawa and Rothenberg 2018). On d0 of reanalysis, almost none of the DN cells belonged to the DN2 stage (PBS: 0.8 %; APAP: 0.53 %) *(Figure 13C-D)*. On d4, frequencies of DN2 cells peaked (PBS: 4.35 %; APAP: 4.93 %), before starting to decline again from d7 to d11. (d7: PBS: 2.39 %; APAP: 2.21 %; d11: PBS: 1.28 %; APAP: 1.46 %). The rise of DN2 frequencies was significant on d4 compared to d0 indicating an ongoing maturation process of both PBS- as well as APAP-exposed cells.

DN3 cells can be identified by the expression of CD25 but an absence of CD44 expression (Shah and Zúñiga-Pflücker 2014, Ciofani and Zúñiga-Pflücker 2007, Hosokawa and Rothenberg 2018). At the beginning of co-culture no DN3 cells could be detected *(Figure 13E-F)*. The frequencies of DN3 cells started to increase slightly on d4 until averagely 3-4 % of DN cells belonged to the DN3 stage on d11 (d0: PBS: 0 %; APAP: 0 %; d4: PBS: 0.89 %; APAP: 0.72 %; d7: PBS: 1.81 %; APAP:

2.1 %). On d11 (PBS: 3.04 %; APAP: 4.06 %) a significant increase in cell frequencies in both groups was observed compared to d0.

DN4 cells neither express CD25 nor CD44 (Shah and Zúñiga-Pflücker 2014, Ciofani and Zúñiga-Pflücker 2007, Hosokawa and Rothenberg 2018). At the beginning of co-culture, almost none of DN cells belonged to the DN4 stage (d0: PBS: 4 %; APAP: 3.13 %; d4: PBS: 3.35 %; APAP: 3.18 %; d7: PBS: 5.9 %; APAP: 4.86 %) *(Figure 13G-H)*. This remained the case until the frequency of DN4 cells increased significantly in both treatment groups on d11 (PBS: 51.8 %; APAP: 43.7 %). In direct comparison, the frequency of DN4 cells remained significantly lower when cells were prenatally exposed to APAP compared to cells exposed to PBS (d14).
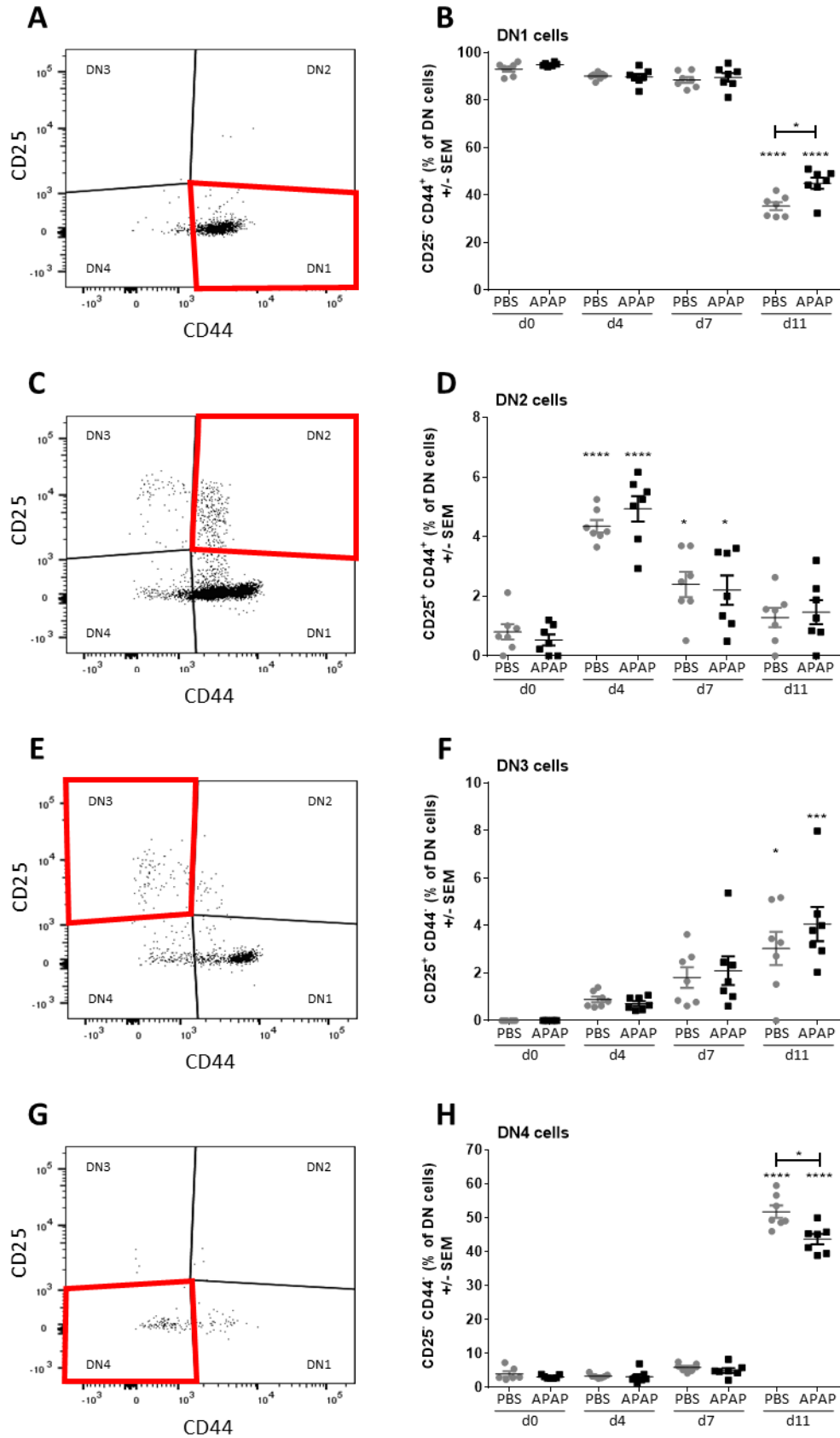
Figure 13: Frequencies of distinct double negative stages in co-culture of HSC isolated from cryo-preserved fetal liver cells with OP9-DLL1 cells in 24-well plate.
Pregnant mice were treated with 250 mg/kg APAP (n = 7) or PBS (n = 7) i.p. On E 14.5 fetuses were collected. Fetal liver cells were cryo-preserved prior to HSC (lin$^-$, c-Kit$^+$, Sca-1$^+$) isolation *via* fluorescence-activated cell sorting. HSC were co-cultured with OP9-DLL1 cells. Cells were analyzed by flow cytometry for the expression of CD4, CD8, CD25, and CD44. Representative dot plots showing the four stages of double negative (DN; CD4$^-$CD8$^-$) cells, DN1, DN2, DN3, and DN4 on d0 (A), d4 (C), d7 (E), d11 (G). Frequencies of DN1 (B), DN2 (D), DN3 (F), and DN4 (H) in co-culture. The plotted significant stars refer to d0 of the respective treatment group. *P ≤ 0.05, ***P ≤ 0,001, ****P ≤ 0.0001.

In ES2 (fresh cell, 24-well plates), frequencies of DN1 cells (CD44$^+$, CD25$^-$) were almost 100 % on d0 (PBS: 99.63 %; APAP: 99.66 %; APAP+NAC: 99.8 %) and d4 *(Figure 14A)*. However, at d4 of reanalysis, significantly lower cell frequencies were detected in the DN1 stage when HSC were prenatally exposed to APAP (88.18 %) in comparison to PBS- (99.63 %) or APAP+NAC-exposed cells (99.8 %). The trend of declining DN1 cell frequencies continued on d7. At this time point, the decrease in cell frequencies was significant compared to d0 in all three groups. Nevertheless, this decline was more pronounced in the APAP group (87.4 %) compared to the two other treatment groups (PBS: 91.2 %; APAP+NAC: 93.68 %). This difference was significant when APAP-exposed cells were compared to cells from the APAP+NAC-treated group but not in comparison to the PBS group.

Before cells were co-cultured with OP9-DLL1 cells (d0), none of the fetal liver HSC expressed both CD25 and CD44, therefore no DN2 cells could be detected (PBS: 0.06 %; APAP: 0.06 %; APAP+NAC: 0.07 %) *(Figure 14B)*. This changed as cells were exposed to DLL1 in the co-culture system. On d4, frequencies of DN2 cells increased in all three groups (PBS: 4.78 %; APAP: 8.13 %; APAP+NAC: 3.44 %). When frequencies of d4 were compared to d0 in the APAP and PBS group, the increase was significant. Interestingly, the frequencies were significantly higher in the APAP group compared to the other treatment groups. On d7, DN2 frequencies declined again, as cells appeared to have adopted a more mature stage (PBS: 2.91 %; APAP: 2.64 %; APAP+NAC: 2.04 %) such as DN3.

In the DN3 stage developing T cells neither express CD25 nor CD44 (Shah and Zúñiga-Pflücker 2014, Ciofani and Zúñiga-Pflücker 2007, Hosokawa and Rothenberg 2018). In ES2, frequencies of DN3 cells started to rise at d4 of co-culture (d0: PBS: 0 %; APAP: 0 %; APAP+NAC: 0 %) *(Figure 14C)*. Here, it seemed that APAP-exposed cells had a higher frequency of DN3 cells than the cells of the other two groups (PBS: 0.55 %; APAP: 1.02 %; APAP+NAC: 0.11 %). However, this difference was not significant. On d7 of reanalysis, the frequencies of DN3 cells declined again, this was similar in all three treatment groups (PBS: 0.6 %; APAP: 0.92 %; APAP+NAC: 0.35 %), therefore no significant differences between the groups were detected.

Additionally, frequencies of CD25$^-$, CD44$^-$ DN4 cells were low on d0 (PBS: 0.3 %; APAP: 0.24 %; APAP+NAC: 0.15 %) *(Figure 14D)*. Frequencies increased on d4 (PBS: 2.37 %; APAP: 2.67 %; APAP+NAC: 1.76 %) until they reached their maximum on d7 of co-culture (PBS: 5.28 %; APAP: 9.04 %; APAP+NAC: 3.93 %). On d7, significantly more cells in the APAP group (9.04 %) belonged to the DN4 stage in comparison to the other two remaining treatment groups, PBS and APAP+NAC (PBS: 5.28 %; APAP+NAC: 3.93 %). Moreover, on d7 significantly higher frequencies of APAP- and PBS- but not the APAP+NAC- exposed cells belonged to the DN4 stage compared to d0.

Considering, the results in this experiment, where cells were not frozen prior to flow cytometric sort and HSC were co-cultured with OP9-DLL1 cells in 24-well plates, it seemed that fetal liver cells

prenatally exposed to APAP progressed faster through the DN stages than cells that were treated with PBS or APAP+NAC.

These findings additionally showed that NAC reversed the effect of APAP on the developing HSC.

Figure 14: Frequencies of distinct double negative stages in co-culture of fetal liver HSC with OP9-DLL1 cells in 24-well plate.
On E 12.5 pregnant mice were treated with 250 mg/kg APAP (n = 4), PBS (n = 4), or 250 mg/kg APAP+1200 mg/kg NAC (n = 4) i.p. On E 14.5 dams were sacrificed and fetal liver HSC (lin⁻, c-Kit⁺, Sca-1⁺) were isolated *via* fluorescence-activated cell sorting. HSC were co-cultured with OP9-DLL1 cells over 7 days in 24-well plates. Cells were analyzed by flow cytometry on d0, d4, and d7 regarding the expression of CD4, CD8, CD25, and CD44. Frequencies of the four stages of double negative (DN; CD4⁻CD8⁻) cells, DN1 (CD44⁺ CD25⁻) (A), DN2 (CD44⁺ CD25⁺) (B), DN3 (CD44⁻ CD25⁺) (C), and DN4 (CD44⁻ CD25⁻) (D) throughout co-culture. The plotted significant stars refer to d0 of the respective treatment group. *P ≤ 0.05, ***P ≤ 0,001, ****P ≤ 0.0001.

In ES3 (fresh cells, 48-well plates), fetal liver HSC also progressed through the distinct DN stages, DN1 to DN4.

In the beginning, HSC mainly belonged to the DN1 stage (CD44+, CD25-) *(Figure 15A)*. D0 to d7 almost all of the cells were DN1 cells (d0: PBS: 93.93 %; APAP: 92.7 %; d4: PBS: 93.2 %; APAP: 93.45 %; d7: PBS: 94.85 %; APAP: 96 %). From d11 of co-culture, frequencies of DN1 cells started to decline continuously (d11: PBS: 85.7 %; APAP: 84.38 %; d14: PBS: 52.95 %; APAP: 68.22 %) until on d18 averagely less than 20 % of DN cells were in the DN1 stage (PBS: 14.7 %; APAP: 15.14 %). This decrease was significant on d14 and d18 in both treatment groups, APAP and PBS, compared to d0. Nevertheless, no significant differences were observed between APAP- and PBS-treated cells. Compared to ES1 and ES2, it seemed that the onset of

maturation of DN cells was delayed, as frequencies of DN1 cells only began to decrease on d14 of co-culture with OP9-DLL1 cells.

Before co-culture (d0), almost none of the isolated fetal liver cells were DN2 cells (PBS: 0.05 %; APAP: 0.1 %) *(Figure 15B)*. On d4 frequencies increased slightly in both groups (PBS: 3.33 %; APAP: 2.83 %), before DN2 cell frequencies declined again on d7 in both treatment groups (PBS: 1.45 %; APAP: 1.12 %). However, this development was temporary. On d11 more cells belonged to the DN2 state (d11: PBS: 4.14 %; APAP: 5.65 %: d14: PBS: 3.93 %; APAP: 3.3 %). On d18 of reanalysis the maximum of DN2 cells was reached (PBS: 10.03 %; APAP: 7.82 %). Here, the frequency of DN2 cell frequency was significantly higher compared to d0. Interestingly, both treatment groups were similarly affected by DLL1-exposition, so no significant differences were observed between APAP-and PBS-treated cells at any time point.

Fetal liver HSC gave rise to DN3 cells from d11 onwards *(Figure 15C)*. At earlier reanalysis time points almost no DN3 cells were detected (d0: PBS: 0 %; APAP: 0 %; d4: PBS: 0.39 %; APAP: 0.28 %; d7: PBS: 1.02 %; APAP: 0.63 %; d11: PBS: 4.33 %; APAP: 2.94 %; d14: PBS: 30.02 %; APAP: 16.26 %). After 14 days in the co-culture system, the frequency of DN3 cells in the PBS-treated group was significantly higher compared to d0. On d18 the peak of DN3 cells was reached in both treatment groups (PBS: 57.85 %; APAP: 37.4 %), which was significantly higher compared to d0 in the APAP group as well as in the PBS group.

Finally, fetal liver HSC gave rise to DN4 cells *(Figure 15D)*. Until d11 of co-culture almost none of the developing cells were DN4 cells (d0: PBS: 0.6 %; APAP: 0.59 %; d4: PBS: 1.9 %; APAP: 1.8 %; d7: PBS: 1.64 %; APAP: 0.93 %; d11: PBS: 3.47 %; APAP: 3.66 %). On d11 frequencies started to rise until the maximum was reached on d18 (d14: PBS: 8.57 %; APAP: 7.71 %; d18: PBS: 15.65 %; APAP: 38.5 %). At this point of reanalysis, the frequency of DN4 cells in the APAP group was significantly higher than on d0. The development regarding the DN4 state was very similar in both treatment groups and apparently not influenced by the substances the cells were prenatally exposed to.
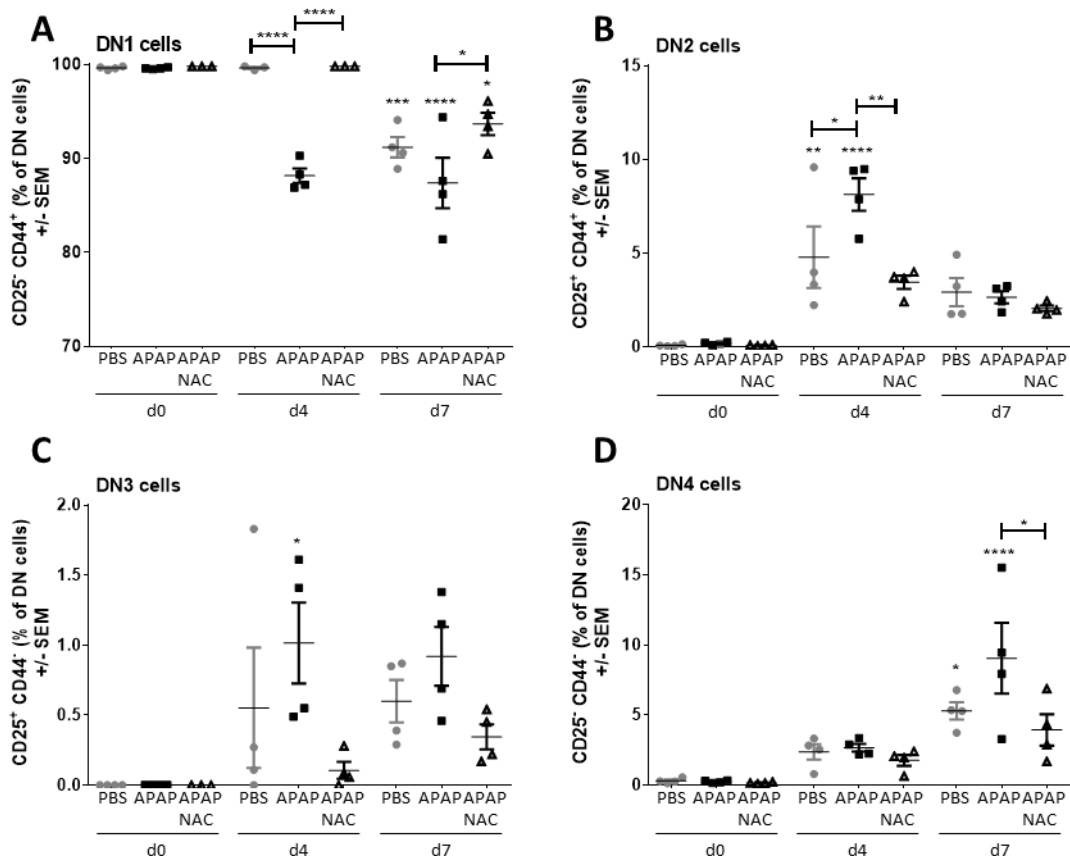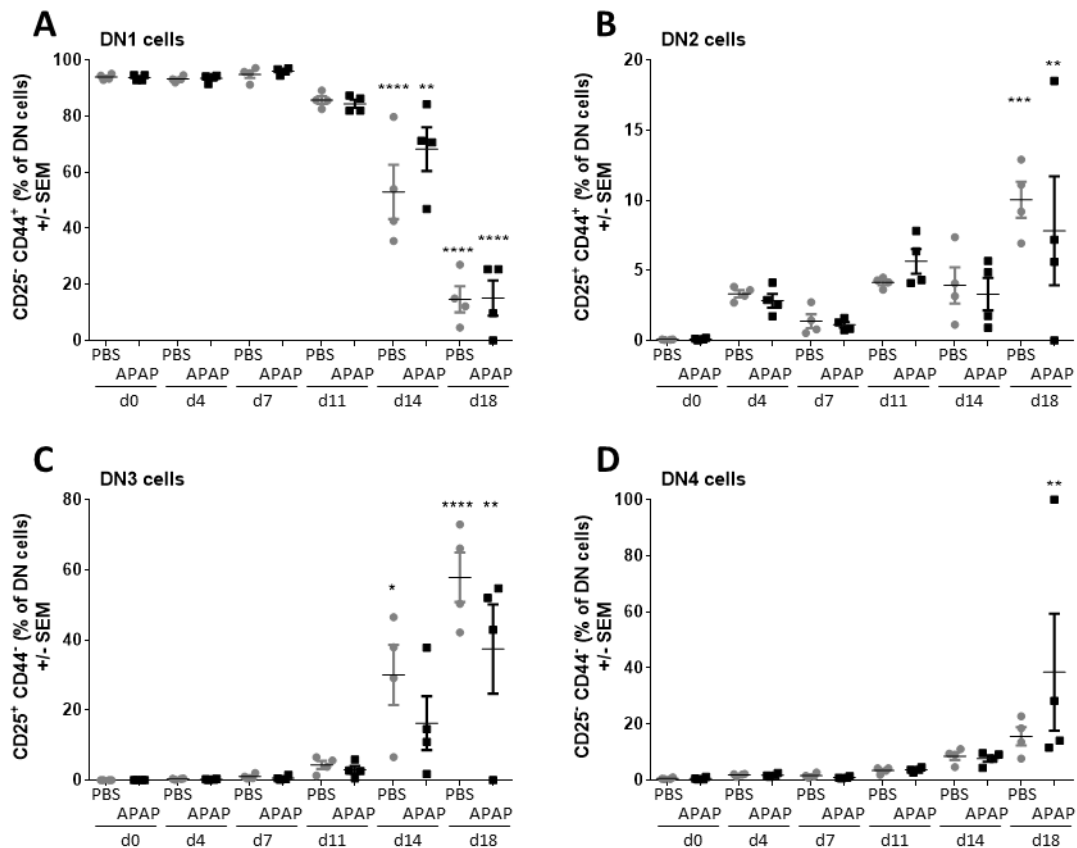
Figure 15: Frequencies of distinct double negative stages in co-culture of fetal liver HSC with OP9-DLL1 cells in 48-well plate.
On E 12.5 pregnant mice were treated with 250 mg/kg APAP (n = 4) or PBS (n = 4) i.p. On E 14.5 dams were sacrificed and fetal liver HSC (lin⁻, c-Kit⁺, Sca-1⁺) were isolated *via* fluorescence-activated cell sorting. HSC were co-cultured with OP9-DLL1 cells over 18 days in 48-well plates. Cells were analyzed by flow cytometry on d0, d4, d7, d11, d14, and d18 regarding the expression of CD4, CD8, CD25, and CD44. Frequencies of the four stages of double negative (DN; CD4⁻ CD8⁻) cells, DN1 (CD44⁺ CD25⁻) (A), DN2 (CD44⁺ CD25⁺) (B), DN3 (CD44⁻ CD25⁺) (C), and DN4 (CD44⁻ CD25⁻) (D) throughout co-culture. The plotted significant stars refer to d0 of the respective treatment group. *P ≤ 0.05, ***P ≤ 0,001, ****P ≤ 0.0001, ****P ≤ 0.0001.

3.7 Effects of prenatal APAP exposure on the development of CD4/CD8 double positive cells in the OP9-DLL1 co-culture system

After immature T cell progenitors progressed through the DN stages during their development, they begin to upregulate CD4 and CD8 (Shah and Zúñiga-Pflücker 2014, Singer, Adoro, and Park 2008). The state of the DP cells, expressing both CD4 and CD8 on the surfaces, was analyzed.

At the beginning of ES1 with previously frozen HSC, almost none of the living cells expressed both CD4 and CD8 (PBS: 0.92 %; APAP: 1.11 %) *(Figure 16A)*. In contrast, when cells were incubated with DLL1-expressing OP9 cells, the frequencies of DP cells increased continuously (d4: PBS: .09 %; APAP: 2.83 %; d7: PBS: 16.4 %; APAP: 18.35 %), until it reached a maximum at the end of co-culture, on d11 (PBS: 30.53 %; APAP: 34.29 %). At this time point, the frequency of DP cells was significantly higher than on d0 in both treatment groups. The two treatment groups showed similar cell frequencies at all time points of reanalysis. Therefore, no significant differences between the treatment groups could be observed.

Pre- and post-selection DP cells can be distinguished by their CD5 and CD69 expression (Gangadharan et al. 2006). Interestingly, it was shown that cells in the co-culture system with OP9-DLL1 cells did not progress to CD5$^+$, CD69$^+$ post-selection DP cells *(Figure 16C)*. They rather rested in the pre-selection DP state (CD5^{int} CD69$^-$) (d4: PBS: 94.13 %; APAP: 94.36 %; d7: PBS: 98.22 %; APAP: 98 %; d11: PBS: 96.27 %; APAP: 97.87 %) *(Figure 16B)*. This was observed in both treatment groups, so no difference between cells exposed to APAP or PBS was detected.

Figure 16 Frequencies of overall CD4 and CD8 double positive (DP) cells as well as pre-and post-selection DP cells in co-culture of HSC isolated from cryo-preserved fetal liver cells with OP9-DLL1 cells in 24-well plate.
On E 12.5 pregnant mice were treated with 250 mg/kg APAP (n = 7) or PBS (n = 7) i.p. On E 14.5 dams were sacrificed and fetuses collected. Fetal liver cells were cryo-preserved prior to HSC (lin$^-$, c-Kit$^+$, Sca-1$^+$) isolation *via* fluorescence-activated cell sorting. HSC were co-cultured with OP9-DLL1 cells over 11 days in 24-well plates. Cells were analyzed by flow cytometry on d0, d4, d7, and d11 for the expression of CD4, CD8, CD5, and CD69. Frequencies of CD4 and CD8 DP cells throughout co-culture (A). Frequencies of pre- (CD5^{int} CD69$^-$) and post-selection (CD5$^+$ CD69$^+$) DP cells (B-C). The plotted significant stars refer to d0 of the respective treatment group. ****P $\leq$ 0.0001.

In ES2 (non-frozen cells, 24-well plates), frequencies of DP cells similarly increased continuously over 7 days in co-culture (d0: PBS: 0.95 %; APAP: 1.54 %; APAP+NAC: 0.86 %; d4: PBS: 2.26 %; APAP: 2.53 %; APAP+NAC: 1.48 %, d7: PBS: 2.85 %; APAP: 3.27 %; APAP+NAC: 1.77 %) *(Figure 17A)*. However, the percentages of DP cells were generally much lower than in ES1. At all time points of reanalysis, APAP-exposed HSC tended to have higher DP frequencies than the other groups. Moreover, DP cells did not progress into post-selection DP cells and instead rested in the pre-selection DP state (d4: PBS: 66.88 %; APAP: 52.13 %; APAP+NAC: 75.63 %; d7: PBS: 73.45 %; APAP: 85.65 %; APAP+NAC: 83 %) *(Figure 17B-C)*. However, different from

ES1, the total sum of pre-and post-selection DPs was not 100 %, therefore there seemed to be cells belonging neither to the pre- nor to the post-selection DP state. This was similarly observed in all three treatment groups, although on d0 frequencies of pre-selection DP cells were slightly lower when exposed to APAP.

Figure 17: Frequencies of overall CD4 and CD8 double positive (DP) cells as well as pre-and post-selection DP cells in co-culture of fetal liver HSC with OP9-DLL1 cells in 24-well plate.
On E 12.5 pregnant mice were treated with 250 mg/kg APAP (n = 4), PBS (n = 4), or 250 mg/kg APAP+1200 mg/kg NAC (n = 4) i.p. On E 14.5 dams were sacrificed and fetal liver HSC (lin-, c-Kit+, Sca-1+) were isolated *via* fluorescence-activated cell sorting. HSC were co-cultured with OP9-DLL1 cells over 7 days in 24-well plates. Cells were analyzed by flow cytometry on d0, d4, and d7 for the expression of CD4, CD8, CD5, and CD69. Frequencies of CD4 and CD8 DP cells throughout co-culture (A). Frequencies of pre- (CD5int CD69-) and post-selection (CD5+ CD69+) DP cells (B-C).

In ES3, frequencies of DP cells were slightly higher on d0 (PBS: 1.21 %; APAP: 1.02 %) than on d4 (PBS: 0.21 %; APAP: 0.26 %) and d7 (PBS: 0.15 %; APAP: 0.16 %) in the APAP-treated group as well as in the PBS-treated group *(Figure 18A)*. Nevertheless, this variation was not significant. From d11, the frequencies continuously started to rise until d18 (d11: PBS: 1.55 %; APAP: 1.88 %; d14: PBS: 2.04 %; APAP: 2.73 %; d18: PBS: 3.06 %; APAP: 1.99 %). In both groups, the cell frequencies developed comparably. Again, similar to the other two experiments, it was shown that cells rested in the pre-selection DP stage (d7: PBS: 35.18 %; APAP: 15.78 %; d11: PBS: 53.5 %; APAP: 53.73 %; d14: PBS: 65.63 %; APAP: 62.98 %; d18: PBS: 92.68 %; APAP: 63.73 %) and almost no post-selection DP cells were detectable at any time point of reanalysis (d7: PBS: 5.65 %; APAP: 0 %; d11: PBS: 0 %; APAP: 0 %; d14: PBS: 1.65 %; APAP: 1.13 %; d18: PBS: 0.46 %; APAP: 3.55 %) *(Figure 18B-C)*. Nevertheless, the sum of pre-and post-selection DP cells did not

account for 100 %, comparable to ES2. Furthermore, generally lower pre-selection DP cell frequencies were detected in the APAP group. However, overall HSC developed similarly in both treatment groups as significant differences were not observed.
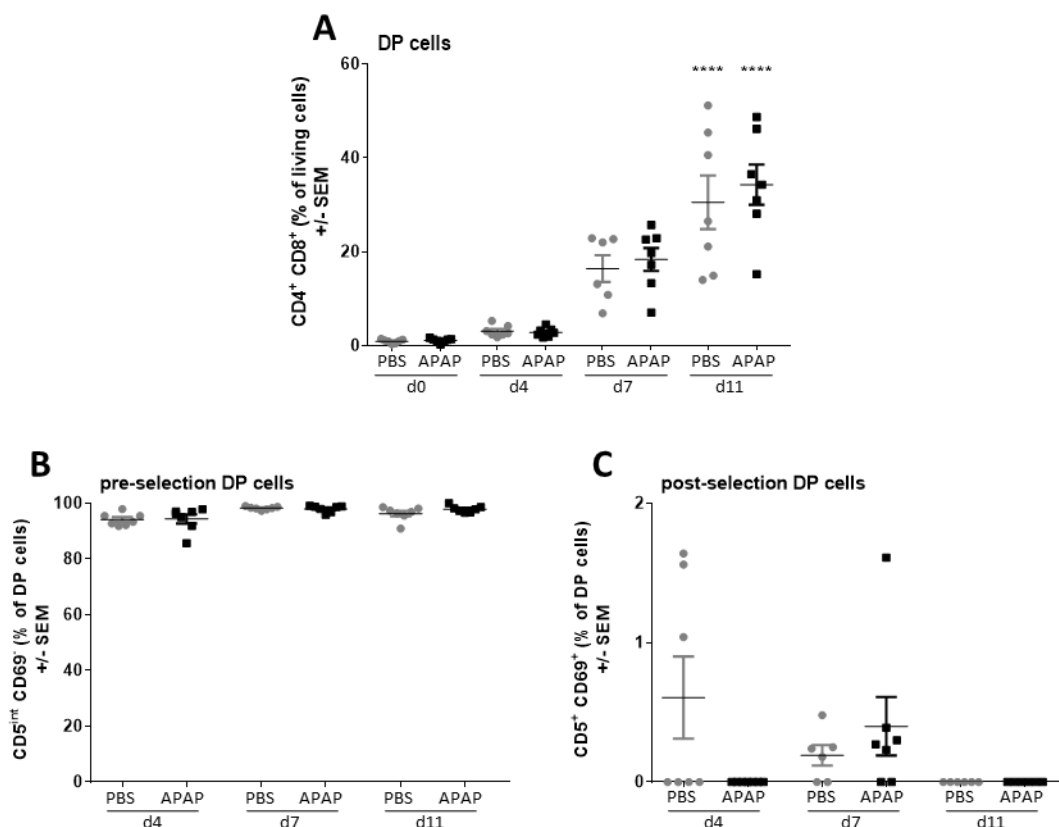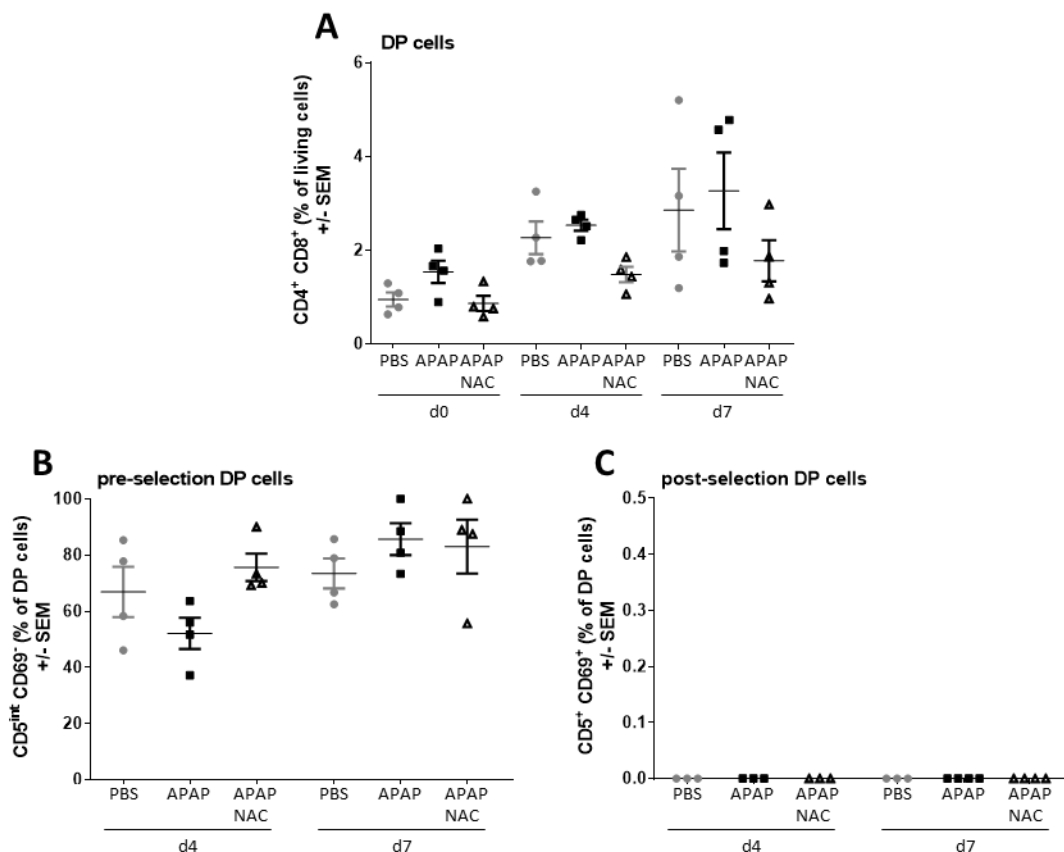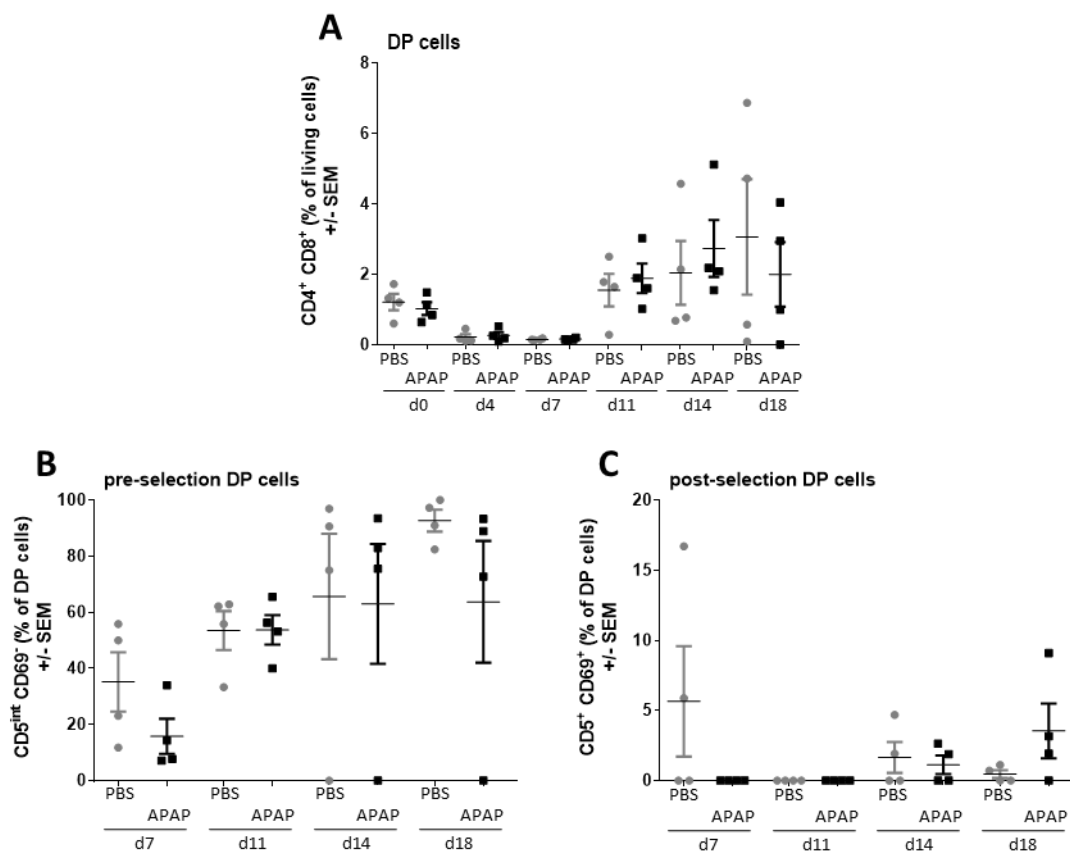

Figure 18: Frequencies of overall CD4 and CD8 double positive (DP) cells as well as pre-and post-selection DP cells in co-culture of fetal liver HSC with OP9-DLL1 cells in 48-well plate.
On E 12.5 pregnant mice were treated with 250 mg/kg APAP (n = 4) or PBS (n = 4) i.p. On E 14.5 dams were sacrificed and fetal liver HSC (lin⁻, c-Kit⁺, Sca-1⁺) were isolated *via* fluorescence-activated cell sorting. HSC were co-cultured with OP9-DLL1 cells over 18 days in 48-well plates. Cells were analyzed by flow cytometry on d0, d4, d7, d11, d14, and d18 for the expression of CD4, CD8, CD5, and CD69. Frequencies of CD4 and CD8 DP cells throughout co-culture (A). Frequencies of pre- (CD5^{int} CD69$^-$) and post-selection (CD5$^+$ CD69$^+$) DP cells (B-C).

3.8 Effect of prenatal APAP exposure on the rise of immature CD8-expressing T cells (ISP8) in the OP9-DLL1 co-culture system

After developing T cells progressed through the DN stages, CD8 SP cells evolve (Shah and Zúñiga-Pflücker 2014; Singer, Adoro, and Park 2008). When cells were in co-culture with DLL1$^+$ OP9 cells in ES1 (frozen, 24-well plates), the frequency of CD4$^-$, CD8$^+$ cells increased over time (d0: PBS: 0.75 %, APAP: 0.63 %; d4: PBS: 0.95 %; APAP: 0.85 %; d7: PBS: 0.99 %; APAP: 0.72 %; d11: PBS: 1.89 %; APAP: 2.71 %) *(Figure 19A)*. However, almost none of the CD8 SP cells expressed the maturation marker TRC-β, which indicated that these cells were ISP8 cells (Shah and Zúñiga-Pflücker 2014, Singer, Adoro, and Park 2008) (d4: PBS: 100 %; APAP: 100 %; d7: PBS: 100 %; APAP: 100 %; d11: PBS: 100 %; APAP: 100 %) *(Figure 19B)*. When ISP8 cells

were displayed as a frequency of all living cells *(Figure 19C)*, the pattern of frequency growth was similar to CD8 SP cells *(Figure 19A)*. This emphasized that the CD8 SP cells, which evolved over time, were immature (d0: PBS: 0.67 %, APAP: 0.51 %; d4: PBS: 0.95 %; APAP: 0.85 %; d7: PBS: 0.97 %; APAP: 0.72 %; d11: PBS: 1.82 %; APAP: 2.69 %). This effect appeared to be independent of treatment.

Figure 19: Frequencies of CD8 single positive (SP) cells and immature CD8 single positive cells (ISP8) in co-culture of HSC isolated from cryo-preserved fetal liver cells with OP9-DLL1 cells in 24-well plate.
On E 12.5 pregnant mice were treated with 250 mg/kg APAP (n = 7) or PBS (n = 7) i.p. On E 14.5 dams were sacrificed and fetuses collected. Fetal liver cells were cryo-preserved prior to HSC (lin⁻, c-Kit⁺, Sca-1⁺) isolation *via* fluorescence-activated cell sorting. HSC were co-cultured with OP9-DLL1 cells over 11 days in 24-well plates. Cells were analyzed by flow cytometry on d0, d4, d7, and d11 regarding the expression of CD4, CD8, and TCR-β. Frequencies of CD8 SP cells (CD4⁻ CD8⁺) (A) and ISP8 cells (CD8⁺, TCR-β⁻) as a frequency of CD8 SP cells (B). ISP8 cells as a frequency of living cells (C). The plotted significant stars refer to d0 of the respective treatment group. *P ≤ 0.05, **P ≤ 0.01, ****P ≤ 0.0001.

When cells were co-cultured over 7 days in ES2 (fresh cells; 24-well plate), CD8 SP cells developed as well *(Figure 20)*. However, this occurred already after 4 days *(Figure 20A)*. On d0, none of the fetal liver HSC were CD8 SP cells. On d4 of reanalysis, the frequency of CD8 SP cells increased in all three treatment groups. This increase was significantly higher in the APAP group than in the PBS or APAP+NAC treatment group. On d7, CD8 SP cell frequencies decreased again, this decline was similar in all three treatment groups. Nevertheless, the frequencies of CD8 SP cells were significantly higher when compared to d0. Also, in this experiment almost all of the CD8 SP cells were TCR-β⁻, therefore could also be identified as ISP8 cells *(Figure 20B)*. This was confirmed when the frequencies of ISP8 cells were displayed as a frequency of living cells *(Figure 20C)*. Again, the

pattern of the alterations of the frequencies was similar to the overall CD8 SP cell frequencies *(Figure 20A)*.

Figure 20: Frequencies of CD8 single positive (SP) cells and immature CD8 single positive cells (ISP8) in co-culture of fetal liver HSC with OP9-DLL1 cells in 24-well plate.
On E 12.5 pregnant mice were treated with 250 mg/kg APAP (n = 4), PBS (n = 4), or 250 mg/kg APAP+1200 mg/kg NAC (n = 4) i.p. On E 14.5 dams were sacrificed and fetal liver HSC (lin⁻, c-Kit⁺, Sca-1⁺) were isolated *via* fluorescence-activated cell sorting. HSC were co-cultured with OP9-DLL1 cells over 7 days in 24-well plates. Cells were analyzed by flow cytometry on d0, d4, and d7 regarding the expression of CD4, CD8, and TCR-β. Frequencies of CD8 SP cells (CD4⁻ CD8⁺) (A) and ISP8 cells (CD8⁺, TCR-β⁻) as a frequency of CD8 SP cells (B). ISP8 cells as a frequency of living cells (C). The plotted significant stars refer to d0 of the respective treatment group. *P ≤ 0.05, **P ≤ 0.01, ****P ≤ 0.0001.

In ES3 (fresh cells, 48-well plates) it was similarly shown that cells differentiated into CD8 SP cells *(Figure 21A)*. On d0 there were almost no CD8 SP cells (PBS: 3.29 %; APAP: 3.66 %). Frequencies increased continuously until the final time point of reanalysis on d18 (d4: PBS: 7.88 %; APAP: 6.1 %; d7: PBS: 14.33 %; APAP: 11.3 %; d11: PBS: 39.83 %; APAP: 38.58 %; d14: PBS: 36.15 %; APAP: 47.63 %; d18: PBS: 46.08 %; APAP: 70.93 %). On d11 and d18 the frequencies of CD8 SP cells were significantly higher than on d0 in both treatment groups. On d14 the increase was only significant in case of cells prenatally exposed to APAP. Aside from that, this development appeared independent of treatment. As described for the experiments above, almost all of the CD8 SP cells were ISP8 cells (d4: PBS: 95.55 %; APAP: 90.95 %; d7: PBS: 98.18 %; APAP: 97.78 %; d11: PBS: 95.38 %; APAP: 94.85 %; d14: PBS: 98.87 %; APAP: 98.7 %; d18: PBS: 99.08 %; APAP: 99.55 %) *(Figure 21B)*. This was confirmed when the frequencies of ISP8 cells were displayed as a frequency of living cells (d0: PBS: 1.87 %; APAP: 2.03 %; d4:

PBS: 7.57 %; APAP: 5.64 %; d7: PBS: 14.12 %; APAP: 11.11 %; d11: PBS: 40.98 %; APAP: 34.05 %; d14: PBS: 35.53 %; APAP: 47.05 %; d18: PBS: 45.75 %; APAP: 70.58 %) *(Figure 21C)*. The pattern of the increase in frequencies was similar to CD8 SP cells *(Figure 21A)* as already seen in the previous two experiments (ES1, ES2).
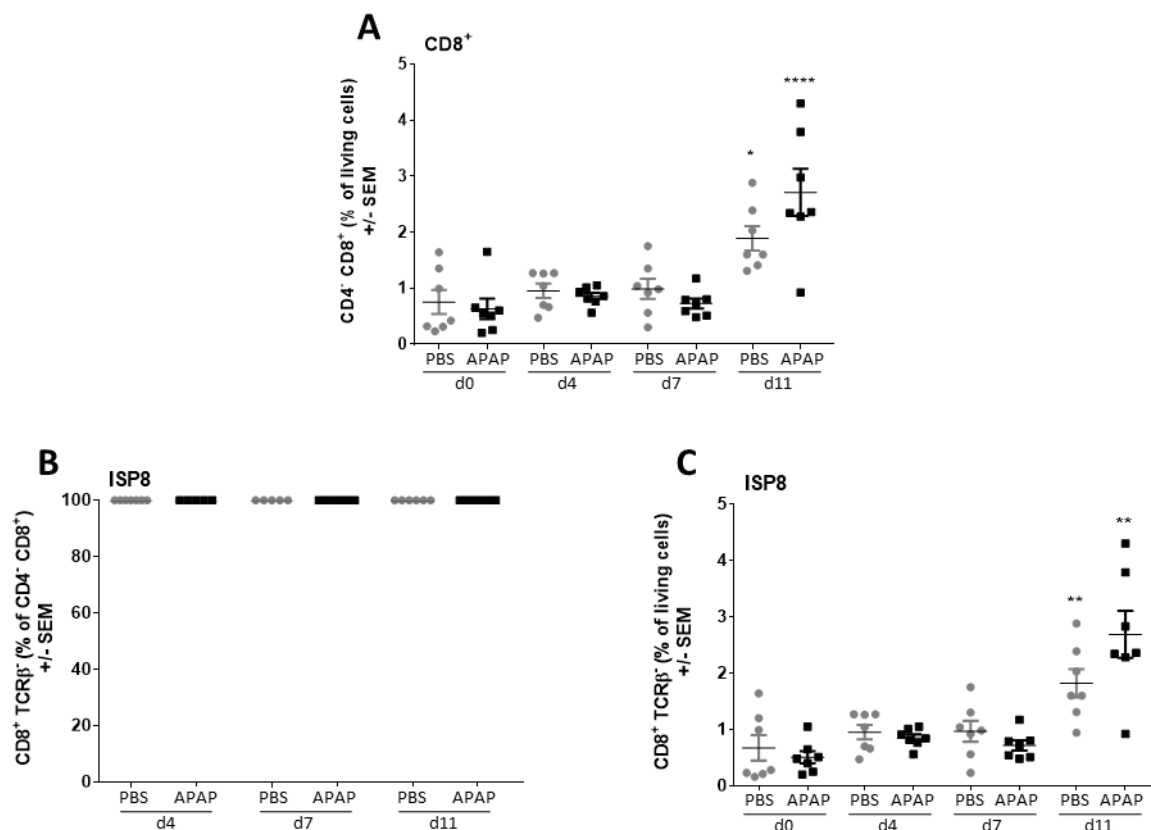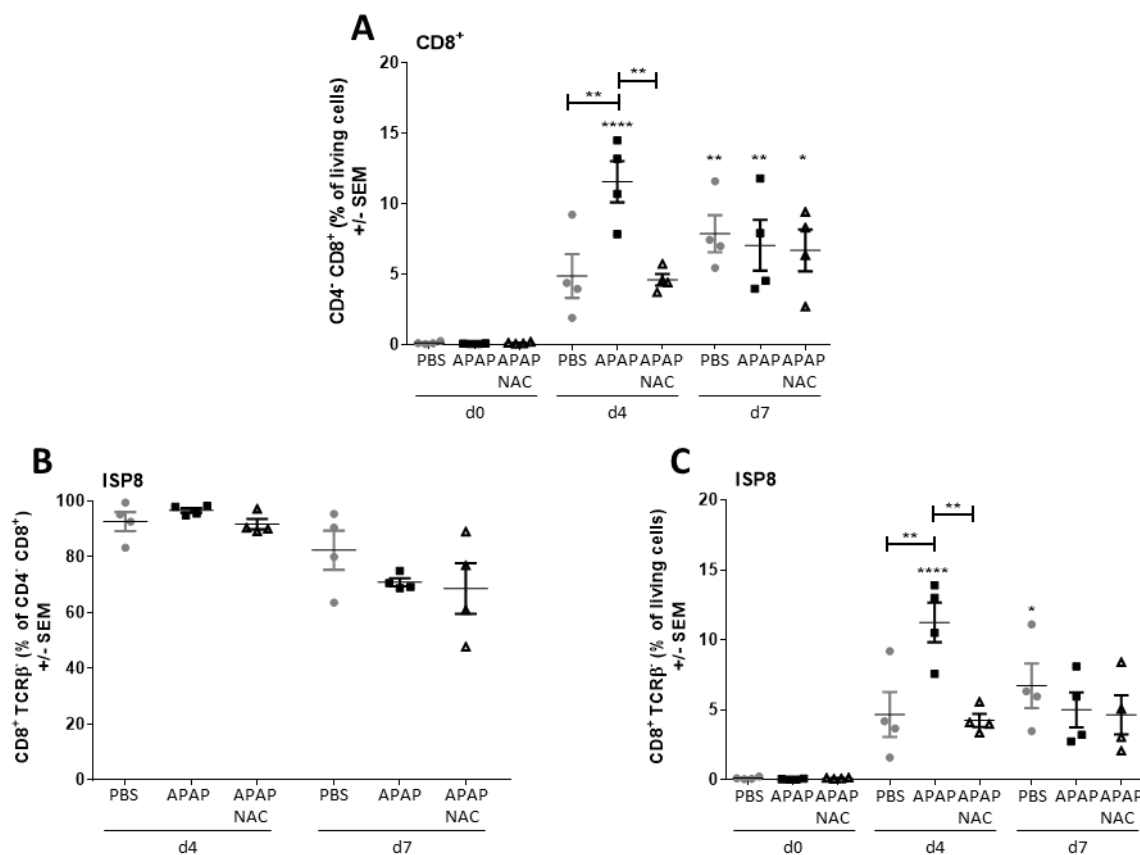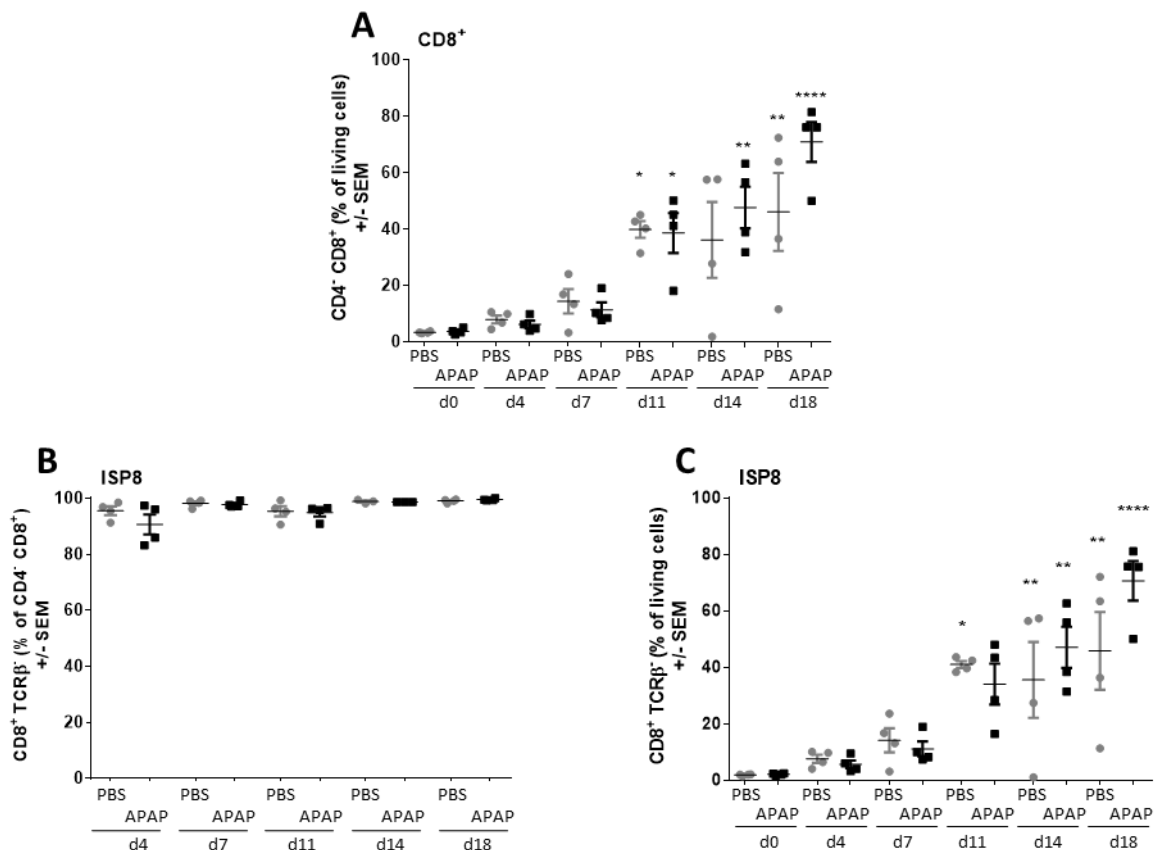

Figure 21: Frequencies of CD8 single positive (SP) cells and immature CD8 single positive cells (ISP8) in co-culture of fetal liver HSC with OP9-DLL1 cells in 48-well plate.
On E 12.5 pregnant mice were treated with 250 mg/kg APAP (n = 4) or PBS (n = 4) i.p. On E 14.5 dams were sacrificed and fetal liver HSC (lin⁻, c-Kit⁺, Sca-1⁺) were isolated *via* fluorescence-activated cell sorting. HSC were co-cultured with OP9-DLL1 cells over 18 days in 48-well plates. Cells were analyzed by flow cytometry on d0, d4, d7, d11, d14, and d18 regarding the expression of CD4, CD8, and TCR-β. Frequencies of CD8 SP cells (CD4⁻ CD8⁺) (A) and ISP8 cells (CD8⁺, TCR-β⁻) as a frequency of CD8 SP cells (B). ISP8 cells as a frequency of living cells (C). The plotted significant stars refer to d0 of the respective treatment group. *P ≤ 0.05, **P ≤ 0.01, ****P ≤ 0.0001.

In all three experiments (ES1-ES3) cells were able to develop into CD8 SP cells *(Figure 19, 20, 21)*. Moreover, it appeared that those CD8 SP cells were predominantly immature in all experiments. Notably, in ES1 *(Figure 19)* the frequencies of CD8 SP cells were generally lower compared to ES2 *(Figure 20)* and ES3 *(Figure 21)*.

Interestingly, only in ES2 *(Figure 20)*, significant differences in frequencies of CD8 SP cells between the treatment groups was observed. Here, it seemed that differentiation to CD8 SP cells was accelerated when HSC were prenatally exposed to APAP.

3.9 Effect of prenatal APAP exposure on the development of CD4-expressing T cells in the OP9-DLL1 co-culture system

In ES1 (frozen, 24-well plates) frequencies of CD4 SP cells decreased throughout co-culture with OP9-DLL1 cells *(Figure 22)*. On d0 approximately a third of living cells expressed CD4 on their surface (PBS: 34.1 %; APAP: 33.84 %). Here, it should be mentioned that these cells were identified as HSC, therefore these CD4$^+$ cells were still stem cells. On d4 CD4 SP cell frequencies decreased (PBS: 18.84 %; APAP: 18.49 %). On d7 and d11 of reanalysis, CD4 SP cell frequencies were further reduced (< 10 %) (d7: PBS: 5.47 %; APAP: 5.05 %; d11: PBS: 6.86 %; APAP: 6.55 %). Additionally, the number of CD4 SP cells on d4, d7, and d11 was significantly lower compared to d0. Cell frequency development was similar in both treatment groups.
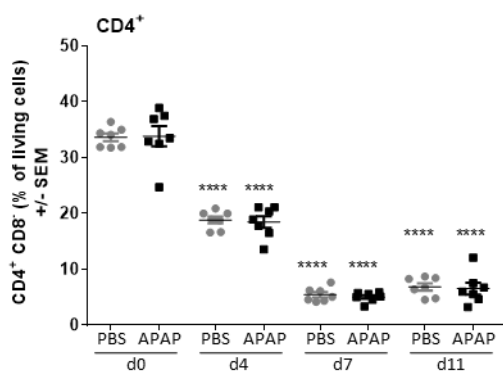
Figure 22: Frequencies of CD4 single positive cells in co-culture of HSC isolated from cryo-preserved fetal liver cells with OP9-DLL1 cells in 24-well plate.
On E 12.5 pregnant mice were treated with 250 mg/kg APAP (n = 7) or PBS (n = 7) i.p. On E 14.5 dams were sacrificed and fetuses collected. Fetal liver cells were cryo-preserved prior to HSC (lin$^-$, c-Kit$^+$, Sca-1$^+$) isolation *via* fluorescence-activated cell sorting. HSC were co-cultured with OP9-DLL1 cells over 11 days in 24-well plates. Cells were analyzed by flow cytometry on d0, d4, d7 and d11 regarding the expression of CD4 and CD8. Frequencies of CD4 SP cells (CD4$^+$ CD8$^-$). The plotted significant stars without a bar refer to d0 of the respective treatment group. ****P ≤ 0.0001.

In ES2 (fresh cells, 24-well plates), interestingly, CD4$^+$ cell frequencies were generally much lower *(Figure 23)* than in the first experiment when fetal liver cells were frozen *(Figure 22)*. The cell frequencies varied between 2 and 8 % throughout co-culture (d0: PBS: 1.95 %; APAP. 4.42 %; APAP+NAC: 1.15 %; d4: PBS: 2.47 %; APAP: 3.7 %; APAP+NAC: 2.48 %; d7: PBS: 4.83 %; APAP: 5.26 %; APAP+NAC: 3.16 %) *(Figure 23)*. However, cells that were prenatally exposed to APAP tended to have slightly higher CD4 SP cell frequencies on d0 and d4. Nevertheless, this difference was not significant when the APAP group was compared to cells treated with PBS or APAP+NAC.
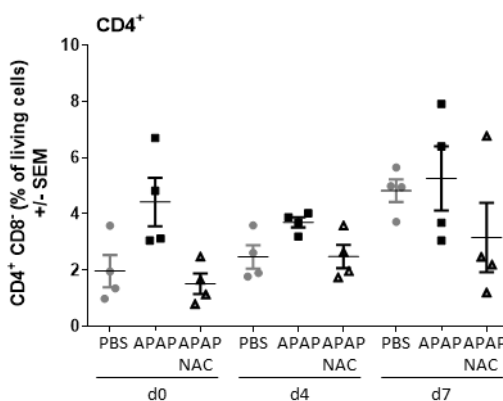
Figure 23: Frequencies of CD4 single positive cells in co-culture of fetal liver HSC with OP9-DLL1 cells in 24-well plate.
On E 12.5 pregnant mice were treated with 250 mg/kg APAP (n = 4), PBS (n = 4), or 250 mg/kg APAP+1200 mg/kg NAC (n = 4) i.p. On E 14.5 dams were sacrificed and fetal liver HSC (lin$^-$, c-Kit$^+$, Sca-1$^+$) were isolated *via* fluorescence-activated cell sorting. HSC were co-cultured with OP9-DLL1 cells over 7 days in 24-well plates. Cells were analyzed by flow cytometry on d0, d4, and d7 regarding the expression of CD4 and CD8. Frequencies of CD4 SP cells (CD4$^+$ CD8$^-$).

Under conditions of ES3 (fresh cells, 48-well plates) frequencies of CD4 SP cells were very low *(Figure 24)*. On every day of reanalysis, almost none of the living cells expressed CD4 exclusively. However, on d4 in both groups cell frequencies of CD4 SP cells increased. But this increase of CD4 SP cells was not significant when compared to the other reanalysis time points (d0: PBS: 0.08 %; APAP: 0.16 %; d4: PBS: 0.71 %; APAP: 1.01 %; d7: PBS: 0.25 %; APAP: 0.25 %; d11: PBS: 0.28 %; APAP: 0.17 %; d14: PBS: 0.16 %; APAP: 0.22 %; d18: PBS: 0.07 %; APAP: 0.12 %). Cells in both treatment groups were similarly affected in their development.
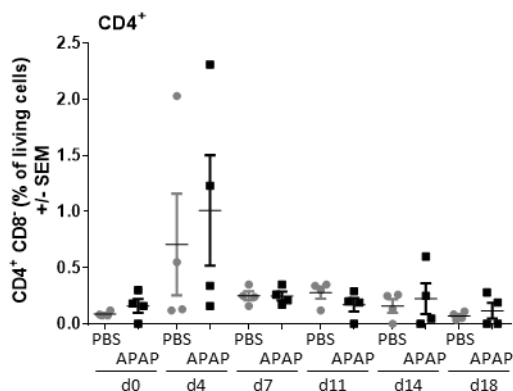
Figure 24: Frequencies of CD4 single positive cells in co-culture of fetal liver HSC with OP9-DLL1 cells in 48-well plate.
On E 12.5 pregnant mice were treated with 250 mg/kg APAP (n = 4) or PBS (n = 4) i.p. On E 14.5 dams were sacrificed and fetal liver HSC (lin⁻, c-Kit⁺, Sca-1⁺) were isolated *via* fluorescence-activated cell sorting. HSC were co-cultured with OP9-DLL1 cells over 18 days in 48-well plates. Cells were analyzed by flow cytometry on d0, d4, d7, d11, d14 and d18 regarding the expression of CD4 and CD8. Frequencies of CD4 SP cells (CD4⁺ CD8⁻).

Overall, it was observed that in ES1 (frozen cells, 24-well plates) *(Figure 22)* relatively high frequencies of cells were already CD4⁺ but CD8⁻ before cells were co-cultured with OP9-DLL1 cells, although they additionally exhibited HSC characteristics *(Figure 7)*. The expression of CD4 was downregulated over time in the co-culture system *(Figure 22)*. In ES2 and ES3 this effect was not observed *(Figure 23Figure 24)*. Cells that were identified as HSC *(Figure 8,Figure 9)* before co-culture, did not express CD4 before co-culture. In fact, in ES2, frequencies of CD4 SP cells tended to increase during incubation with DLL1-expressing OP9 cells. In ES3, almost no CD4⁺SP cells were detected at any time point of reanalysis *(Figure 23Figure 24)*.

3.10 T cell differentiation in co-culture system with OP9 -LIE cells that lack DLL1

In order to investigate whether the exposure to DLL1 is essential for HSC development, cells were co-cultured with OP9-DLL1 cells as well as with OP9-LIE cells in 24-well plates. To generate OP9-LIE cells, OP9 cells were transduced with an empty vector, so they were lacking DLL1-expression. Developing cells were analyzed by flow cytometry on d0, d4, d7, and d11 of co-culture, and the expression of CD4 and CD8 was considered *(Figure 25)*.

On d0, before fetal liver HSC were given into a co-culture system with either OP9-DLL1 or OP9-LIE cells, the majority of fetal liver HSC sparsely expressed CD4 or CD8 *(Figure 25A)*. This was also the case on d4 of reanalysis *(Figure 25B, E)*. On d7 and d11 it was shown that HSC exposed to DLL1 upregulated the expression of CD8 *(Figure 25C, D)*. By contrast, fetal liver HSC that were incubated with OP9-LIE cells were not able to give rise to CD8 SP cells *(Figure 25F, G)*.

It has to be noted, that on d11 of co-culture fewer cells were analyzed in both groups. This indicated that HSC were not able to proliferate anymore, in fact, they lost their viability and died, independent of DLL1-exposure.
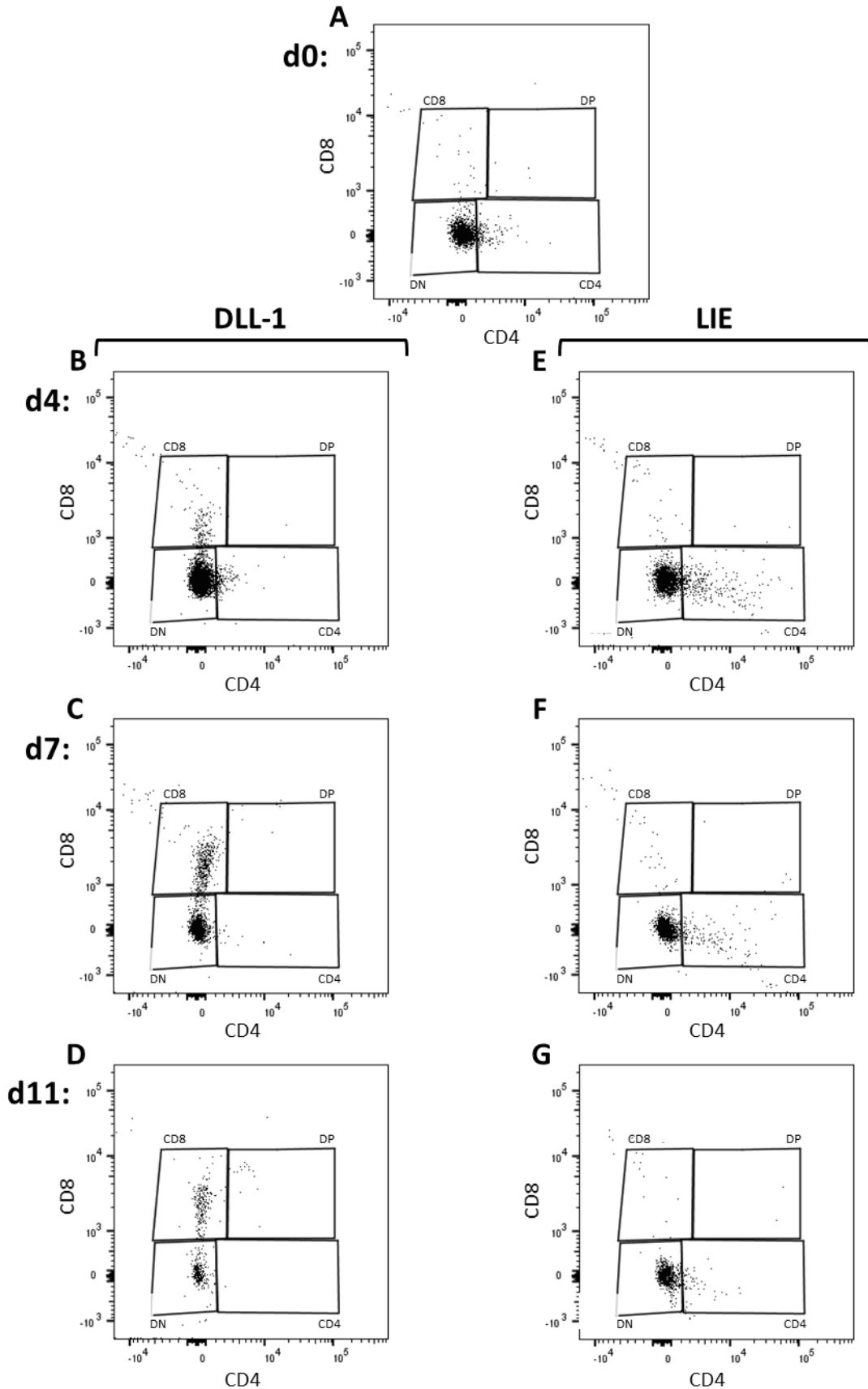
Figure 25: T cell maturation in a co-culture system with OP9-DLL1 cells vs. co-culture system with OP9-LIE cells.
On E 14.5 dams were sacrificed and fetal liver HSC (lin-, c-Kit+, Sca-1+) were isolated *via* fluorescence-activated cell sorting. Isolated HSC were co-cultured with OP9 cells expressing DLL1 or with OP9 cells not expressing DLL1 (LIE). These cells were analyzed by flow cytometry regarding their CD4 and CD8 expression on d0 (A), d4, and d7 of co-culture. Developing cells co-cultured with OP9-DLL-1 cells (B)-(D) were compared to cells co-cultured with OP9-LIE cells (E)-(G).

46

In conclusion, our results demonstrated that maternal APAP administration during pregnancy induced liver damage in dams. Additional treatment with the APAP-specific antidote, NAC, reversed the adverse effects of APAP on maternal livers. Moreover, it was observed that maternal weight gain during the course of pregnancy was negatively affected by the application of APAP. However, when pregnancy outcome and fetal development were assessed, no APAP-specific effect could be observed in terms of litter sizes, numbers of miscarriages, fetal weights. Interestingly, numbers of non-frozen HSC isolated from fetal livers tended to be lower when prenatally exposed to APAP compared to PBS or APAP+NAC (ES1-3), however, this was not significant.

When isolated fetal liver HSC were exposed to DLL1 in the OP9-system, cells lost their stem cell characteristics (c-Kit$^+$, Sca-1$^+$). In fact, HSC isolated from fetal livers were able to give rise to T cell precursors. They distinctively progressed through the DN stages. Strikingly, when cells were incubated with DLL1-expressing OP9 cells, they were more likely to exclusively express CD8 instead of CD4 on their surfaces. However, these CD8 SP cells were lacking TCR-β-expression and turned out to be immature CD8 SP cells (ISP8), representing an intermediate T cell precursor stage before cells expressed both CD4 and CD8 to become DP cells.

In general, fetal liver cells that were cryo-preserved prior to final HSC purification seemed not to be a disadvantage with regard to viability and purity. Nonetheless, these cells seemed to mature faster in the OP9-co-culture system.

Cells that were not frozen and co-cultured with OP9-DLL1 cells in 48-well plates proliferated extensively, which resulted in more time points for reanalysis. Although proliferation occurred sufficiently it appeared that differentiation of T cells was decelerated compared to cells incubated in 24-well plates. Furthermore, non-frozen cells co-cultured in 24-well plates resulted in accelerated T cell differentiation when prenatally exposed to APAP. Here, the preventive effect of additional NAC treatment was observed, as it reversed APAP-induced alterations in T cell development.

Finally, these studies again provided evidence that DLL1 expression is essential for T cell development. HSC co-cultured with DLL1-expressing OP9 cells were able to upregulate CD8 expression while HSC not exposed to DLL1, persisted in the DN state.

4 Discussion

APAP is a frequently prescribed and applied drug to treat fever and pain. It is available over-the-counter and therefore often taken as self-medication. This facilitates unintentional overdose potentially resulting in liver damage.

Moreover, APAP is the only analgesic drug that is licensed in all three trimesters of pregnancy as it is considered as safe for the mother as well as for the child. However, several epidemiological studies on APAP use in pregnancy implied negative effects on mothers and unborn children.

There seems to be an association between maternal APAP application and higher susceptibility for the child to develop wheezing after birth and childhood asthma later in life (Persky et al. 2008, Rebordosa et al. 2008, Eyers et al. 2011). It has also been found that mice prenatally exposed to APAP had decreased frequencies of HSC in fetal livers, therefore it might have an impact on fetal immune development (Karimi et al. 2015).

Collectively, these findings arouse concerns about the safety of APAP use in pregnancy. Especially, the association between APAP and the development of asthma as well as the reduced frequencies of HSC in the offspring might indicate that APAP has an impact on the HSC compartment and therefore on the offspring´s immune system. Nonetheless, there is still not enough data that explain the mechanisms behind the effects of APAP on the fetus.

4.1 Establishment of experimental conditions

These studies aimed to investigate the influence of prenatal exposition to APAP on the immune development of the offspring and whether additional application of the APAP-specific antidote, NAC, has protective effects.

To identify the changes that occur in T cell differentiation due to APAP exposition during embryogenesis, T cell differentiation of fetuses prenatally exposed to PBS, APAP, or APAP+NAC was observed using the co-culture system with the stromal OP9 cells expressing DLL1. DLL1 is a Notch-ligand that was found to be essential for T cell differentiation (Brandstadter and Maillard 2019).

Moreover, it was important to test for ideal experimental conditions that warrant sufficient cell proliferation, differentiation, and survival.

Three experimental setups were tested and evaluated regarding their quality and applicability. However, the overall protocol used for HSC purification from fetal liver tissue was identical. Only in ES1, fetal liver cells were cryo-preserved and stored at -80°C for one week prior to final HSC purification *via* FACS according to the protocol by Motashami *et al.* (Mohtashami, Zarin, and Zúñiga-Pflücker 2016). Then fetal liver HSC were co-cultured with DLL1-expressing OP9 cells.

As animals became pregnant on consecutive days, freezing and final HSC purification *via* FACS of all cells after one week of cryo-preservation (as in ES1) was the only way to start co-cultivation of all isolated fetal liver HSC with OP9-DLL1 cells on the same day.

Moreover, different well sizes were applied to identify optimal conditions for HSC to proliferate and to survive. In ES1 and ES2 24-well plates were used and in ES3 HSC were co-cultured with OP9-DLL1 cells in 48-well plates where wells were smaller.

4.2 APAP applied to pregnant mice caused liver damage while NAC had protective effects

APAP applied to pregnant mice can either have direct or indirect effects on the immune development of the offspring. It freely crosses the placental barrier and may therefore affect the fetus directly (Thiele et al. 2015). However, liver damage in dams caused by APAP application might also lead indirectly to altered fetal immune development either due to inflammatory cytokines or toxic substances, formed in the maternal liver and passing the placental barrier.

To investigate whether APAP administration in pregnant mice causes liver damage and whether additional NAC treatment is protective, substances were applied on E 12.5, and serum ALT levels were measured 24 h after APAP, APAP+NAC, or PBS injection.

Pregnant mice treated with 250 mg/kg bodyweight APAP exhibited significantly elevated serum ALT levels in comparison to PBS-or APAP+NAC-treated animals. This was confirmed by extensive necrotic areas in liver sections of APAP-treated mice which were absent in the other two treatment groups.

The APAP dose of 250 mg/kg bodyweight, that was applied in these experiments, has been found to induce severe hepatotoxicity in dams, whereas this dose only slightly enhanced ALT and AST levels in non-pregnant female mice. Nevertheless, this APAP dose, results in a 100 % survival rate in pregnant and non-pregnant mice (Karimi et al. 2015). For pregnant mice this was also observed in this study.

Overdosage of APAP is likely to cause liver damage in humans and in mice (Mossanen and Tacke 2015, Ramachandran and Jaeschke 2018). APAP is metabolized in the liver where it is conjugated with glucuronic acid or sulfate, and finally excreted *via* the urine (McGill and Jaeschke 2013). When APAP is overdosed, the toxic metabolite NAPQI accumulates. If the capacity of NAPQI detoxification by glutathione is exhausted, the formation of NAPQI-protein adducts results in mitochondrial damage and consequently in hepatocyte necrosis (McGill and Jaeschke 2013). Cell necrosis causes the generation of free radicals like superoxide (Yan et al. 2010). It is produced in mitochondria and can react with nitric oxide to form peroxynitrite. This metabolite is highly reactive and can modulate protein functions, potentially causing further hepatocyte damage (Radi 2018).

These mechanisms similarly play a role in pregnant mice. In fact, elevated progesterone and estrogen levels influence metabolic functions and impair the excretory potential of the liver. This might explain why pregnant mice are more prone to develop hepatic injury upon APAP administration compared to non-pregnant animals (Karimi et al. 2015). Moreover, female sex hormones were found to induce structural damage in hepatic mitochondria facilitating the development of acute fatty liver in pregnancy (Grimbert et al. 1995). Therefore, these pregnancy-related changes in liver function might provide explanation why APAP was also harmful to our pregnant animals.

In contrast, treatment with 250 mg/kg bodyweight APAP and additional 1200 mg/kg bodyweight NAC did not cause elevated serum ALT levels in pregnant mice. Therefore, NAC had a protective effect on the liver. NAC prevents hepatic injury and is used in clinics to treat liver failure caused by APAP overdosage (Hodgman and Garrard 2012). In APAP-induced liver damage, glutathione stores are depleted which results in the accumulation of the toxic APAP metabolite, NAPQI. Now, NAC can help to replenish hepatic glutathione stores as it provides cysteine, a rate-limiting amino acid for glutathione biosynthesis. This facilitates the elimination of NAPQI (Prescott et al. 1977).

As shown here, the protective mechanisms of NAC which prevented APAP-induced liver failure in pregnant mice, seem to be similar to those observed in non-pregnant animals or humans.

4.3 The application of APAP at mid-gestation seemed to have no impact on pregnancy outcome

The influence of APAP on pregnancy outcome was assessed. Litter sizes, numbers of miscarriages, and fetal weights did not seem to be affected by prenatal APAP exposition, as no difference in pregnancy outcome between the three treatment groups was shown. The fact that APAP was only applied 48 h before pregnancy outcome evaluation, might be causal that no differences were discovered. "Macroscopic" effects of APAP on fetal health and maternal pregnancy adaptation (e.g., litter sizes, numbers of miscarriages, fetal weights) might take longer than only two days to establish. Furthermore, miscarriages or birth defects are dependent on multiple factors, therefore identification of a single cause would have been difficult in any case (Cuny et al. 2020). Interestingly, studies in pregnant women demonstrated that intake of non-steroidal anti-inflammatory drugs (NSAIDs) around conception increases the risk for miscarriages, but not when these drugs were applied at later time points (D. K. Li et al. 2018). This might also be transferred to these results. Although NSAIDs have different mechanisms of action than APAP, the injection at mid-gestation (E 12.5), as performed in these studies, might also not have had an impact on miscarriages and rate of implantations. Moreover, several other studies similarly showed that implantations and abortion rates are not influenced by maternal APAP administration. These studies also evaluated fetal weights upon *in utero* APAP exposition. They demonstrated that 24 h and 96 h after APAP administration fetal

weights were lower compared to weights of fetuses exposed to PBS (Karimi et al. 2015, Thiele et al. 2015). In contrast, our results indicated that fetal weight development was not impaired by prenatal APAP exposition.

4.4 APAP applied to pregnant mice reduced weight gain during pregnancy

Moreover, maternal weight development throughout pregnancy was evaluated. It was found that dams treated with APAP gained less weight over the course of pregnancy compared to the other two groups. Here, weight gain in mice exposed to APAP was significantly lower when compared to PBS-exposed dams. An explanation might be that APAP-treated animals developed liver injury and therefore discomfort and morbidity. This in turn might have caused lower food intake and subsequently less gain of weight. Additionally, the fact that numbers of implantations and fetal weights were similar in all three treatment groups implied that these aspects cannot be causal for less weight increase in APAP-exposed dams.

4.5 APAP reduced HSC numbers in fetal livers while DMSO seemed to diminish the HSC-reducing effect of APAP

The fetal liver is the main site of HSC production during embryogenesis. At later time points HSC migrate into the fetal spleen, thymus, and finally bone marrow (Ciriza et al. 2013).

In ES2, numbers of HSC purified per fetal liver were slightly lower in fetuses exposed to APAP than treated with PBS or APAP+NAC. In ES3, a similar trend was observed. Less fetal liver HSC were isolated from fetuses prenatally exposed to APAP compared to PBS-treated mice. Due to small samples sizes (n = 4/treatment group) and a wide variance in this experiment, the difference was not significant, as well.

Comparing HSC numbers of all three experiments, it appeared that cryo-preservation prior to fetal liver HSC sort, as performed in ES1, did not influence purity and HSC frequencies.

To protect cells from freezing damage, dimethyl sulfoxide (DMSO) was applied in ES1. Studies that investigated the effect of freezing and thawing of cells found that using DMSO as a cryoprotectant agent resulted in higher rates of cell survival after thawing, compared to other cryoprotectants (Falk et al. 2018). However, although purity and cell numbers were not affected by cell freezing, it seemed that the emerging HSC-reducing effect of APAP, as described in ES2 and ES3, was diminished by freezing.

Still, the suggested reduced numbers of HSC isolated from fetal livers after APAP exposition, observed in ES2 and ES3, is in line with literature: Studies in mice demonstrated a decrease in fetal liver HSC percentages following APAP exposition (Karimi et al. 2015). However, it has to be noted that this group isolated fetal liver HSC on E 16.5, which is 48 h later than in our project. Since on E 16.5 fetal HSC already begin to seed into the fetal thymus we decided for an earlier isolation time

point (E 14.5) (Solano et al. 2011). Nevertheless, also investigations in humans revealed lower HSC frequencies in cord blood when mothers were treated with APAP during pregnancy (Bremer et al. 2017).

Moreover, the application of NAC reversed the APAP-induced reduction of HSC frequencies in fetal livers. Besides the protective effects on maternal livers, this implied that NAC also affects fetal livers. Like APAP, NAC freely crosses the placental barrier. It has been demonstrated that infants of mothers treated with NAC after APAP intoxication had elevated levels of NAC in cord blood and cardiac blood. Furthermore, these children did not exhibit symptoms of APAP-related toxicity, although, it was shown that APAP, once got into the fetal circulation, is hepatically eliminated (Wilkes, Clark, and Herrera 2005, Horowitz et al. 1997). The authors subsequently concluded that NAC has also direct antidotal effects on the fetuses due to placental transfer, at least in humans (Horowitz et al. 1997).

4.6 Cryo-preservation of cells and treatment with DMSO seemed to accelerate cell maturation

Normally, T cells mature in the thymus. To investigate T cell differentiation *in vitro*, isolated fetal liver HSC were co-cultured with OP9 cells that express DLL1, a Notch-signaling pathway activator essential for T cell development (Kopan and Ilagan 2009).

Firstly, we showed in all experiments, that HSC lost their stem cell characteristics over time in the co-culture system, which indicated that HSC matured when incubated with OP9-DLL1 cells. However, interestingly it appeared that cryo-preserved cells already lost c-Kit and Sca-1 surface expression earlier than non-frozen cells. Studies on the pharmacology of DMSO reported that adding it to cell cultures enhances cell differentiation and function, especially of leukemic cells in mice, rats, and humans (Jacob and Herschler 1986). Furthermore, it was shown that DMSO treatment facilitates the responsiveness towards differentiation signals in pluripotent stem cells and therefore induces differentiation among all germ layers (Chetty et al. 2013). Hence, one can assume that cryo-preservation of HSC using DMSO also lead to increased sensitivity towards differentiation signals in the OP9-system.

4.7 APAP caused accelerated progression through DN stages while cryo-preservation and massive cell proliferation blunted this effect

Initially, maturing T cells neither express CD4 nor CD8. They belong to the DN cells (Shah and Zúñiga-Pflücker 2014).

Our data suggest that frequencies of general DN cells decreased over time in the co-culture system with OP9-DLL1 cells in all three experiments. This points out that cells attain a higher degree of maturity when exposed to OP9-DLL1 cells.

Strikingly, when HSC were cryo-preserved, lower frequencies of DN cells were detected on d0 of co-culture than when cells were not frozen. In this case, it is particularly worth mentioning that on d0 there were already cells expressing CD4 and simultaneously belonging to the HSC compartment. This evokes the impression that freezing and/ or treatment with DMSO facilitates surface expression of CD4 although cells still exhibit stem cell characteristics (c-Kit$^+$, Sca-1$^+$; discussed later). This would subsequently result in lower percentages of DN cells at the beginning of co-culture after cryo-preservation of fetal liver cells.

Interestingly, in ES2 NAC reversed the effect of APAP on the frequencies of DN cells on d4. Although fewer cells belonged to the DN cell stage when exposed to APAP (d4), this was not the case when cells were additionally treated with the antidote, NAC. Indeed, cell frequencies in the APAP+NAC group resembled that of cells only exposed to PBS. This emphasizes that besides of abrogating APAP-related effects in the mother, NAC also has a protective impact on fetal cells (Wilkes, Clark, and Herrera 2005, Horowitz et al. 1997).

HSC cultured in 48-well plates proliferated extensively most likely due to more sufficient cell-cell interactions. Cells were therefore maintained over 18 days, so that even less cells belonged to the DN cell stage at the end of co-culture, compared to the other two experiments. Consistent with literature, the longer HSC are exposed to DLL1 the better they can develop into more sophisticated T cell precursors (Kutleša et al. 2009).

Moreover, DN cells can be distinguished into DN1-4 stages *via* the expression of CD25 and CD44 (Shah and Zúñiga-Pflücker 2014).

Generally, this study demonstrated that HSC were able to progress through all DN cell stages when exposed to DLL1 in the OP9-system. This is consistent with the literature. Since it was found that DLL1 is essential for T cell development *in vivo*, stromal OP9 cells transduced with DLL1 became indispensable for T cell research as they provide ideal conditions to investigate T cell differentiation *in vitro* (Schmitt and Zúñiga-Pflücker, 2002, Schmitt et al. 2004).

Interestingly, only in ES2, it appeared that fetal liver HSC prenatally exposed to APAP progressed faster through the DN cell stages. On d4 significantly less APAP-exposed cells belonged to the DN1 stage. However, at that time point these cells were already more mature, namely, DN2 and DN3 cells.

Furthermore, on d7, higher frequencies of DN4 cells were observed in the APAP group than in the PBS and APAP+NAC treatment group.

Again, HSC development of APAP+NAC- and PBS-exposed cells was similar. Therefore, it appeared that NAC reversed the impact of APAP on the fetal liver HSC.

The accelerated maturation that appeared in ES2 but not in ES1 could be potentially attributed to the fact that cells were frozen in ES1: Although cryo-preservation of cells in DMSO is supposed to protect from severe damage, the freeze-thaw processes might cause molecular and structural alterations to the cells (Falk et al. 2018). For successful cryo-preservation with high survival rates after freezing, it is crucial that primary cells are in good condition, such as high viability (Ramos et al. 2014). In ES1, freezing challenged cells as they were exposed to tough environmental conditions. Cryo-preservation followed by thawing potentially selected HSC that were "healthier", according to the principle of the survival of the fittest. Taking this assumption into account, only cells might have been co-cultured with OP9-DLL1 cells that were not severely affected by APAP treatment.

Moreover, DMSO is also known for its properties to scavenge free radicals (Verheijen et al. 2019). High doses of APAP induce oxidative stress, which is one of the reasons for hepatocyte damage in APAP-related liver injury (Du, Ramachandran, and Jaeschke 2016). Given that APAP crosses placental barriers, it might cause formation of free radicals in fetal livers too. Therefore, DMSO treatment of processed fetal liver cells might reduce APAP-induced fetal hepatocyte damage by scavenging free radicals in the co-culture system, thus *ex vivo*.

Another peculiarity in the behavior of cryo-preserved HSC was observed: On d11 high frequencies of DN4 cells were detected. However, in ES3 these high DN4 cell frequencies were recorded when cells were maintained in co-culture with OP9-DLL1 cells for 18 days. Therefore, it seemed that cryo-preserved cells matured faster. This can be attributed to the fact that DMSO induces cell differentiation, which was represented by faster cell maturation in these studies (Jacob and Herschler 1986, Chetty et al. 2013).

Yet, it is striking that HSC co-cultured in smaller wells over 18 days (ES3) seemed to mature generally slower than HSC co-cultured in 24-well plates (ES1 and ES2). Apparently, in ES3 higher frequencies of DN2, DN3, and DN4 cells were only reached on d14 while DN1 cell frequencies only started to decline significantly on d14, as well.

In smaller wells, as applied in ES3, better cell-interactions facilitated proliferation (Breems et al. 1998, Vaidya and Kale 2015). This was subsequently followed by higher cell numbers per well. Eventually, concentrations of cytokines that were added to the medium, as described in ***Materials and Methods***, were not enough for sufficient cell maturation but for cell proliferation.

For example, Kutleša *et al.* showed that EML cells co-cultured with OP9-DLL1 cells require IL-7, SCF, and Flt3L for proliferation as well as for differentiation (Kutleša et al. 2009). Similarly, Wang *et al.* demonstrated the importance of those cytokines in T cell development in the OP9-system.

Furthermore, they revealed the distinct roles of each cytokine in the process of T cell maturation and they interestingly found that these effects on cell proliferation and differentiation are dose-dependent (Wang, Pierce, and Spangrude 2006). This might explain the decelerated T cell maturation in 48-well plates, as cytokine concentrations were eventually not sufficient for proliferating cells in ES3. Consequently, higher concentrations of cytokines should be applied in future experiments.

Moreover, accelerated progression through DN stages following maternal APAP administration, as in ES2, was not observed in ES3. High proliferation rates eventually altered cell culture conditions in ES3 in that manner that only HSC not affected by APAP survived. Potentially, these cells were less dependent on sufficient cytokine concentrations than isolated HSC that were severely damaged due to APAP exposure. This led to the selection and cultivation of only unaffected HSC, so that no significant difference between the treatment groups was seen.

An alternative explanation for lower frequencies of more mature T cell stages in ES3 is that progenitors proliferated extensively in 48-well plates so that percentages of less mature T cell stages remained higher. This potentially evoked the impression that T cells matured slower although T cell differentiation proceeded.

4.8 In co-culture with OP9-DLL1 cells, only immature CD8 T cells evolved

After developing T cells passed the DN stages they give rise to immature CD8 SP cells that do not express TCR-β on their surfaces yet and are referred to as ISP8 (Gegonne et al. 2018).

In our studies, T cells exclusively expressing CD8 on surfaces were analyzed. In all experiments, it was evident, that cells upregulated CD8-expression as HSC were co-cultured with OP9-DLL1 cells. However, when TCR-β-expression of $CD8^+$ cells was assessed, it turned out that TCR-β was absent, therefore these CD8 SP cells were identified as ISP8, the intermediate state between DN and DP cells (Gegonne et al. 2018).

Interestingly, when fetal liver cells were cryo-preserved before the final HSC sort, frequencies of CD8 SP cells were lower at all reanalysis time points than in the other two experiments. At first, this evoked the impression that cells were not able to progress beyond the state of DN cells.

On the contrary, when higher maturation stages were considered, e.g., DP cells, cryo-preserved cells already persisted in this state. Comparing DP cells of all experiments, the maximum of DP frequencies of cryo-preserved cells was considerably higher than when cells were not frozen. Again, these data supported the notion that cryo-preserved cells matured faster. In fact, it seemed that developing HSC almost bypassed the ISP8 state, as frequencies were rather low at any time point of reanalysis. Again, this could be explained by the application of DMSO which is known to drive differentiation (Jacob and Herschler 1986).

In the other two experiments where non-frozen cells were co-cultured and analyzed, ISP8 cells differentiated as well. However, frequencies of ISP8 cells were considerably elevated compared to ES1. Respectively, relatively more cells were in the ISP8 stage, as they did not give rise to more mature cells, yet.

In ES2, the maximum frequency of ISP8 cells was reached on d4. However, looking at DP frequencies it appeared that those cells had higher frequencies on d7, indicating that cells matured from ISP8 cells to DPs during co-culture. Furthermore, APAP-exposed HSC seemed to be faster in differentiation, as there were significantly increased frequencies of ISP8 cells on d4 compared to the other two treatment groups. This was also underlined by DP frequencies: On d7 there tended to be higher frequencies of DP cells in the APAP group compared to the two other treatment groups. However, here the difference was not significant.

Treatment with the antidote, NAC also reversed APAP-induced alterations in ISP8 cell development. Again, suggesting that NAC reversed the effect of APAP.

Fetal liver HSC co-cultured with OP9-DLL1 cells in 48-well plates proliferated extensively, which resulted in more reanalysis time points. In ES3 significant increase in ISP8 cell frequencies was only observed on d11 of co-culture, whereas significant growth in ISP8 frequencies in ES2 was already seen on d4 and d7. However, on d18 the majority of cells developed into ISP8 cells. These high ISP8 frequencies were not reached in ES2, where HSC were only co-cultured for 7 days.

This observation was also found by a group that co-cultured the multipotent EML (erythroid, myeloid, lymphoid) cell line. They demonstrated that cells needed more than 7 days for CD4 and CD8 upregulation (Kutleša et al. 2009). Therefore, in future experiments, longer periods of co-culture should be considered.

4.9 In co-culture with OP9-DLL1 cells maturing T cells did not undergo positive-selection

At the stage of DP cells, most of the cells have successfully undergone TCR gene rearrangement and express a functional TCR on the cell surface (Sawicka et al. 2014). On the one hand, DPs that recognize MHC-self-peptide complexes with low affinity endure positive-selection. On the other hand, DP cells with too high affinities to MHC-self-peptide complexes are neglected and eliminated by negative-selection. Therefore, DP cells can be divided into pre-/ and post-selection DPs (Sawicka et al. 2014).

Our data indicated that T cells developing in the OP9-system did not undergo positive-selection because the majority of DP cells persisted in the pre-selection DP state. However, conspicuously, especially in ES2 and ES3 there were DPs that were neither identified as pre-selection nor as post-selection DPs.

The pre- and post-selection states are distinguished through surface expression of CD5 and CD69 (Gangadharan et al. 2006). Studies demonstrated that the extent of CD5-expression is reliant on TCR signaling. Experiments in mice deficient for MHC-I and MHC-II demonstrated that DP cells expressed low levels of CD5. Subsequently, the authors concluded that continuous signaling *via* the TCR or pre-TCR is required to maintain intermediate levels of CD5 expression on DP cells (Azzam et al. 1998).

Furthermore, literature confirmed that culture systems with OP9-DLL1 cells fail to support all aspects of proper positive-selection as especially MHC-II-expression on OP9 cells is missing (de Pooter and Zúñiga-Pflücker, 2007, Kutleša et al. 2009). Taking both these aspects into consideration, it is likely that lacking of MHC-II molecules impaired continuous TCR signaling in our study resulting in DP cells neither being identified as CD5^{int} nor CD5^{+}, thus as pre-or post-selection DP cells. Moreover, insufficient MHC-II-expression in the OP9-system might be responsible for the generation of DPs that were not able to progress through positive-selection.

4.10 CD4-expression requires proper MHC-II signaling

Frequencies of CD4-expressing T cells did not increase over time in all three experiments. When fetal liver HSC were cryo-preserved before final purification by FACS, more than 30 % expressed CD4 at the beginning of co-culture, while cells were actually identified as HSC (lin^{-}, c-Kit^{-}, Sca-1^{-}). Interestingly, studies in mice showed that there are pluripotent stem cells in bone marrow that partly express CD4 on their surfaces (Wineman et al. 1992). Therefore, it cannot be ruled out that stem cells are simultaneously able to express CD4. Having this in mind, cryo-preservation and treatment with DMSO could potentially initiate CD4-expression on pluripotent HSC. Because OP9 cells lack MHC-II-expression, maturing T cells do not get signals for CD4 maintenance which may have caused CD4 downregulation during co-culture of cryo-preserved cells.

In the other two experiments (ES2 and ES3), it was observed that HSC scarcely expressed CD4 on the cell surface. This was also demonstrated by other groups. They similarly showed that T cells developing in the OP9-system were more likely to express CD8 instead of CD4. Moreover, T cells expressing CD4 turned out to be immature intermediates (Schmitt and Zúñiga-Pflücker 2002). This again reflects that OP9-DLL1 cells without MHC-II-expression were not able to induce differentiation of mature CD4^{+} T cells in these studies.

4.11 DLL1-expression is essential for T cell differentiation

Notch-ligands, such as DLL1, are essential for T cells to evolve. The expression of those Notch-pathway activators suppresses B cell development and facilitates T cell differentiation instead (Brandstadter and Maillard 2019). To confirm the importance of DLL1 in T cell differentiation, fetal liver HSC were also co-cultured with OP9 cells that did not express DLL1 (OP9-LIE cells). Our data confirmed that while cells exposed to DLL1 lost the DN state, HSC that were not exposed to DLL1 did not get past the DN stage in order to become more mature T cell progenitors.

4.12 Conclusions for future investigations

Summarizing all the results, we demonstrated that under every experimental condition fetal liver HSC were able to differentiate in co-culture with OP9-DLL1 cells. Moreover, we showed that under specific experimental conditions maternal APAP intake during pregnancy affected fetal T cell development and it seemed that it accelerated T cell maturation. However, this effect was only observed in one experiment.

Interestingly, additional NAC treatment reversed APAP-induced effects in dams and offspring. It prevented liver injury in pregnant mice, and in fetuses, it reversed APAP-induced T cell differentiation alterations.

Moreover, to establish optimal conditions for HSC cultivation and T cell maturation, three different experimental setups were tested and evaluated.

Cryo-preservation of fetal liver cells prior to final HSC sort seemed not to affect cells in their viability and the ability for T cell differentiation. However, it is widely known that cryo-preservation and application of DMSO as a cryo-protectant agent might affect cells. Moreover, DMSO can manipulate behavior of cells in the co-culture system as it was shown to enhance cell differentiation (Jacob and Herschler 1986).

Identification of triggers that potentially alter T cell differentiation in the OP9-system can be difficult. Furthermore, discrimination whether changes in T cell development are induced due to cryo-preservation and DMSO treatment, APAP application, or other external and internal factors are challenging and therefore, cryo-preservation of cells should be avoided in future experiments.

Additionally, fetal liver HSC were co-cultured with OP9-DLL1 cells in 48-well plates where wells were smaller. We found that cells proliferated more sufficiently which resulted in more reanalysis time points. Because T cells need time to mature properly (Kutleša et al. 2009), it is advantageous to co-culture HSC for at least 14 days to be able to analyze all differentiation stages and to identify potential changes in fetal immune ontogeny caused by maternal APAP administration. In future experiment is should be considered to adjust cytokine concentrations to higher cells numbers.

In order to obtain more reliable results that allow to make clear statements about APAP-induced changes in fetal T cell differentiation, it is necessary to perform more experiments under uniform conditions. This will increase sample sizes indispensable for statistically significant results.

If future experiments can reproduce the incipient observations that were made in these studies and if they prove the influence of APAP on fetal immune ontogeny, new treatment guidelines regarding maternal APAP treatment during pregnancy are inevitable. Evidence of the protective effect of additional NAC treatment would revolutionize analgesic treatment in pregnancy, as it potentially provides a solution to the problem of APAP application in pregnant women which is potentially harmful to the mother and the child.

5 Outlook

These studies examined the effect of maternal APAP application during pregnancy on fetal T cell differentiation using the OP9-DLL1 co-culture system. To identify potential alterations in fetal immune ontogeny, it was necessary to establish a suitable experimental setup.

As other groups have already proven, the results of these investigations showed that fetal liver HSC incubated with DLL1-expressing OP9 cells were able to give rise to T cells. Moreover, it became apparent that APAP-exposed fetal liver HSC tended to be faster in maturation than unexposed cells. In contrast, treatment with the APAP-specific antidote, NAC, seemed to reverse the effects of APAP. This was shown when maternal liver damage was assessed but also when T cell differentiation in the OP9-system was analyzed: In terms of T cell differentiation behavior, cells exposed to APAP+NAC resembled those exposed to PBS, when compared to APAP-treated cells.

Nonetheless, further investigations have to be performed to identify clear mechanisms of how *in utero* APAP exposition influences immune development in offspring.

Although these studies contribute to the development of a suitable experimental setup to investigate APAP-specific effects on T cell development, more experiments need to be done which improve this *in vitro* model. When a model was established, that eliminated all confounding factors and potentially demonstrated differences in T cell differentiation due to APAP treatment, the analysis of genes that regulate T cell differentiation and apoptosis during the different developmental stages would be of great interest. This would help to understand the clear mechanisms that play a role in T cell differentiation and how they were potentially modified by APAP application.

To identify whether APAP itself, the toxic intermediate, NAPQI, or other factors are involved in immune alterations in the offspring, NAPQI should be measured in maternal blood serum as well as in fetal livers.

Both the general act of injection of APAP to pregnant mice and the subsequent liver damage is likely to induce stress reactions and inflammatory processes in dams, leading to secretion of stress hormones but also inflammatory factors. Those analyses possibly help to determine a direct or indirect effect of maternal APAP application to the offspring, or both.

Another point of interest is whether the effect of APAP can be simulated *in vitro*. For this purpose, HSC can be treated with APAP and NAPQI and then co-cultured with OP9-DLL1 cells. This would even help to modify the experimental model, as it makes it independent on external conditions that potentially influence the analyses, such as stress induction through injection of pregnant mice, or other animal-related factors. To simulate the protective effect of NAC, it should also be applied to HSC *in vitro*.

As epidemiological studies found a higher susceptibility towards wheezing and childhood asthma when *in utero* exposed to APAP (Eyers et al. 2011), the examination of children that were prenatally exposed to APAP would be useful to transfer *in vitro* studies *in vivo*. Although reduced numbers of HSC in cord blood were already found after maternal APAP intake in humans (Bremer et al. 2017), the exploration of different immune cells, such as eosinophils and leukocytes would shed more light on the mechanisms. This would be particularly important since studies in mice demonstrated more severe airway inflammation when prenatally exposed to APAP, as demonstrated by leukocyte and eosinophil infiltration into the airways (Karimi et al. 2015). Also, the investigation of T_{reg} would be interesting, as these cells regulate the immune reaction, and seem to play a crucial role in the development of asthma (Zhao and Wang 2018). Finally, the main goal of future experiments should be to identify the link between altered T cell differentiation and asthma development after prenatal APAP exposition.

As APAP-induced immune deviation in offspring is of great interest, in general, the alterations in monocytes and macrophages are also focus of ongoing research. In this field, co-culture systems with OP9 cells are also applied.

Taking all these aspects into consideration, the application of APAP during pregnancy does not seem to be as safe as initially expected. Despite its importance to treat fever and pain, which may also have adverse effects on the fetus, the indication for treatment with APAP in pregnant women should be thoroughly evaluated. Moreover, by providing clear information about APAP to pregnant women and the general population, the risk for negative effects can be reduced.

6 Summary

Acetaminophen (APAP) is a frequently applied drug that treats fever and pain. In pregnancy, it is the only analgesic that is licensed throughout all three trimesters as it is considered to be safe for the mother as well as for the child. However, epidemiological studies showed impaired health in offspring whose mothers were treated with APAP in pregnancy, such as a higher risk for childhood asthma. As the development of asthma is T cell-dependent, the aim of this thesis was to identify alterations in T cell differentiation in offspring that were prenatally exposed to APAP.

To establish a suitable experimental setup that provides ideal conditions for these investigations, three independent experiments with slightly different protocols were performed.

In general, allogeneically mated female mice were treated on embryonic day (E) 12.5. They were either injected with APAP or PBS intraperitoneally. To investigate a potential protective effect of additional treatment with N-acetylcysteine (NAC), the antidote of APAP, pregnant mice were injected with APAP and NAC. On E 14.5 dams were sacrificed. Maternal livers and fetuses were collected for further processing. For T cell differentiation, HSC, isolated from fetal livers, were co-cultured with OP9-DLL1 cells and analyzed *via* FACS.

APAP induced liver damage in pregnant mice assessed by elevated serum ALT levels and hepatocyte necrosis. In contrast, protective effects of additional NAC treatment on maternal livers were observed. Moreover, dams treated with APAP gained less weight over the course of pregnancy than animals in the other treatment groups.

Additionally, we could demonstrate that fetal liver HSC exposed to DLL1-expressing OP9 cells lost their stem cell characteristics (c-Kit$^+$, Sca-1$^+$) and gave rise to T cell precursors. They distinctively progressed through the double negative (DN) stages, neither expressing CD4 nor CD8. However, as cells matured, they were more likely to express CD8 on their cell surface rather than CD4. These CD8-expressing cells were identified as immature CD8 cells, as they were lacking TCR-β. In general, cryo-preserved fetal liver cells were not disadvantaged in terms of survival and purity, however, they seemed to mature faster in the OP9-system. Non-frozen cells that were co-cultured with OP9-DLL1 cells in 48-well plates proliferated extensively, which allowed more time points for reanalysis. Although they proliferated sufficiently it appeared that differentiation of T cells was decelerated compared to non-frozen cells incubated in 24-well plates. Furthermore, cells co-cultured in 24-well plates showed accelerated T cell differentiation when prenatally exposed to APAP. Here, a protective effect of additional NAC treatment was observed.

These data indicated that prenatal APAP exposition affected fetal T cell differentiation, while the application of NAC reversed APAP-specific effects and might therefore have protective properties. However, in order to verify these findings, further *in vitro* experiments have to be performed under well-defined conditions.

7 Zusammenfassung

Acetaminophen (APAP) ist ein häufig eingesetztes Schmerz- und Fiebermittel. Als einziges Schmerzmedikament ist es während der gesamten Schwangerschaft zugelassen. Studien zeigten jedoch, dass die Gesundheit von Kindern, dessen Mütter während der Schwangerschaft mit APAP behandelt wurden, beeinträchtigt wird. Demnach haben diese ein höheres Risiko für die Entwicklung von T Zell-vermitteltem Asthma. Ziel dieser Arbeit war es, Veränderungen in der T Zell Differenzierung bei Nachkommen, die vor der Geburt APAP ausgesetzt waren, zu identifizieren.

Um ein geeignetes experimentelles Design zu etablieren, wurden drei unabhängige Experimente, mit etwas unterschiedlichen Protokollen, durchgeführt.

Allogen verpaarte Mäuse wurden an Gestationstag (E) 12.5 behandelt. Entweder wurde APAP, PBS oder APAP und zusätzlich das Antidot, N-acetylcystein (NAC), intraperitoneal injiziert. An E 14.5 wurden mütterliche Lebern und Föten entnommen. Zur Differenzierung von T Zellen aus fötalen Leber HSC wurden diese mit OP-DLL1 Zellen kultiviert und durchflußzytometrisch analysiert.

APAP verursachte einen Leberschaden in den schwangeren Mäusen. Im Gegensatz dazu wurde ein schützender Effekt auf das mütterliche Lebergewebe durch die Gabe von NAC beobachtet. Im Vergleich zu den anderen Gruppen, nahmen Mütter, die ausschließlich mit APAP behandelt wurden, weniger Gewicht während der Schwangerschaft zu.

Die Exposition von fötalen Leber HSC gegenüber OP9-DLL1 Zellen führte dazu, dass sie ihre Stammzell-Eigenschaften (c-Kit$^+$, Sca-1$^+$) verloren. Sie entwickelten sich zu T Zell-Vorläufern, wobei sie die einzelnen Stadien der doppelt negativen (DN) Zellen durchliefen. Zudem exprimierten die heranreifenden T Zellen eher CD8 als CD4 auf ihrer Oberfläche. Diese Zellen wurden jedoch als unreife CD8 Zellen identifiziert, da sie noch keinen TCR-β besaßen.

Fötale HSC hatten keinen Nachteil, wenn sie nach der Entnahme und Aufarbeitung eingefroren wurden, bevor sie mit OP9-DLL1 Zellen kultiviert wurden. Im Hinblick auf Überlebensrate und Reinheit konnten keine Unterschiede zu den frisch-isolierten HSC festgestellt werden. Dennoch, reiften sie in der Co-Kultur schneller heran. Nicht-gefrorene HSC, die auf 48-well Platten mit den OP9-DLL1 Zellen ausgesät wurden, proliferierten, sodass die Reanalysen der Zellen an mehr Zeitpunkten stattfinden konnten. Trotz der Proliferation, war der Reifungsprozess bei dieser Zellpopulation langsamer als bei fötalen Leber HSC, die nicht gefroren, aber in 24-well Platten kultiviert wurden: Hier zeigten frische Zellen außerdem ein schnelleres Reifungsverhalten, wenn sie *in utero* gegenüber APAP exponiert waren. Außerdem konnte hier ein präventiver Einfluss von NAC bestätigt werden.

Die Daten weisen darauf hin, dass die pränatale Exposition mit APAP einen Einfluss auf die fötale T Zell Entwicklung hat. Zudem wurde dieser Effekt durch NAC aufgehoben, was dafürspricht, dass diese Substanz eventuell schützende Eigenschaften aufweist. Dennoch müssen weitere Versuche unter gleichen Bedingungen erfolgen, die diese Erkenntnisse bestätigen.

8 References

Anderson B J (2008) Paracetamol (Acetaminophen): Mechanisms of Action. *Paediatric Anaesthesia*. 18: 915-921.

Artavanis-Tsakonas S, Rand M D, and Lake R J (1999) Notch Signaling: Cell Fate Control and Signal Integration in Development. *Science.* 284(5415): 770-776.

Azzam H S, Grinberg A, Lui K, Shen H, Shores E W, and Love P E (1998) CD5 Expression Is Developmentally Regulated by T Cell Receptor (TCR) Signals and TCR Avidity. *Journal of Experimental Medicine*. 188(12): 2301-23111.

Azzoni E, Frontera V, McGrath K E, Harman J, Carrelha J, Nerlov C, Palis J, Jacobsen S E W, and Bruijn M (2018) Kit Ligand Has a Critical Role in Mouse Yolk Sac and Aorta–Gonad–Mesonephros Hematopoiesis. *EMBO Reports*. 19(10): e45477.

Bessems J G M, and Vermeulen N P E (2001) Paracetamol (Acetaminophen)-Induced Toxicity: Molecular and Biochemical Mechanisms, Analogues and Protective Approaches. *Critical Reviews in Toxicology*. 31(3): 55-138.

Brandstadter J D, and Maillard I (2019) Notch Signalling in T Cell Homeostasis and Differentiation. *Open Biology*. 9(11): 190187.

Bray S J (2006) Notch Signalling: A Simple Pathway Becomes Complex. *Nature Reviews Molecular Cell Biology*. 7(9): 678-689.

Breems D A, Blokland E A W, Siebel K E, Mayen A E M, Engels L J A, and Ploemacher R E (1998) Stroma-Contact Prevents Loss of Hematopoietic Stem Cell Quality during Ex Vivo Expansion of CD34+ Mobilized Peripheral Blood Stem Cells. *Blood*. 91(1): 111-117.

Bremer L, Goletzke J, Wiessner C, Pagenkemper M, Gehbauer C, Becher H, Tolosa E, et al. (2017) Paracetamol Medication During Pregnancy: Insights on Intake Frequencies, Dosages and Effects on Hematopoietic Stem Cell Populations in Cord Blood From a Longitudinal Prospective Pregnancy Cohort. *EBioMedicine*. 26: 146-151.

Brune K, Renner B, and Tiegs G (2015) Acetaminophen/Paracetamol: A History of Errors, Failures and False Decisions. *European Journal of Pain (United Kingdom)*. 19(7): 953-965.

Cheelo M, Lodge C J, Dharmage S C, Simpson J A, Matheson M, Heinrich J, and Lowe A J (2015) Paracetamol Exposure in Pregnancy and Early Childhood and Development of Childhood Asthma: A Systematic Review and Meta-Analysis. *Archives of Disease in Childhood*. 100(1): 81-89.

Chetty S, Walton Pagliuca F, Honore C, Kweudjeu A, Rezania A, and Melton D A (2013) A Simple Tool to Improve Pluripotent Stem Cell Differentiation. *Nature Methods*. 10(6): 553-556.

Choi K, Kennedy M, Kazarov A, Papadimitriou J C, and Keller G (1998) A Common Precursor for Hematopoietic and Endothelial Cells. *Development*.125(4): 725-732.

Ciofani M, and Zúñiga-Pflücker J C (2007) The Thymus as an Inductive Site for T Lymphopoiesis. *Annual Review of Cell and Developmental Biology*. 23: 463-493.

Ciriza J, Thompson H, Petrosian R, Manilay J O, and García-Ojeda M E (2013) The Migration of Hematopoietic Progenitors from the Fetal Liver to the Fetal Bone Marrow: Lessons Learned and Possible Clinical Applications. *Experimental Hematology*. 41(5): 411-423.

Cosmi L, Maggi L, Santarlasci V, Liotta F, and Annunziato F (2014) T Helper Cells Plasticity in Inflammation. *Cytometry Part A*. 85(1): 36-42.

Cuny H, Rapadas M, Gereis J, Martin E M M A, Kirk R B , Shi H, and Dunwoodie S L (2020) NAD Deficiency Due to Environmental Factors or Gene–Environment Interactions Causes Congenital Malformations and Miscarriage in Mice. *Proceedings of the National Academy of Sciences of the United States of America*. 117(7): 3738-3747.

Dong H, Haining R L, Thummel K E, Rettie A E, and Nelson S D (2000) Involvement of Human Cytochrome P450 2D6 in the Bioactivation of Acetaminophen. *Drug Metabolism and Disposition*. 28(12): 1397-1400.

Dorsch M, Zheng G, Yowe D, Rao P, Wang Y, Shen Q, Murphy C, et al. (2002). Ectopic Expression of Delta4 Impairs Hematopoietic Development and Leads to Lymphoproliferative Disease. *Blood*. 100(6): 2046-2055.

Du K, Ramachandran A, and Jaeschke H(2016) Oxidative Stress during Acetaminophen Hepatotoxicity: Sources, Pathophysiological Role and Therapeutic Potential. *Redox Biology*. 10: 148-156.

Ewijk van W, Shores E W, and Singer A(1994) Crosstalk in the Mouse Thymus. *Immunology Today*. 15(5): 214-217.

Eyers S, Weatherall M, Jefferies S, and Beasley R (2011) Paracetamol in Pregnancy and the Risk of Wheezing in Offspring: A Systematic Review and Meta-Analysis. *Clinical and Experimental Allergy*. 41(4): 482-489.

Fahy J V (2015) Type 2 Inflammation in Asthma-Present in Most, Absent in Many. *Nature Reviews Immunology*. 15(1): 57-65.

Falk M, Falková I, Kopečná O, Bačíková A, Pagáčová E, Šimek D, Golan M, et al. (2018) Chromatin Architecture Changes and DNA Replication Fork Collapse Are Critical Features in Cryopreserved Cells That Are Differentially Controlled by Cryoprotectants. *Scientific Reports*. 8(1): 14694.

Flora S De, Izzotti A, Agostini F D, and Balansky R M (2001) Mechanisms of N-Acetylcysteine in the Prevention of DNA Damage and Cancer, with Special Reference to Smoking-Related End-Points. *Carcinogenesis*. 22(7): 999-1013.

Fowlkes B J, and Robey E A (2002) A Reassessment of the Effect of Activated Notch1 on CD4 and CD8 T Cell Development. *The Journal of Immunology*.169(4): 1817-1821.

Gangadharan D, Lambolez F, Attinger A, Wang-Zhu Y, Sullivan B A, and Cheroutre H 2006 Identification of Pre- and Postselection TCRαβ+ Intraepithelial Lymphocyte Precursors in the Thymus. *Immunity*.25(4): 631-641.

Gao X, Xu C, Asada N, and Frenette P S (2018) The Hematopoietic Stem Cell Niche: From Embryo to Adult. *Development (Cambridge)*.145(2): dev139691.

Gegonne A, Chen Q R, Dey A, Etzensperger R, Tai X, Singer A, Meerzama D, Ozato K, and Singer D S (2018) Immature CD8 Single-Positive Thymocytes Are a Molecularly Distinct Subpopulation, Selectively Dependent on BRD4 for Their Differentiation. *Cell Reports*. 24(1): 117-129.

Gelotte C K, Auiler J F, Lynch J M, Temple A R, and Slattery J T (2007) Disposition of Acetaminophen at 4, 6, and 8 g/Day for 3 Days in Healthy Young Adults. *Clinical Pharmacology and Therapeutics*. 81(6): 840-848.

Givan A L (2011) Flow Cytometry: An Introduction." *Methods in Molecular Biology (Clifton, N.J.)*. 699: 1-29.

Graham G G, and Scott K F (2005) Mechanism of Action of Paracetamol." *American Journal of Therapeutics*. 12(1): 46-55.

Grimbert S, Fisch C, Deschamps D, Berson A, Fromenty B, Feldmann G, and Pessayre D (1995) Effects of Female Sex Hormones on Mitochondria: Possible Role in Acute Fatty Liver of Pregnancy. *American Journal of Physiology - Gastrointestinal and Liver Physiology*. 268(1): G107-G115.

Han D, Dara L, Win S, Than T A, Yuan L, Abbasi S Q, Liu Z X, and Kaplowitz N (2013) Regulation of Drug-Induced Liver Injury by Signal Transduction Pathways: Critical Role of Mitochondria. *Trends in Pharmacological Sciences*. 34(4): 243-253.

Hay-Schmidt A, Ejlstrup Finkielman O T, Jensen B A H, Høgsbro C F, Holm J B, Haurum Johansen K, Jensen T K, et al. (2017) Prenatal Exposure to Paracetamol/Acetaminophen and Precursor Aniline Impairs Masculinisation of Male Brain and Behaviour *Reproduction*. 154(2): 145-152.

Hinz B, Cheremina O, and Brune K (2008) Acetaminophen (Paracetamol) Is a Selective Cyclooxygenase-2 Inhibitor in Man. *FASEB Journal*. 22(2): 383-390.

Hodgman M J, and Garrard A R(2012) A Review of Acetaminophen Poisoning. *Critical Care Clinics*. 28(4): 499-516.

Holgate S T (2012) Innate and Adaptive Immune Responses in Asthma. *Nature Medicine*.18(5): 673-683.

Horowitz R S, Dart R C, Jarvie D R, Bearer C F, and Gupta U(1997) Placental Transfer of N-Acetylcysteine Following Human Maternal Acetaminophen Toxicity. *Journal of Toxicology - Clinical Toxicology*. 35(5): 447-451.

Hosokawa H, and Rothenberg E V (2018) Cytokines, Transcription Factors, and the Initiation of T-Cell Development. *Cold Spring Harbor Perspectives in Biology*. 10(5): a028621.

Hosoya T, Kuroha T, Moriguchi T, Cummings D, Maillard I, Lim K C, and Engel J D (2009) GATA-3 Is Required for Early T Lineage Progenitor Development. *Journal of Experimental Medicine*. 206(13): 2987-3000.

Imaeda A B, Watanabe A, Sohail M A, Mahmood S, Mohamadnejad M, Sutterwala F S, Flavell R A, and Mehal W Z (2009) Acetaminophen-Induced Hepatotoxicity in Mice Is Dependent on Tlr9 and the Nalp3 Inflammasome. *Journal of Clinical Investigation*. 119(2): 305-314.

Jacob S W, and Herschler R (1986) Pharmacology of DMSO. *Cryobiology*.23(1): 14-27.

Jensen M S, Cristina Rebordosa C, Thulstrup A M, Toft G, Sørensen H T, Bonde J P, Henriksen T B, and Olsen J (2010) Maternal Use of Acetaminophen, Ibuprofen, and Acetylsalicylic Acid during Pregnancy and Risk of Cryptorchidism. *Epidemiology*. 21(6): 779-785.

Kanamori M, Nakatsukasa H, Okada M, Lu Q, and Yoshimura A (2016) Induced Regulatory T Cells: Their Development, Stability, and Applications. *Trends in Immunology*. 37(11): 803-811.

Karimi K, Keßler T, Thiele K, Ramisch K, Erhardt A, Huebener P, Barikbin R, Arck P, and Tiegs G (2015) Prenatal Acetaminophen Induces Liver Toxicity in Dams, Reduces Fetal Liver Stem Cells, and Increases Airway Inflammation in Adult Offspring. *Journal of Hepatology*. 62(5): 1085-1091.

Kodama H, Nose M, Niida S, Nishikawa S, and Nishikawa S (1994) Involvement of the C-Kit Receptor in the Adhesion of Hematopoietic Stem Cells to Stromal Cells. *Experimental Hematology*. 22(10): 879-884.

Kondo K, Ohigashi I, and Takahama Y (2019) Thymus Machinery for T-Cell Selection. *International Immunology*. 31(3): 119-125.

Kopan R, and Ilagan M X G (2009) The Canonical Notch Signaling Pathway: Unfolding the Activation Mechanism." *Cell*. 137(2): 216-233.

Kristensen D M, Mazaud-Guittot S, Gaudriault P, Lesné L, Serrano T, Main K M, and Jégou B (2016) Analgesic Use-Prevalence, Biomonitoring and Endocrine and Reproductive Effects. *Nature Reviews Endocrinology*.12(7): 381-393.

Kristensen D M, Hass U, Lesn L, Lottrup G, Rosenskjold Jacobsen P, Desdoits-Lethimonier C, Boberg J, et al. (2011) Intrauterine Exposure to Mild Analgesics Is a Risk Factor for Development of Male Reproductive Disorders in Human and Rat. *Human Reproduction*. 26(1): 235-244.

Kumar B V, Connors T J, and Farber D L(2018) Human T Cell Development, Localization, and Function throughout Life. *Immunity*.48(2): 202-213.

Kutleša S, Zayas J, Valle A, Levy R B, and Jurecic R (2009) T-Cell Differentiation of Multipotent Hematopoietic Cell Line EML in the OP9-DL1 Coculture System. *Experimental Hematology*. 37(8): 909-923.

Larson A M, Polson J, Fontana R J, Davern T J, Lalani E, Hynan L S, Reisch J S, et al. (2005) Acetaminophen-Induced Acute Liver Failure: Results of a United States Multicenter, Prospective Study. *Hepatology*. 42(6): 1264-1272.

Lee G R (2018) The Balance of Th17 versus Treg Cells in Autoimmunity." *International Journal of Molecular Sciences*. 19(3): 730.

Lee W M (2004) Acetaminophen and the U.S. Acute Liver Failure Study Group: Lowering the Risks of Hepatic Failure. *Hepatology*. 40(1): 6-9.

Lee W M (2017) Acetaminophen (APAP) Hepatotoxicity—Isn't It Time for APAP to Go Away? *Journal of Hepatology*. 67(6): 1324-1331.

Lewkowich I P, Herman N S, Schleifer K W, Dance M P, Chen B L, Dienger K M, Sproles A A, et al. (2005) CD4+CD25+ T Cells Protect against Experimentally Induced Asthma and Alter Pulmonary Dendritic Cell Phenotype and Function. *Journal of Experimental Medicine*. 202(11): 1549-1561.

Li D K, Ferber J R, Odouli R, and Quesenberry C (2018) Use of Nonsteroidal Antiinflammatory Drugs during Pregnancy and the Risk of Miscarriage. *American Journal of Obstetrics and Gynecology*. 219(3): 275.e1-275.e8.

Li P, Spolski R, Liao W, and Leonard W J (2014) Complex Interactions of Transcription Factors in Mediating Cytokine Biology in T Cells. *Immunological Reviews*. 261(1): 141-156.

Liew Z, Ritz B, Rebordosa C, Lee P C, and Olsen J (2014) Acetaminophen Use during Pregnancy, Behavioral Problems, and Hyperkinetic Disorders. *JAMA Pediatrics*. 168(4): 313-320.

Mahe E, Pugh T, and Kamel-Reid S (2018) T Cell Clonality Assessment: Past, Present and Future. *Journal of Clinical Pathology*. 71(3): 195-200.

Mazaleuskaya L L, Sangkuhl K, Thorn C F, Fitzgerald G A, Altman R B, and Klein T E (2015) PharmGKB Summary: Pathways of Acetaminophen Metabolism at the Therapeutic versus Toxic Doses. *Pharmacogenetics and Genomics*.25(8): 416-426.

McGill M R, and Jaeschke H (2013) Metabolism and Disposition of Acetaminophen: Recent Advances in Relation to Hepatotoxicity and Diagnosis. *Pharmaceutical Research*. 30(9):2174-2187.

Mims J W (2015) Asthma: Definitions and Pathophysiology." *International Forum of Allergy and Rhinology*. 5: Suppl1: S2-6.

Mittrücker H W, Visekruna A, and Huber M 2014. "Heterogeneity in the Differentiation and Function of CD8+ T Cells." *Archivum Immunologiae et Therapiae Experimentalis* 62(6): 449-458.

Mohtashami M, Zarin P, and Zúñiga-Pflücker J C (2016) Induction of T Cell Development in Vitro by Delta-like (Dll)-Expressing Stromal Cells. In *T-Cell Development: Methods and Protocols*. 1323: 159-167.

Mossanen J C, and Tacke F (2015) Acetaminophen-Induced Acute Liver Injury in Mice. *Laboratory Animals*. 49(Suppl1): 30-36.

Nakano T (1995) Lymphohematopoietic Development from Embryonic Stem Cells in Vitro. *Seminars in Immunology*. 7(3): 197-203.

Nowell C S, Farley A M, and Blackburn C C (2007) Thymus Organogenesis and Development of the Thymic Stroma. *Methods Mol Biol.* 380: 125-162.

Okeke E B, and Uzonna J E (2019) The Pivotal Role of Regulatory T Cells in the Regulation of Innate Immune Cells. *Frontiers in Immunology*. 10: 680.

Otto G P, Rathkolb B, Oestereicher M A, Lengger C J, Moerth C, Micklich K, Fuchs H, Gailus-Durner V, Wolf E, and Hrabě De Angelis M (2016) Clinical Chemistry Reference Intervals for C57BL/6J, C57BL/6N, and C3HeB/FeJ Mice (Mus Musculus). *Journal of the American Association for Laboratory Animal Science*. 55(4): 375-386.

Patra A K, Avots A, Zahedi R P, Schüler T, Sickmann A, Bommhardt U, and Serfling E (2013) An Alternative NFAT-Activation Pathway Mediated by IL-7 Is Critical for Early Thymocyte Development. *Nature Immunology*. 14(2): 127-135.

Pei Y, Liu H, Yang Yi, Yang Ya, Jiao Y, Tay F R, and Chen J (2018) Biological Activities and Potential Oral Applications of N-Acetylcysteine: Progress and Prospects. *Oxidative Medicine and Cellular Longevity*. 2018: 2835787.

Pérez-Giraldo C, Rodriguez-Benito A, Morán F J, Hurtado C, Blanco M T, and Gómez-García A C (1997) Influence of N-Acetylcysteine on the Formation of Biofilm by Staphylococcus Epidermidis. *Journal of Antimicrobial Chemotherapy*. 39(5): 643-646.

Persky V, Piorkowski J, Hernandez, Chavez E N, Wagner-Cassanova C, Vergara C, Pelzel D, Enriquez R, Gutierrez S, and Busso A (2008) Prenatal Exposure to Acetaminophen and Respiratory Symptoms in the First Year of Life. *Annals of Allergy, Asthma and Immunology*. 101(3): 271-278.

Petersen T G, Liew Z, Nybo Andersen A M, Andersen G L, Kragh Andersen P, Martinussen T, Olsen J, et al. (2018) Use of Paracetamol, Ibuprofen or Aspirin in Pregnancy and Risk of Cerebral Palsy in the Child. *International Journal of Epidemiology*. 47(1): 121-130.

Pooter, Renée de, and Juan Carlos Zúñiga-Pflücker. 2007. "T-Cell Potential and Development in Vitro: The OP9-DL1 Approach." *Current Opinion in Immunology*. https://doi.org/10.1016/j.coi.2007.02.011.

Porritt H E, Rumfelt L L, Tabrizifard S, Schmitt T M, Zúñiga-Pflücker J C, and Petrie H T (2004) Heterogeneity among DN1 Prothymocytes Reveals Multiple Progenitors with Different Capacities to Generate T Cell and Non-T Cell Lineages. *Immunity*. 20(6): 735-745

Prescott L F (1983) Paracetamol Overdosage: Pharmacological Considerations and Clinical Management. *Drugs*. 25(3): 290-314.

Prescott L F, Ballantyne A, Proudfoot A T, Park J, and Adriaenssens P (1977) TREATMENT OF PARACETAMOL (ACETAMINOPHEN) POISONING WITH N-ACETYLCYSTEINE. *The Lancet*. 2(8035): 432-434.

Puel A, Ziegler S F, Buckley R H, and Leonard W J (1998) Defective IL7R Expression in T-B+NK+ Severe Combined Immunodeficiency. *Nature Genetics*. 20(4): 394-397.

Radi R (2018) Oxygen Radicals, Nitric Oxide, and Peroxynitrite: Redox Pathways in Molecular Medicine. *Proceedings of the National Academy of Sciences of the United States of America*. 115(23): 5839-5848.

Radtke F, Wilson A, Stark G, Bauer M, Van Meerwijk J, MacDonald H R, and Aguet M (1999) Deficient T Cell Fate Specification in Mice with an Induced Inactivation of Notch1. *Immunity*. 10(5): 547-558.

Ramachandran A, and Jaeschke H (2018) Acetaminophen Toxicity: Novel Insights into Mechanisms and Future Perspectives. *Gene Expression*. 18(1): 19-30.

Ramos T V, Mathew A J, Thompson M L, and Ehrhardt R O (2014) Standardized Cryopreservation of Human Primary Cells. *Current Protocols in Cell Biology*. 64: A.3l.1-8.

Rebordosa C, Kogevinas M, Sørensen H T, and Olsen J (2008) Pre-Natal Exposure to Paracetamol and Risk of Wheezing and Asthma in Children: A Birth Cohort Study. *International Journal of Epidemiology*. 37(3): 583-590.

Rojo J M, Bello R, and Portolés P (2008) T-Cell Receptor. *Advances in Experimental Medicine and Biology*. 640: 1-11.

Romagnani S (1994) Lymphokine Production by Human T Cells in Disease States. *Annual Review of Immunology*. 12: 227-257.

Rothenberg E V (2019) Programming for T-Lymphocyte Fates: Modularity and Mechanisms. *Genes and Development*. 33(17-18): 1117-1135.

Sawicka M, Stritesky G L, Reynolds J, Abourashchi N, Lythe G, Molina-París C, and Hogquist K A (2014) From Pre-DP, Post-DP, SP4, and SP8 Thymocyte Cell Counts to a Dynamical Model of Cortical and Medullary Selection. *Frontiers in Immunology*. 5: 19.

Schmitt T M, de Pooter R F, Gronski M A, Cho S K, Ohashi P S, and Zúñiga-Pflücker J C (2004) Induction of T Cell Development and Establishment of T Cell Competence from Embryonic Stem Cells Differentiated in Vitro. *Nature Immunology*. 5(4): 410-417.

Schmitt T M, and Zúñiga-Pflücker J C (2002) Induction of T Cell Development from Hematopoietic Progenitor Cells by Delta-like-1 in Vitro. *Immunity*. 17(6): 749-756.

Seita J, and Weissman I L (2010) Hematopoietic Stem Cell: Self-Renewal versus Differentiation. *Wiley Interdisciplinary Reviews: Systems Biology and Medicine*. 2(6): 640-653.

Shah D K, and Zúñiga-Pflücker J C (2014) An Overview of the Intrathymic Intricacies of T Cell Development. *The Journal of Immunology*. 192(9): 4017-4023.

Singer A, Adoro S, and Park J-H (2008) Lineage Fate and Intense Debate: Myths, Models and Mechanisms of CD4- versus CD8-Lineage Choice. *Nature Reviews Immunology*. 8(10): 788-801.

Smyth E M, Grosser T, Wang M, Yu Y, and FitzGerald G A (2009) Prostanoids in Health and Disease. *Journal of Lipid Research*. 50 Suppl(Suppl) S423-428.

Solano M E, Jago C, Pincus M K, and Arck P C (2011) Highway to Health; or How Prenatal Factors Determine Disease Risks in the Later Life of the Offspring. *Journal of Reproductive Immunology*. 90(1): 3-8.

Su D M, Navarre S, Oh W J, Condie B G, and Manley N R (2003)A Domain of Foxn1 Required for Crosstalk-Dependent Thymic Epithelial Cell Differentiation. *Nature Immunology*. 4(11): 1128-1135.

Thiele K, Kessler T, Arck P C, Erhardt A, and Tiegs G (2013) Acetaminophen and Pregnancy: Short- and Long-Term Consequences for Mother and Child. *Journal of Reproductive Immunology*. 97(1): 128-139.

Thiele K, Solano M E, Huber S, Flavell R A, Kessler T, Barikbin R, Jung R, Karimi K, Tiegs T, and Arck P C (2015) Prenatal Acetaminophen Affects Maternal Immune and Endocrine Adaptation to Pregnancy, Induces Placental Damage, and Impairs Fetal Development in Mice. *American Journal of Pathology*. 185(10): 2805-2818.

Tovo-Rodrigues L, Schneider B C, Martins-Silva T, Del-Ponte B, Loret De Mola C, Schuler-Faccini L, Sales Luiz Vianna F, et al. (2018) Is Intrauterine Exposure to Acetaminophen Associated with Emotional and Hyperactivity Problems during Childhood? Findings from the 2004 Pelotas Birth Cohort. *BMC Psychiatry*. 18(1): 368.

Tsukamoto T (2019) HIV Impacts CD34+ Progenitors Involved in T-Cell Differentiation during Coculture with Mouse Stromal OP9-DL1 Cells. *Frontiers in Immunology*. 10: 81.

Tumes D J, Papadopoulos M, Endo Y, Onodera A, Hirahara K, and Nakayama T (2017) Epigenetic Regulation of T-Helper Cell Differentiation, Memory, and Plasticity in Allergic Asthma. *Immunological Reviews*. 278(1): 8-19.

Ueno H, Sakita-Ishikawa M, Morikawa Y, Nakano T, Kitamura T, and Saito M (2003) A Stromal Cell-Derived Membrane Protein That Supports Hematopoietic Stem Cells. *Nature Immunology*. 4(5): 457-63.

Vaidya A, and Kale V (2015) Hematopoietic Stem Cells, Their Niche, and the Concept of Co-Culture Systems: A Critical Review. *Journal of Stem Cells*. 10(1): 13-31.

Vantourout P, and Hayday A (2013) Six-of-the-Best: Unique Contributions of Γδ T Cells to Immunology. *Nature Reviews Immunology*. 13(2): 88-100.

Verheijen M, Lienhard M, Schrooders Y, Clayton O, Nudischer R, Boerno S, Timmermann B, et al. (2019) DMSO Induces Drastic Changes in Human Cellular Processes and Epigenetic Landscape in Vitro. *Scientific Reports*. 9(1): 4641.

Wang H, Pierce L J, and Spangrude G J (2006) Distinct Roles of IL-7 and Stem Cell Factor in the OP9-DL1 T-Cell Differentiation Culture System. *Experimental Hematology*. 34(12): 1730-1740.

Weber B N, Wei Shine Chi A, Chavez A, Yashiro-Ohtani Y, Yang Q, Shestova O, and Bhandoola A (2011) A Critical Role for TCF-1 in T-Lineage Specification and Differentiation. *Nature*. 476(7358): 63-68.

Wilkes J M, Clark L E, and Herrera J L (2005) Acetaminophen Overdose in Pregnancy. *Southern Medical Journal*. 98(11): 1118-1122.

Wineman J P, Gilmore G L, Gritzmacher C, Torbett B E, and Muller-Sieburg C E (1992) CD4 Is Expressed on Murine Pluripotent Hematopoietic Stem Cells. *Blood*. 80(7): 1717-1724.

Wu L, Aster J C, Blacklow S C, Lake R, Artavanis-Tsakonas S, and Griffin J D (2000) MAML1, a Human Homologue of Drosophila Mastermind, Is a Transcriptional Co-Activator for NOTCH Receptors. *Nature Genetics*. 26(4): 484-489.

Yan H-M, Ramachandran A, Bajt M L, Lemasters J J, and Jaeschke H (2010) The Oxygen Tension Modulates Acetaminophen-Induced Mitochondrial Oxidant Stress and Cell Injury in Cultured Hepatocytes. *Toxicological Sciences*. 117(2): 515-523.

Zhao S-T, and Wang C-Z (2018) Regulatory T Cells and Asthma. *Journal of Zhejiang University: Science B*. 19(9): 663-673.

Zúñiga-Pflücker, J C (2004) T-Cell Development Made Simple. *Nature Reviews Immunology*. 4(1): 67-72.

9 Danksagung

Mein besonderer Dank gilt Frau Prof. Gisa Tiegs für die Überlassung dieses interessanten und klinisch relevanten Themas und die Möglichkeit, meine Doktorarbeit am Institut für Experimentelle Immunologie und Hepatologie anfertigen zu dürfen. Ich danke ihr herzlich für die vielen Anregungen und die Freiheit zum selbstständigen Arbeiten.

Für die Bereitstellung des Stipendiums danke ich dem iPRIME-Else-Kröner-Promotionskollegium und den Koordinatoren Prof. Tobias Huber und Prof. Ulf Panzer.

Ein ganz besonderer Dank geht an Dr. Laura Berkhout für die Übernahme meiner direkten Betreuung und die stetige Hilfsbereitschaft. Die vielen wertvollen Diskussionen und Anregungen trugen einen maßgeblichen Beitrag zum Gelingen dieser Arbeit bei.

Des Weiteren möchte ich mich herzlich bei Dr. Birgit Schiller bedanken, dass sie mich zwischenzeitlich bei der Durchführung und Planung der Experimente unterstützt hat. Ich bin dankbar für das jederzeit offene Ohr, dass sie für mich hatte und ihren einmaligen Einsatz. Auch bei Dr. Lars Bremer bedanke ich mich für die Einarbeitung in das Thema und die anfängliche Planung dieses Projektes.

Außerdem möchte ich mich bei den Mitgliedern meiner Betreuungskommission Prof. Linda Diehl und Prof. Eva Tolosa bedanken. Dankbar bin ich für die Vorschläge für weiterführende Experimente und die Bereitstellung der OP9 Zellen durch Prof. Eva Tolosa.

Auch Dr. Anna Gieras danke ich für die Informationen über das OP9 Ko-Kultursystem.

Ich möchte Elena Tasika und Carsten Rothkegel für die hervorragende technische Unterstützung sowie die nette Atmosphäre im Labor bedanken. Auch gilt mein Dank allen weiteren Mitarbeitern und Doktoranden des Instituts, die immer für Fragen offen waren und ebenfalls zum guten Arbeitsklima beigetragen haben.

Auch meinen Freunden möchte ich dafür danken, dass sie immer für mich da sind und auch in schwierigen Zeiten für Ablenkung und Ermutigung sorgen. Insbesondere danke ich meinen Uni-Mädels, die mich seit Anfang des Studiums begleiten und mir in jeder Lebenslage mit Rat und Tat zur Seite stehen.

Zu guter Letzt gilt mein größter Dank meiner Familie, auf die ich immer zählen kann. Vor allem danke ich meinen Eltern für ihre allumfassende Unterstützung und bedingungslose Liebe, die sie mir und meinen Geschwistern entgegenbringen. Ohne euch wäre mein Studium und diese Arbeit

wahrscheinlich nie möglich gewesen. Auch bin ich meinen Geschwistern, Tiara und David, und meinem Freund, Philip, für ihre immer aufbauenden Worte und Taten dankbar.

10 Curriculum vitae

<u>Laura Enrica Mayer, *17.01.1997</u>

<u>Ausbildung:</u>

<u>seit 10/2015:</u>   Studium der Humanmedizin am Universitätsklinikum
                        Hamburg-Eppendorf (UKE), voraussichtlicher Abschluss 12/2022

<u>06/2015:</u>   Abitur am Helene-Lange-Gymnasium Hamburg

<u>Auslandsaufenthalte:</u>

<u>08/2012-06/2013:</u>   Bradfield College, Reading, England (10. Klasse)

<u>Dissertation:</u>

<u>seit 10/2018:</u>   Experimentelle Doktorarbeit am Institut für Experimentelle
                        Immunologie und Hepatologie am UKE unter der Leitung von
                        Prof Dr. rer. nat. Gisa Tiegs

<u>Förderung:</u>

<u>10/2018-09/2019:</u>   Stipendium durch das iPRIME-Else-Kröner-Promotionskollegium

<u>Praktika:</u>

<u>08/2018:</u>   Famulatur in der Allgemein- und Viszeralchirurgie,
                        Asklepios Klinik Wandsbek, Hamburg

<u>08/2020:</u>   Famulatur in der Allgemein-internistischen Praxis, Rodigallee,
                        Hamburg

<u>09/2020:</u>   Famulatur im MVZ Rheumatologie und Autoimmunmedizin,
                        Hamburg

<u>03/2021:</u>   Famulatur in der Poliklinik für Dermatologie,
                        Universitäsklinikum Hamburg-Eppendorf

Hamburg, 20.02.2022

L. Mayer

11 Eidesstattliche Versicherung

Ich versichere ausdrücklich, dass ich die Arbeit selbständig und ohne fremde Hilfe verfasst, andere als die von mir angegebenen Quellen und Hilfsmittel nicht benutzt und die aus den benutzten Werken wörtlich oder inhaltlich entnommenen Stellen einzeln nach Ausgabe (Auflage und Jahr des Erscheinens), Band und Seite des benutzten Werkes kenntlich gemacht habe.

Ferner versichere ich, dass ich die Dissertation bisher nicht einem Fachvertreter an einer anderen Hochschule zur Überprüfung vorgelegt oder mich anderweitig um Zulassung zur Promotion beworben habe.

Ich erkläre mich einverstanden, dass meine Dissertation vom Dekanat der Medizinischen Fakultät mit einer gängigen Software zur Erkennung von Plagiaten überprüft werden kann.

Unterschrift: